Aspects of global symmetry in quantum many-body systems.

A Dissertation Presented

by

Abhishodh Prakash

to

The Graduate School

in Partial Fulfillment of the Requirements

for the Degree of

Doctor of Philosophy

in

Physics

Stony Brook University

June 2018

Stony Brook University

The Graduate School

Abhishodh Prakash

We, the dissertation committee for the above candidate for the Doctor of Philosophy degree, hereby recommend acceptance of this dissertation.

Tzu-Chieh Wei – Dissertation Advisor
Associate Professor, C.N. Yang Institute for Theoretical Physics

Alexander Abanov – Chairperson of Defense
Professor, Simons Center for Geometry and Physics.

Eden Figueroa
Assistant Professor, Department of Physics and Astronomy.

Robet Konik
Chair of CMPMS Division
Brookhaven National Laboratory.

This dissertation is accepted by the Graduate School.

Charles Taber
Dean of the Graduate School

Abstract of the Dissertation

Aspects of global symmetry in quantum many-body systems.

by

Abhishodh Prakash

Doctor of Philosophy

in

Physics

Stony Brook University

2018

Symmetries lie at the heart of understanding many physical phenomena - from solids and liquids to fundamental forces. In particular, the existence of distinct phases of matter, which has consequences as important as the very existence of life, is in several cases a consequence of the manner in which global symmetries interplay with dynamics. One important route for the formation of phases is when symmetry is *spontaneously broken*. Examples include the transition of a liquid to solid or fluid to superfluid. Indeed, there was a time when all known examples of phases were believed to be understood in this framework leading to speculations that symmetry-breaking was the ultimate theory of phases and phase transitions. In the recent decades however, several examples of phases that lie outside the symmetry-breaking paradigm have been discovered both experimentally and theoretically like quantum hall phases, topological insulators and the Haldane phase. It is now understood that in order to have non-trivial phases,the presence of global symmetries is not essential and if present, they need not be broken. In this thesis, we will study various quantum

many-body systems, their phases and the effect of global symmetries from this modern viewpoint.

In the first part, we will study how to detect various phases of one-dimensional spin chains via appropriately designed order parameters when we know the global symmetry of the system and test this out on a model Hamiltonian. Next, we will explore how so-called symmetry-protected topological (SPT) phases which are non-trivial phases without broken symmetries can be *unwound* by extending the symmetry. In the second part, we demonstrate how certain SPT phases can serve also as *computational phases of matter* i.e. phases of matter that can be used to obtain resource states for quantum computation. In the last part, we explore disorder-driven out-of-equilibrium phases of matter, dubbed *eigenstate phases* and their stability in the presence of different kinds of global symmetries.

Publications

This thesis is based on the work included in the following publications. Significant emphasis is given to [1,3,6,7].

1. Abhishodh Prakash, Juven Wang, Tzu-Chieh Wei,
   Unwinding Short-Range Entanglement, arXiv:1804.11236 [quant-ph]

2. Yanzhu Chen, Abhishodh Prakash, Tzu-Chieh Wei,
   Universal quantum computing using $(\mathbb{Z}_d)^3$ symmetry-protected topologically ordered states,
   Phys. Rev. A 97, 022305 (2018), arXiv:1711.00094 [quant-ph].

3. Abhishodh Prakash, Sriram Ganeshan, Lukasz Fidkowski, Tzu-Chieh Wei, *Eigenstate phases with finite on-site non-Abelian symmetry*,
   Phys. Rev. B 96, 165136 (2017), arXiv:1706.06062 [cond-mat.dis-nn].

4. David T. Stephen, Dong-Sheng Wang, Abhishodh Prakash, Tzu-Chieh Wei, Robert Raussendorf,
   Computational Power of Symmetry-Protected Topological Phases,
   Phys. Rev. Lett. 119, 010504 (2017), arXiv:1611.08053 [quant-ph].

5. Robert Raussendorf, Dongsheng Wang, Abhishodh Prakash, Tzu-Chieh Wei, David Stephen,
   Symmetry-protected topological phases with uniform computational power in one dimension,
   Phys. Rev. A 96, 012302 (2017), arXiv:1609.07549 [quant-ph].

6. Abhishodh Prakash, Colin G. West, Tzu-Chieh Wei,
   Detection of gapped phases of a 1D spin chain with onsite and spatial symmetries,
   Phys. Rev. B 94, 045136 (2016), arXiv:1604.00037 [cond-mat.str-el].

7. Abhishodh Prakash, Tzu-Chieh Wei,
   Ground states of 1D symmetry-protected topological phases and their utility as resource states for quantum computation,
   Phys. Rev. A 92, 022310 (2015), arXiv:1410.0974 [quant-ph].

To the unacknowledged, who defend the truth passionately, speak it freely and inspire us to pursue it without fear.

Contents

List of Figures

List of Tables

Acknowledgements

Acknowledgements here

Chapter 1

Introduction

1.1 The importance of phases

The existence of matter in distinct phases has several consequences. The most important example is perhaps that of water. Without any change in its chemical composition, depending on external conditions like temperature and pressure, water molecules can organize themselves into several phases- solid, liquid and gas. In its liquid form, water is understood to be crucial for the existence of life [1]. It is for this reason that in order to search for extraterrestrial life, NASA's Kepler observatory looks for Earth-like planets, called *Goldilocks planets* that exist in the so-called *habitable zone* *i.e.* the range of orbits around a star within which a planetary surface can support liquid water [2]. Not just the existence of different phases but also *phase transitions* *i.e.* the ability to go from one phase to another by varying external parameters is also very important. By freezing water into ice, it can be used to preserve things and by boiling it into steam, it can be used to power engines. The ability to melt metals into its liquid form has proven very useful in remodeling them to desired shapes. Finally, different phases respond differently to electrical and thermal currents and this has been used extensively for various practical purposes– good insulators are used to build shelters that provide protection from the elements and good metals are used to distribute heat and electricity.

From an academic point of view, the study of phases and phase transitions is highly interesting even when disconnected from commercial and practical uses and this study has a long history which we will briefly glimpse below.

1.1.1 What makes up stuff?

The study of phases of matter is closely linked with the search for the fundamental constituents of matter. Interestingly, the best theory for what the universe is made up of had been more-or-less the same for close to two millenia. These were called the classical elements– earth, fire, air and water. While the origin of this is commonly attributed to ancient Greece (during the fourth century B.C.), similar lists have also been found in the ancient cultures of Babylon, Japan, Tibet, India and China [3]. It was the *scientific revolution* [4] with its new ideas, rigor and techniques like experimentation, mathematical modeling and empericism that brought about a significant improvement of the understanding of the building blocks of the universe. The first list of indivisible constituents, called elements, was published by Antoine-Laurent de Lavoiser in 1789 which included oxygen, nitrogen, hydrogen and others which are part of the modern list of elements we well as 'light' and 'caloric' which are not. A significant achievement of this line of study was the publication of the *periodic table* by Dimitri Mendeleev in 1869 [5] that not only organized a large number of observed elements but also made predictions for undiscovered ones (which were subsequently proven). It is now known that elements themselves are further divisible and the modern viewpoint of fundamental building blocks, called the *standard model of elementary particles* is phrased in terms of fundamental fields and their excitation quanta, called fundamental particles. This too is believed to be incomplete and the search for a more general theory is an active area of ongoing research.

1.1.2 What the stuff that make up stuff make up?

In the early nineteenth century, the English chemist, Humphry Davy observed that of the 40 chemical elements known, twenty-six had metallic properties. He further conjectured that elements that were then believed to be gases, such as nitrogen and hydrogen could be liquefied under the right conditions and would then behave as metals [6]! Clearly, Davy understood that even though the constituents of a substance were unchanged (indivisible elements even), in large numbers, they could organize themselves into different *phases*. Davy's conjectures were subsequently proven– in 1823, Michael Faraday, then an assistant in Davy's lab, successfully liquefied chlorine and most known gaseous elements and by 1908, James Dewar and Kamerlingh Onnes were successfully able to liquefy hydrogen and helium, respectively. The emerging picture of phases and phase transitions was as shown in fig. 1.1 (taken from ref. [7]). The discovery of superconductivity in 1911 by Kamerlingh Onnes and superfluidity in liquid helium by Pyotr Kapitsa and John Allen in 1937 compelled

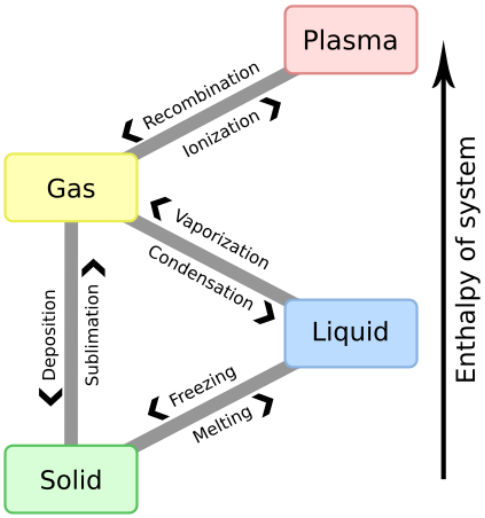

Figure 1.1: Schematic of phases and phase transitions.

the need for a systematic understanding of phases and phase transitions.

1.2 The role of symmetries

1.2.1 Orders of phase transitions

One of the earliest and most successful attempts at a systematic understanding of phases and phase transitions is the theory of *spontaneous symmetry breaking* (SSB). Before understanding SSB, we need to understand the notion of an order of a phase transitions. Roughly, phase transitions can be of two types:

1. First-order: Characterized by an abrupt change in the free energy, latent heat and a co-existence of phases near phase transitions.

2. Continuous/ second-order: Characterized by a divergent susceptibility and an infinite correlation length but no abrupt change in the free energy.

It can be said that it is the continuous phase transitions which are the interesting ones. This is because first order phase transitions can either be circumvented or avoided by appropriately tuning external parameters (like how the water-steam phase transition as a function of pressure disappears beyond a certain temperature) or they turn into second order phase transitions. The

Landau-Ginzburg phase transitions via SSB describes a class of continuous phase transitions [8].

1.2.2 Spontaneous symmetry breaking and universality

A symmetry can be thought of as the collection of actions that leaves something of interest invariant. For example, if the thing of interest is a triangle, there are six actions that leaves it invariant. These symmetry actions can be generated by a combination of a 120 degree rotation about the center and reflection about one of the *axes of symmetry* as shown in fig.1.2. The

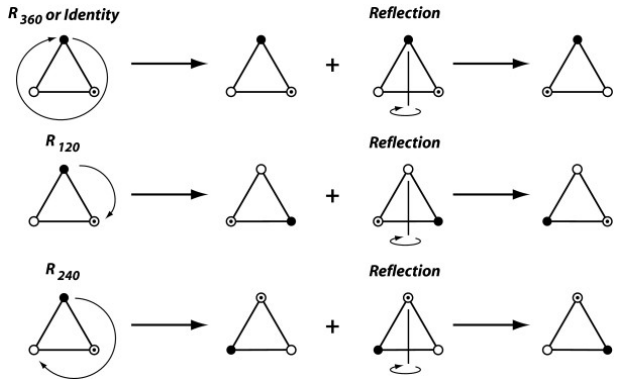

Figure 1.2: Symmetries of the triangle.

mathematical framework that describes the set of symmetry actions and their properties is *group theory*. Spontaneous symmetry breaking can be understood in a nutshell as a phenomenon where a *problem* has a set of symmetries but its solutions have only a subset of those symmetries. A clear illustration of the essential features of this phenomenon, taken from the review of symmetry breaking and ordered media by Michael [9] is as follows. The problem is very simple– what is the curve joining the four corners of a square of unit length? The problem clearly has the symmetries of the square. However, the solutions, shown in fig. 1.3 which are curves of length $1 + \sqrt{3}$ clearly have symmetries fewer than that of the square. Specifically, the solutions are longer invariant under a 90 degree rotation about the center of the square. The number of *degenerate* solutions are the same as the number of symmetries of the problem divided by the number of symmetries of the solutions. In fact, the *broken symmetry generator* of rotation of the square by 90 degrees relates the two solutions as can be seen in fig. 1.3. In the Ginzburg-Landau framework, phases can be thought of as being described by a family of problems, parametrized by a set of continuous parameters (temperature, pressure, magnetic field, ...)

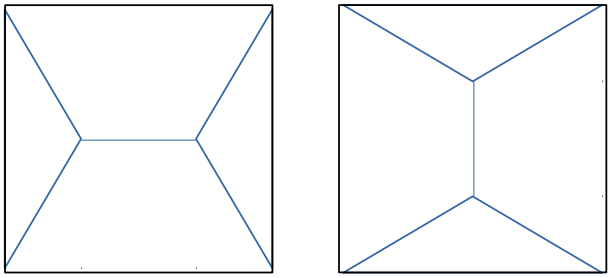

Figure 1.3: Illustrative example of spontaneous symmetry breaking.

with a certain set of symmetries, and the solutions with a subset of those symmetries. A SSB phase transition between a disordered phase (when the symmetries of the problem are also those of the solution) to an ordered phase (when some of the symmetries of the problem are broken and are not the symmetries of the solutions) happens at some value of the parameters which is called the *critical point*. What the problem is depends on whether we are looking at *classical* or *quantum* phases. For classical phases, the problem is to find configurations of the system that minimizes a certain quantity called the *free energy*. For quantum phases, the problem is to find minimum energy *quantum states* called the ground states of the system. The symmetries of the problem are reflected in the symmetries of the quantity that defines the *dynamics* of the system- the *energy function* for a classical system and the *Hamiltonian* for a quantum system.

More formally, the Ginzburg-Landau framework is a phenomenological approach to phases and phase transitions based on SSB. In this framework, phases are classified by some universal quantities independent of microscopic details: space-time dimensions, unbroken and broken symmetries. Furthermore, phase transitions can be classified and divided into placed in *universality classes* based on a set of numbers, called *critical exponents* which can be measured experimentally. Furthermore, the framework posits that near a phase transition, a system in equilibrium can be described by a set of local *order parameters*. The information about the unbroken and broken symmetries are encoded in the symmetry properties of the order parameter and critical exponents are obtained by studying the *effective field theory* that describes the dynamics of these order parameters with the aid of tools and techniques like *renormalization group*.

1.3 Going beyond spontaneous symmetry breaking

The Ginzburg-Landau framework was so successful that there were speculations that *all* phases and phase transitions could be understood within this framework. For the existence of a non-trivial phase of a system in equilibrium, the Ginzburg-Landau framework requires the following in the physical system:

1. The presence of global symmetries.

2. The spontaneous breaking of some of these symmetries.

We will see that both of these requirements can be relaxed to obtain equilibrium phases and phase transitions that are outside the scope of SSB. We will also see that the very existence of equilibrium may be inessential to the existence of a phase which can be defined rather generally.

The main challenge to the sovereignty of the Ginzburg-Landau framework over the study of phases came with the experimental discovery of the *quantum Hall effect* (QHE) [10]– a phenomenon observed in a two-dimensional electronic gas in the presence of strong magnetic field perpendicular to the plane of the gas as shown in fig. 1.4. It was found that for a fixed strength of magnetic

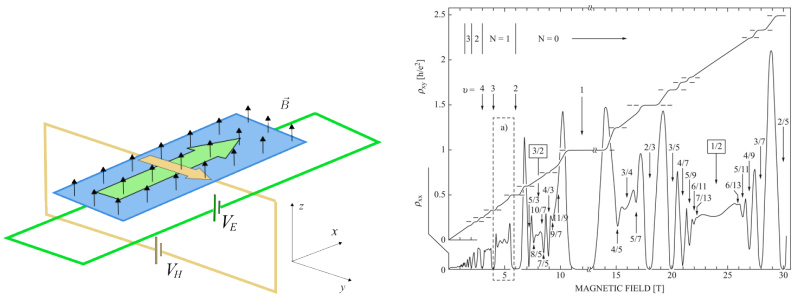

Figure 1.4: Schematic set-up of the quantum Hall experiment (left), experimental results (right)

field, the conductance in one of the planar directions after the application of a voltage in the perpendicular planar direction (called Hall response) was quantized to be integer multiples of the fundamental unit of conductance, $\frac{e^2}{h}$ (subsequently, Hall responses of rational multiples were also discovered). This quantization was stable to perturbations of the magnetic field. It was soon clear that each quantized Hall response corresponded to a distinct phase of matter which could not be characterized by the spontaneous breaking of any symmetries. Furthermore, it is believed that essential features of these

phases, especially of systems with a non-integer Hall response (called fractional quantum Hall systems) do not even rely on the presence of any symmetries, let alone their spontaneous breaking. Such phases are said to possess *topolgical order*.

A second counter example to the symmetry breaking picture is the successful prediction [11, 12] and discovery [13] of topological insulators. These are non-trivial band insulators that possess global symmetries which are essential to distinguish them from ordinary insulators but are not spontaneously broken. Topological insulators belong to a prominent example of a non-trivial *symmetry protected topological (SPT) phase*. We will return to SPT phases in the chapters contained in the first two parts of this thesis.

A third example is perhaps the most drastic departure- the study of out-of-equilibrium phases. The earliest instance of such an example is that of systems which have Anderson localization [14]. These are weakly interacting quantum systems with quenched disorder which show an absence energy and charge transport. A renewal of interest in these systems was motivated by the seminal work of Basko et. al. [15] who showed that localization can persist even in the presence of strong interactions. Such systems with *many-body localization* [16] are believed to belong to a new type of phase of matter whose members violate the so-called eigenstate thermalization hypothesis (ETH) [17]. It is believed that the existence of such phases, usually observed in systems with strong quenched disorder, require no symmetries to be present and whose signatures can be detected at high energies and large ambient temperatures. We will return to such phases in the third part of this thesis.

1.4 Phases of matter in perspective

Let us explore the notion of a phases in a little more holistic manner. At a grand level, we wish to take the collection of all physical systems and define a way to partition them. These partitions can schematically be called phases. While appealing in its generality and simplicity, this definition is severely lacking in some important details:

- What do we mean by physical systems?
- On what basis do we partition them?
- How do we study them?

Rather than thinking of these questions as having or lacking absolute answers, we will think about them as additional pieces of information that needs

to be specified to complete the formulation of the problem. Let us understand each of these questions separately.

1.4.1 What do we mean by physical systems?

We will first list a set of characteristics that are considered to be essential for any physical system to investigate the question of phases.

- ***Thermodynamic limit***: First, it has been shown that a sharp notion of a phase is obtained when we are considering systems in the *thermodynamic limit i.e.* when the degrees of freedom of the physical system are infinitely many. One way to arrive at this limit is when the system is built out of a large number of individual units each with its own set of degrees of freedom. A degree of freedom can be thought of as a random variable for classical systems and as the dimensionality of the Hilbert space for quantum systems. Note that care must be taken to interpret this in quantum systems. For example, a single harmonic oscillator or a hydrogen atom itself lives in an infinite dimensional Hilbert space but cannot be thought of as a system in the thermodynamic limit while an infinite number of harmonic oscillators or hydrogen atoms can be. A system in thermodynamic limit does not need to be built out of individual units at all. For example, dimer-coverings of a lattice [18] are commonly studied as representing the degrees of freedom of a classical system or as labeling the basis states of the Hilbert space of a quantum system in thermodynamic limit.

- ***Locality and dimensionality***: A reasonable attribute for a physical system is its dimensionality. This usually has a visual description in terms of the individual units of the system– particles, spins etc. being placed on or the dimer coverings being defined on a lattice of a certain dimension. However, in order to meaningfully talk about dimensionality, we must also talk about the locality of interactions. Let us restrict ourselves to quantum systems for this discussion. The evolution of a state of a quantum system is described by a *Hamiltonian* operator which is a Hermitian operator that acts on the Hilbert space of the system. The Hamiltonian is *local* if it is a sum of local operators. An operator is said to be local at a point if it acts non-trivially on the Hilbert space associated to a finite neighborhood of the point. For example, for qubits on a lattice, a local operator at a point x acts as the identity operator on the Hilbert space of spins far away from x and non-trivially on the spins close to x. For dimer coverings, a local operator at x changes the

local dimer configuration near x and leaves the dimer configurations far away unchanged. If the Hamiltonian was not local and if its terms acted on far separated qubits, the location of qubits on the lattice would have very little meaning or consequence and we could, for all purposes imagine them being located on a cluster or a dot. In other words, a non-local Hamiltonian can be thought of as describing a zero dimensional system. Thus, the dimensionality of the system itself can be interpreted as a consequence of the locality of the interaction terms of the Hamiltonian.

So far, we have listed properties that are expected to hold for any reasonable physical system. We will now list attributes that are more optional and serve to make the problem complex and richer:

- ***Symmetry***: As defined before, the symmetries of a system is a set of transformations that leaves the quantity that describes the dynamics of the system invariant. For a classical system, this is the *energy function* which is a function that assigns to a given configuration of the system a number– energy and a symmetry transformation is a set of transformations that does not change the energy when it acts on any configuration. The symmetries of a quantum system are the set of operators that commute with the Hamiltonian.

- ***Spectral properties***: This is a feature of quantum systems in the thermodynamic limit described by time-independent Hamiltonians. A gapped system is one whose Hamiltonian has a finite number of ground states and a finite energy gap separating the first excited state. A gapless system is one whose Hamiltonian has excited states arbitrarily close to the ground state.

1.4.2 On what basis do we partition them?

Once we specify the class of physical systems we wish to study phases of, we need to specify how we want to partition them into phases. To do this, we need to specify an *equivalence relation* between physical systems. An equivalence relation $\sim$ is a binary relation on a set S that has the following properties

1. Reflexivity: $\forall\ s \in S,\ s \sim s$
2. Symmetry: $\forall\ a, b \in S,\ a \sim b \implies b \sim a$
3. Transitivity: $\forall\ a, b, c \in S,\ a \sim b,\ b \sim c \implies a \sim c$

If we interpret the set as the collection of physical systems, the specification of an equivalence relation divides the set into *equivalence classes*. These equivalence classes can be thought of as the different phases of the class of physical systems in consideration. We will look at examples of different equivalence relations on different physical systems in the next section.

1.4.3 How do we study them?

Once we have specified a class of physical systems and the equivalence relation, in order to study the different phases, two lines of investigation are often employed:

1. Classification: The objective of classification is to enumerate the distinct phases and identify their structure.

2. Characterization: The objective of characterization is to identify the set of physical properties common to the members of each distinct phase and to develop methods of identifying these characteristics in any given physical system so as to unambiguously diagnose the phase it belongs to.

The above two programs usually work hand-in-hand. Understanding how to characterize different phases sometimes points to the structure of the phases in their classification and vice versa. A great example is that of integer quantum Hall phases which are characterized by their quantized Hall response by means of which they can be assigned integer labels. This labeling suggests that these phases can be classified to have a group structure of integers, $\mathbb{Z}$.

1.4.4 Examples

Let us understand some examples of phases in the terminology we introduced above.

Equilibrium gapped phases

Local observables of a quantum system in equilibrium at a certain temperature $T = \frac{1}{\beta}$ are described by a time-independent Hamiltonian are obtained using a thermal density matrix

$$\rho_{th} = \frac{e^{-\beta H}}{Tr(e^{-\beta H})} \tag{1.1}$$

It has been shown that a sharp notion of a phase transition can be seen at zero temperature $T = 0$ at which point the thermal density matrix describes the physics in the ground states of H [19]. Such zero temperature phases are sometimes also called quantum phases. When a family $H(\lambda)$ has a gap for some λ, the phase transition happens when the gap closes, at some *critical* λ_c.

Gapped quantum phases in the absence of symmetries are called *topological phases*. Let us list the different aspects of such phases below:

- ***Physical systems***: Local quantum systems in the thermodynamic limit $\{s_i \in \mathcal{S}\}$ described by time independent Hamiltonians $\{H_i \in \mathcal{H}\}$ which have a spectral gap.

- ***Equivalence***: $s_i \sim s_j$ if $\exists s(\lambda)$ described by $H(\lambda) \in \mathcal{H} | H(0) = H_i, H(1) = H_j$. In other words, the Hamiltonians describing two systems in the same phase can be continuously interpolated without closing the gap.

- ***Partial classification***: A class of gapped phases are believed to be described by topological quantum field theories (TQFT) meaning the problem of classification of gapped phases can be mapped into the classification of TQFTs. This is completed in some cases in 1+1 D and 2+1 D. The general picture is still unavailable.

- ***Characterization***: Anyons, topological entanglement entropy, ground state degeneracy, long-range entanglement...

- ***Examples***: quantum Hall phases [10], string net models [20], quantum double models [21]...

The problem of gapped phases with symmetries is a refinement of the above with an additional condition on the set of physical systems under consideration– quantum systems in the thermodynamic limit $\{s_i \in \mathcal{S}\}$ described by time independent Hamiltonians $\{H_i \in \mathcal{H}_G\}$ which have a spectral gap and commute with the representation U_g of some symmetry group G. The equivalence relation that defines the notion of phases is the same as that of gapped phases but on this restricted set of physical systems. This typically increases the number of phases possible. A trivial gapped phase without symmetry can split into different phases with symmetry restriction. Let us list some cases of gapped symmetric phases which are of special interest.

- Gapped phases of symmetric Hamiltonians that have trivial topological order and no spontaneous symmetry breaking are called symmetry protected topological (SPT) phases.

- Gapped phases of symmetric Hamiltonians that have non-trivial topological order and no spontaneous symmetry breaking are called symmetry enriched topological (SET) phases.

- Gapped phases of symmetric Hamiltonians that have trivial topological order and no SPT order correspond to the familiar Ginzburg-Landau phases.

Clearly, there exist combinations of symmetry breaking, topological, SPT and SET ordering that are possible beyond the list above. To classify and characterize all these phases is an ongoing program.

Out-of-equilibrium phases

Unlike the case of equilibrium phases, out-of-equilibrium phases are relatively ill defined poorly understood. However, increasing numerical and experimental evidence points at the promise of several interesting properties present in these systems. This motivates understanding such phases better, by developing adequate analytical tools is a worthwhile endeavor and is an ongoing field of research. Several out-of-equilibrium phases are believed to have *eigenstate order*, meaning that properties that are typically found in the ground states of equilibrium phases are also found in the entire spectrum. However, a clear mechanism of phase transition like gap closure is not available. We list below some details that are known about these so-called eigenstate phases

- ***Physical systems***: Local quantum systems in the thermodynamic limit.

- ***Equivalence***: Unclear.

- ***Classification***: Unclear.

- ***Characterization***: Violation or non-violation of ETH, scaling of entanglement entropy in highly excited states, transport properties, emergence of a complete set of local conserved quantities, level-statistics, ...

- ***Examples***:Systems with low disorder, which satisfy ETH are called thermal systems and systems with high disorder which violate ETH are called MBL systems. The existence of eigenstate phases beyond these two are speculative at best.

Like equilibrium phases, the presence of global symmetries again adds a refinement to the study of out-of-equilibrium phases. Below, we mention some examples of conjectured phases with non-trivial eigenstate order in the presence of global symmetries

- When the dynamics is described by time-independent Hamiltonians, signatures of equilibrium phases like SPT, SET and SSB phases that are observed in ground states are believed to be present in highly excited eigenstates also. These phases are named MBL-SPT [22, 23], MBL-SET and MBL-Spin Glass [24] phases.

- When the dynamics is described by time-dependent Hamiltonians with a single frequency (called Floquet systems), it has been shown that phases with non-trivial eigenstate order can exist [25, 26]. Furthermore, time-periodicity can be interpreted as a global symmetry isomorphic to the group $\mathbb{Z}$. This can be spontaneously broken when the system has non-trivial eigenstate order, giving rise to *time crystals* [27, 28].

- Floquet systems with additional symmetries can have SPT phases that are absent in undriven systems (called Floquet-MBL-SPT phases) [29–31]. These are characterized by boundary modes that are 'pumped out' every Floquet cycle. Similarly, there can also exist SET phases that have no time-independent equilibrium analog.

The third part of this thesis is concerned with the nature of eigenstate phases in the presence of global symmetries.

Computational phases

One of the most successful methods to store and manipulate classical information is the use of magnetic materials in the ordered *ferromagnetic* phase. The advantage is that small changes to the system- fluctuations in temperature, chemical composition does not change the material's utility as a *computational resource state.* Such a class of systems which can be used as computational resource states is called a *computational phase.* The statement that magnetic materials are useful for storing and manipulating information is to say that some symmetry-broken phases also serve as computational phases. It is an interesting question (that may or may not have commercial utility) whether all computational phases useful for classical computation also coincide with symmetry-breaking ordered phases. An equivalent question can be also asked in the context of quantum information processing:

1. Can we define a computational phase of physical systems that can serve as resource states for quantum information processing, perhaps of a given type (topological, circuit-based, measurement-based).

2. Does such a phase coincide with any well-known phases like in the classical case?

There has been increasing evidence to suggest that the answer to both above questions is in the affirmative.

1. It has been shown that anyonic excitations present in certain topological phases can be used for *topological quantum computation* [21]. Such topological phases can also be compuational phases.

2. It has been shown that the short-range-entangled ground states of certain SPT phases can be useful for measurement based quantum computation (MBQC) [32–36].

Let us focus on the case of computational phases useful for MBQC. We want to look for ground states of Hamiltonians that can be resource states for MBQC. As a result, the approach to understand such phases can be posed in a manner similar to that of equilibrium phases.

- ***Physical systems***: Local quantum systems in the thermodynamic limit $\{s_i \in \mathcal{S}\}$ described by time independent Hamiltonians $\{H_i \in \mathcal{H}\}$ whose ground state is a resource state for MBQC.

- ***Equivalence***: $s_i \sim s_j$ if $\exists s(\lambda)$ described by $H(\lambda) \in \mathcal{H} | H(0) = H_i, H(1) = H_j$.

- ***Classification***: Largely unknown

- ***Characterization***: The ability to simulate quantum gates, initialize input quantum information and read out processed result.

- ***Examples***: Certain 1+1D SPT phases [34, 35, 37].

In the second part of the thesis, we explore these questions in detail.

Part I

Equilibrium phases of matter

Chapter 2

Detection of gapped phases of a 1D spin chain.

The contents of this chapter are published in Ref. [38] completed in collaboration with Tzu-Chieh Wei and Colin West.

2.1 Introduction

The program of classifying and characterizing different phases of matter has been revived and actively pursued in recent years. One aspect is to classify phases based on global symmetries. In the Landau-Ginzburg paradigm, given a class of many-body Hamiltonians invariant under a global symmetry defined by a group G, different phases of matter can be enumerated by the *spontaneous symmetry breaking* of G and labeled by the residual symmetry H that G is broken down to. One could also envision the existence of local order parameters which arise from symmetry breaking and hence be able to distinguish between these phases. However, after the discovery of the Quantum Hall Effect [39, 40], it was realized that the Ginzburg-Landau symmetry-breaking picture might not be enough to classify all phases of matter [41]. Some systems like the fractional quantum hall states [40], spin liquids [42], quantum double models [21] and string-net models [20] do not even need symmetries and are called *intrinsic topological phases* or simply *topological phases*. Even with symmetries, several new phases have been discovered which are not classified by symmetry-breaking or characterized by local order parameters; such as topological insulators [11] and the Haldane phase of spin-1 chains [43–45]. These phases are called *symmetry protected topological* (SPT) phases [46, 47]. Furthermore, if we consider global symmetry in systems with intrinsic topological order, we can have more phases called *symmetry enriched topological*

phases [48–50]. In gapped 1D spin chains, which we focus on in this chapter however, it has been shown that there cannot be any intrinsic topological order and hence all phases are either symmetry breaking or SPT phases [46, 51–55].

Given that the classification program has been much explored, there has been interest in developing ways to detect which phase of matter a system belongs to. Since local order parameters are insufficient to detect phases that are not characterized by spontaneous symmetry breaking (SSB), there have been attempts to develop other quantities that can detect SPT phases like non-local 'string' order parameters [54, 56–59] and Matrix Product State (MPS) order parameters [54]. Furthermore, if we include the possibility of both symmetry breaking and SPT phases, there is a rich set of possible phases [52]. Given a global symmetry group G, the ground state can spontaneously break the symmetry to one of its subgroups $H \subset G$. However for each subgroup H, there can exist different SPT phases that do not break symmetry spontaneously. The situation is even more interesting if there are both internal and space-time symmetries like parity and time reversal invariance. In this chapter, we generalize the techniques of Ref [54] and study the phase diagram for a two parameter Hamiltonian of a spin-1 chain which is invariant under a global on-site (internal) A_4 symmetry along with invariance under lattice translation and lattice inversion (parity). Through suitable MPS order parameters, we detect both the different SSB and SPT phases and label them using the classification framework of Ref [52]. A total of eight distinct phases are identified within the parameter space we consider. In particular, we find among these a direct, continuous transition between two topologically nontrivial A_4-symmetric SPT phases, distinguished by the 1D representations of the symmetries, as explained below.

This chapter is organized as follows. In section 2.2, we described the A_4 spin-chain Hamiltonian studied here and present its phase diagram which contains the main results of this chapter. In section 2.3, we review the classification of 1D gapped-spin chains and list parameters which can be used to completely classify phases. In section 2.4, we describe the full details of the phase diagram of the A_4 model, and also enumerate the several possible phases that can in principle exist given the symmetry group of the parent Hamiltonian. Section 2.5 presents, in detail, the numerical techniques by which the states and parameters were obtained, and section 2.6 gives a summary of our results.

2.2 Overview of main results

2.2.1 The Hamiltonian

We will now describe an A_4 and inversion symmetric Hamiltonian whose phase diagram we study in detail. The total Hamiltonian consists of three parts. The first is the Hamiltonian for the spin-1 Heisenberg antiferromagnet which is invariant under the spin-1 representation of $SO(3)$:

$$H_{Heis} = \sum_i \boldsymbol{S}_i \cdot \boldsymbol{S}_{i+1}, \tag{2.1}$$

where $\boldsymbol{S}_i \cdot \boldsymbol{S}_{i+1} \equiv S_i^x S_{i+1}^x + S_i^y S_{i+1}^y + S_i^z S_{i+1}^z$. We add two other combinations, H_q and H_c to the Heisenberg Hamiltonian which breaks the $SO(3)$ symmetry to A_4, the alternating group of degree four and the group of even permutations on four elements (equivalently, the group of *proper* rotations a tetrahedron). These terms are defined as:

$$H_q = \sum_i (S_i^x S_{i+1}^x)^2 + (S_i^y S_{i+1}^y)^2 + (S_i^z S_{i+1}^z)^2,$$

and

$$\begin{aligned} H_c = \sum_i [&(S^x S^y)_i S_{i+1}^z + (S^z S^x)_i S_{i+1}^y + (S^y S^z)_i S_{i+1}^x \\ &+ (S^y S^x)_i S_{i+1}^z + (S^x S^z)_i S_{i+1}^y + (S^z S^y)_i S_{i+1}^x \\ &+ S_i^x (S^y S^z)_{i+1} + S_i^z (S^x S^y)_{i+1} + S_i^y (S^z S^x)_{i+1} \\ &+ S_i^x (S^z S^y)_{i+1} + S_i^z (S^y S^x)_{i+1} + S_i^y (S^x S^z)_{i+1}]. \end{aligned} \tag{2.2}$$

For details on how the perturbations are constructed, see Appendix A.1 or Ref [36].

The operators in H_c are symmetrized so that the Hamiltonian is invariant under inversion as well as lattice translation. With this we have a two-parameter Hamiltonian invariant under an on-site A_4 symmetry along with translation invariance and inversion.

$$H(\lambda, \mu) = H_{Heis} + \lambda H_c + \mu H_q. \tag{2.3}$$

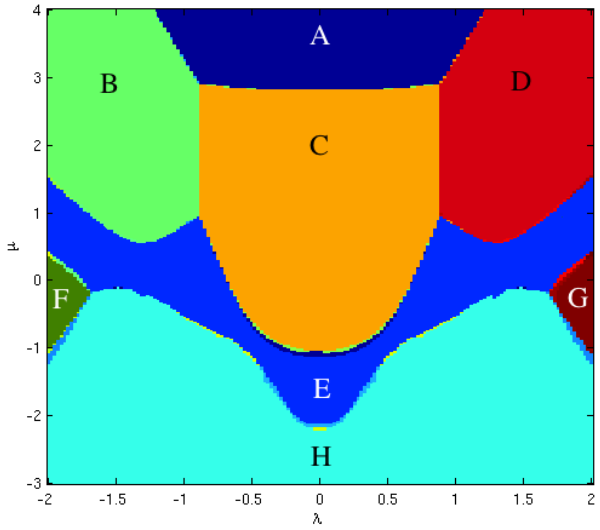

Figure 2.1: The phase diagram for a two-parameter Hamiltonian 2.3 constructed to have an on-site A_4 symmetry, as well as parity translation invariance. The symmetries of the Hamiltonian spontaneously break into five different residual symmetry groups in the ground states. These break down further when classified according to the relevant topological parameters, yielding eight distinct phases overall. The diversity of phases from the comparatively simple Hamiltonian shows the necessity of carefully accounting for all possible symmetries and topological parameters when attempting to characterize the phase of a ground state. For a description of the phases **A-H**, see discussions in the main text.

2.2.2 Summary of numerical results

We employ the iTEBD algorithm [60] to numerically analyze the ground states across a range of parameters $\mu = [-3, 4]$, $\lambda = [-2, 2]$ and find a wide variety of phases. In the parameter space analyzed, a total of eight distinct regions can be identified (labeled with letters **A-H** in Fig. 2.1). These regions are distinguished both by the symmetries of the ground states, and also by the classification parameters of Ref [52].

From the symmetry group G of the parent Hamiltonian, which contains A_4, spatial inversion, and translation symmetries, only the inversion and translation symmetries remain in the ground states of region **A**. Regions **B**, **C**, and **D**, by contrast, all respect the full set of symmetries of the parent Hamiltonians but are differentiated by one of the SPT parameters: namely, the overall complex $U(1)$ phase produced under A_4 transformations. These $U(1)$ phases are different 1D irreducible representations (irreps) of A_4 and correspond to

distinct SPT phases protected by translation and on-site symmetries. In phase **E**, the ground state breaks the symmetry to on-site $\mathbb{Z}_2$ and parity. The translation symmetry in this region is broken down from single-site translation invariance to two-site. This broken, two-site translation symmetry is also present in regions **F** and **G**, but here the remaining symmetries of A_4 and parity are completely preserved. Like regions **B**, **C**, and **D**, regions **F** and **G** have the same symmetry but are distinguished from one another only by the values of their SPT parameters. Finally, in region **H**, the residual symmetry group has an internal $\mathbb{Z}_2 \times \mathbb{Z}_2$ symmetry and parity along with an one-site translation invariance.

Among these eight phases, five correspond to instances of SSB and the remaining three correspond to SPT phases without symmetry breaking. The complete set of such parameters classifying these phases will be described in section 2.3, and the particular values which distinguish them from one another are presented in section 2.4.

Because the phases **B**, **C**, and **D** are not distinguished by any symmetry-breaking criteria (and because none of them are topologically trivial), the boundary lines between them are of particular interest as examples of non-trivial SPT to non-trivial SPT phase transitions. Such transitions are considered uncommon as compared to the more typical case of a transition between SPT and symmetry breaking phases, or trivial to non-trivial SPT phase transitions and have recently attracted particular interest [61–64]. Our analysis, however, shows that this model contains direct nontrivial SPT to SPT transitions, and that the transition is second-order in nature. By directly calculating the ground-state energy and its derivatives, we see sharp divergences in the second derivative, but a continuous first derivative across the boundary between these phases. Representative behavior is shown in Fig. 2.2.

The numerical methods employed here also allows us to probe the central charge of the conformal field theory (CFT) associated with the continuous phase transitions. As one approaches the transition, the correlation length begins to diverge. The central charge of the CFT appears in an important scaling relation between this diverging correlation length and the mid-bond entanglement entropy [65, 66]. In particular, it has been shown that

$$S = \frac{c}{6} \log \xi \tag{2.4}$$

where c is the central charge, and ξ is the correlation length measured in units of lattice spacing. S is the entanglement entropy, given by performing a Schmidt decomposition between sites and computing the entropy of the

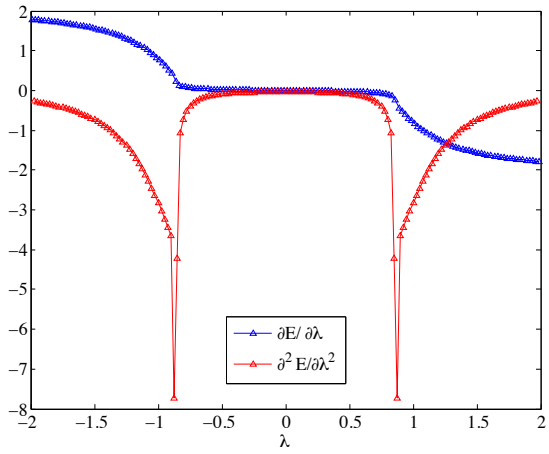

Figure 2.2: Ground state energy derivatives along the line $\mu = 2$ in the phase diagram above show the nature of the phase transitions. The continuous first derivative (blue) contrasts with divergence in the second derivative (red), showing a second-order transition. All three regions are topologically nontrivial SPT phases. Data shown here was computed with a bond dimension of 30, and the behavior has been seen to be stable as the bond dimension increases.

resulting Schmidt coefficients λ_i,

$$S = -\sum_i \lambda_i \log \lambda_i. \tag{2.5}$$

The MPS algorithms employed here to determine the ground state are not well-suited at the actual critical points. This is because the numerical accuracy of these algorithms is controlled by a tunable numerical parameter, the so called "bond dimension." The closer we approach the critical point, the bigger this parameter needs be chosen for the ground states to be computed faithfully. By gradually increasing the bond dimension near the critical point, we obtain states with increasingly large correlation length, allowing us to fit the scaling relation of Eq. 2.4. We can also use this data to estimate the location of the transition, because away from the critical point, the scaling relation will not hold, and S will saturate for large enough ξ (or in practice, for large enough bond dimension). We find the critical lines to be located at $\lambda = \pm 0.865(2)$; fits at multiple points along these lines suggest a central charge of $c = 1.35(1)$, as shown for example in Fig. 2.3.

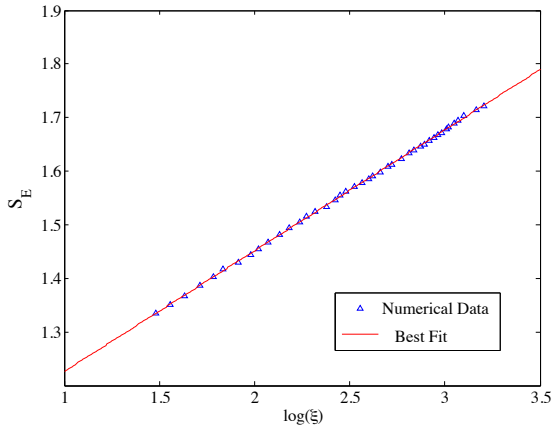

Figure 2.3: Entanglement entropy versus the log of the correlation length for states very close to the transition point. The slope is directly proportional to the central charge of the associated CFT, via Eq. 2.4. Data is generated by computing ground states at the point $\mu = 2, \lambda = 0.865$, and increasing the "bond dimension" of the numerical scheme to allow us to find states closer to the critical point where the correlation length diverges. The behavior shown here is representative of that seen elsewhere along the lines $\lambda = \pm 0.865$. Away from these lines, the entanglement entropy saturates at a finite value of ξ. The best-fit line has a slope of 0.225(1), which corresponds to a central charge of 1.35(1).

2.3 Review of classification of 1D gapped phases of spin chains

We now review the classification of 1D gapped phases of spin chains following [52]. Given the group of global symmetries G, the classification gives us a set of labels whose values distinguishes all possible phases of matter that can exist. We will systematically list these labels for various types of symmetries. It is the value of these labels that we extract numerically to determine the phase diagram presented in Sec 2.2. First, we must give a brief introduction to *matrix product state* (MPS) representations of one dimensional wavefunctions [67], which forms the backbone of the classification scheme.

2.3.1 MPS formalism

Consider a one-dimensional chain of N spins. If each spin is of d-levels *i.e.* the Hilbert space of each spin is d-dimensional, the Hilbert space of the

spin chain itself is d^N-dimensional. A generic state vector in this many body Hilbert space is of the form

$$|\psi\rangle = \sum_{i_1=1}^{d} \dots \sum_{i_N=1}^{d} c_{i_1 \dots i_N} |i_1 \dots i_n\rangle \tag{2.6}$$

This means that the number of coefficients $c_{i_1 \dots i_N}$ needed to describe such a wavefunction grows exponentially with the length of the chain. To write this wavefunction in the MPS form, we need to associate for every spin site (labeled by $m = 1 \dots N$), a $D_m \times D_{m+1}$-dimensional matrix $A_m^{i_m}$ for each basis state $|i_m\rangle = |1\rangle \dots |d\rangle$ such that (assuming periodic boundary conditions without any loss of generality here and henceforth)

$$c_{i_1 \dots i_N} = Tr[A_1^{i_1} A_2^{i_2} \dots A_N^{i_N}]. \tag{2.7}$$

The matrices $A_m^{i_m}$ (which we will call MPS matrices) can, in principle always be obtained via sequential singular value decompositions of the coefficients $c_{i_1 \dots i_N}$, as described in [68]. In practice, it is useful to employ the canonical form of the MPS [67, 68]. For most of the chapter, the term "MPS" shall refer to wavefunctions written in the form

$$|\psi\rangle = \sum_{i_1 \dots i_N} Tr[A_1^{i_1} A_2^{i_2} \dots A_N^{i_N}] |i_1 \dots i_N\rangle. \tag{2.8}$$

Two important features of the MPS representation bear relevance to the numerical methods employed in this chapter. The first is $D = \max_m(D_m)$, called the 'virtual' or 'bond' dimension, which in general may need to be very large. However, if the wavefunction is the ground-state of a gapped Hamiltonian and hence has a finite correlation length, it can be efficiently written as an MPS wavefunction whose bond dimension approaches a constant value that is independent of the size of the chain [68–70]. And as one approaches a critical point, where the correlation length diverges, an increasingly large bond dimension is required to faithfully capture the ground states. Even though the ground states at criticality therefore cannot be accurately represented by an MPS, one can employ the scaling results discussed above and in Fig. 2.3, where increasingly large correlation lengths are probed by gradually increasing the bond dimension.

Secondly, note that when a state possesses translation invariance, the MPS matrices themselves may be chosen to respect the same symmetry. A state invariant under one-site translations, for example, can be represented in the form above with the same MPS tensor at each site, $A_m^{i_m} = A^{i_m}$. This, in turn,

allows a state with translation invariance of any length to be represented by d matrices where d is the dimension of the local Hilbert space. In general, a state with K-site translation invariance requires Kd MPS matrices to represent it.

2.3.2 Symmetry breaking

First, we consider the possibility that the ground state spontaneously breaks the symmetry, G of a Hamiltonian to H. This is the subgroup $H \subset G$ that still leaves the ground state invariant. This residual symmetry group itself acts as one of the labels to indicate the phase of matter. The case of the ground state not breaking any symmetry itself corresponds to $H = G$. However there may exist different SPT phases where the ground state is invariant under the same H. In such a case, we would need more labels along with H to label the phase of matter. These labels depend on what H itself is and will be reviewed next.

We now consider the action of global symmetries on the physical spins and how it translates to the action on the MPS matrices on the virtual level. It was observed that the representation of the symmetry on the virtual level falls into distinct equivalence classes and these classes correspond to the different SPT phases of matter 'protected' by the corresponding symmetry [47, 52–55]. Here, we review the action of various symmetries on the MPS matrices, the different equivalence classes and the labels which distinguish them. The discussions here follow Ref [52].

2.3.3 Onsite/internal symmetry

Let us now consider Hamiltonians that are invariant under the action of a certain symmetry group G_{int} on each spin according to some unitary representation $u(g)$ *i.e.* $[H, U(g)] = 0$ where $U(g) = u_1(g) \otimes \cdots \otimes u_N(g)$. If the ground state $|\psi\rangle$ does not break the symmetry of the Hamiltonian, it is left invariant under the transformation $U(g)$ up to a complex phase

$$U(g)|\psi\rangle = \chi(g)^N |\psi\rangle. \tag{2.9}$$

Eq. (2.9) can be imposed as a condition on the MPS matrix level as [51–54]

$$u(g)_{ij} A^j_M = \chi(g) V^{-1}(g) A^i_M V(g). \tag{2.10}$$

Note that we use the Einstein summation convention wherein repeated indices are summed over. Because u is a group representation, group properties constrain χ to be a 1D representation and V generally to be a *projective rep-*

resentation of G_{int}. A projective representation respects group multiplication up to an overall complex phase.

$$V(g_1)V(g_2) = \omega(g_1, g_2)V(g_1g_2). \tag{2.11}$$

The complex phases $\omega(g_1, g_2)$ are constrained by associativity of group action and fall into classes labeled by the elements of the second cohomology group of G_{int} over $U(1)$ phases $H^2(G_{int}, U(1))$. In other words, *the different elements of $H^2(G_{int}, U(1))$ label different classes of projective representations and hence different SPT phases of matter*. In particular, the identity element of the group $H^2(G_{int}, U(1))$ labels the set of *linear representations* of G_{int} (which respect group multiplication exactly) and the corresponding phase of matter is trivial, containing or adiabatically connected to product ground states.

2.3.4 Lattice translation

Note that we assume an infinite system with periodic boundary conditions for our discussions.

Without on-site symmetry

The group of lattice translations $\mathcal{L}_\mathcal{T}$ is generated by single site shift $\mathcal{S}$ which acts as follows

$$\mathcal{S} : \sum_{i_1 \ldots i_N} c_{i_1 \ldots i_N} |i_1 \ldots i_N\rangle \to \sum_{i_1 \ldots i_N} c_{i_1 \ldots i_N} |i_2, \ldots i_N, i_1\rangle = \sum_{i_1 \ldots i_N} c_{i_N i_1 \ldots i_{N-1}} |i_1 \ldots i_N\rangle. \tag{2.12}$$

In other words,

$$\mathcal{S} : c_{i_1 \ldots i_N} \quad \to \quad c_{i_N i_1 \ldots i_{N-1}} \tag{2.13}$$

$$\mathcal{S} : Tr[A_1^{i_1} \ldots A_N^{i_N}] \quad \to \quad Tr[A_2^{i_1} \ldots A_N^{i_{N-1}} A_1^{i_N}] \tag{2.14}$$

On the MPS matrix level, the single site shift acts as:

$$\mathcal{S} : A_M^i \to A_{M+1}^i. \tag{2.15}$$

The full group, $\mathcal{L}_\mathcal{T}$ generated by $\mathcal{S}$ is

$$\mathcal{L}_\mathcal{T} \quad = \quad \langle \mathcal{S} \rangle = \{e, \mathcal{S}^{\pm 1}, \mathcal{S}^{\pm 2}, \mathcal{S}^{\pm 3} \ldots\}, \tag{2.16}$$

$$S^k \quad : \quad A_M^i \to A_{M+k}^i, \quad k \in \mathbb{Z}. \tag{2.17}$$

For a finite chain with periodic boundary conditions, we have the constraint $\mathcal{S}^N = e$ and hence $\mathcal{L}_\mathcal{T} \cong \mathbb{Z}_N$. For an infinite chain, $\mathcal{L}_\mathcal{T} \cong \mathbb{Z}$. It was shown [52] that *there is only 1 SPT phase protected by $\mathcal{L}_\mathcal{T}$ alone.*

If lattice translation is a symmetry, we can choose

$$A^i_M = A^i_{M'} = A^i \ \ \forall\ M, M' \in \{1, \ldots, N\}, \tag{2.18}$$

that is, the MPS matrices can be chosen to be independent of the site label and the same for all sites.

With on-site symmetry

If lattice translation is a symmetry in addition to on-site symmetry defined by a group G_{int} as described in Sec (2.3.3), the different 1D irreducible representations (irreps) χ that can appear in Eq (2.10) also label different phases of matter. *The different SPT phases protected by $G = G_{int} \times \mathcal{L}_\mathcal{T}$ are labeled by $\{\omega, \chi\}$*

2.3.5 Parity

Without on-site symmetry

The action of inversion or parity, $\mathcal{P}$ in general is generated by a combination of an on-site action by some unitary operator w and a reflection, $\mathcal{I}$ that exchanges lattice sites about a point.

$$\mathcal{P} = w_1 \otimes w_2 \cdots \otimes w_N\ \mathcal{I} \tag{2.19}$$

where, the action of $\mathcal{I}$ is as follows:

$$\mathcal{I} : \sum_{i_1 \ldots i_N} c_{i_1 \ldots i_N} |i_1 \ldots i_N\rangle \to \sum_{i_1 \ldots i_N} c_{i_1 \ldots i_N} |i_N i_{N-1} \ldots i_1\rangle = \sum_{i_1 \ldots i_N} c_{i_N \ldots i_1} |i_1 \ldots i_N\rangle. \tag{2.20}$$

In other words,

$$\begin{aligned} \mathcal{I} : c_{i_1 \ldots i_N} &\to c_{i_N \ldots i_1}, \\ \mathcal{I} : Tr[A^{i_1}_1 A^{i_2}_2 \ldots A^{i_N}_N] &\to Tr[A^{i_N}_1 A^{i_{N-1}}_2 \ldots A^{i_1}_N] \\ &= Tr[(A^{i_1}_N)^T (A^{i_2}_{N-1})^T \ldots (A^{i_N}_1)^T]. \end{aligned}$$

In the last equation, we have used the fact that the trace of a matrix is invariant under transposition. On the MPS matrix level, the action is

$$\mathcal{I} : A^i_M \to (A^i_{N-M+1})^T \tag{2.21}$$

The full action of parity is

$$\begin{aligned} \mathcal{P} : c_{i_1 \ldots i_N} &\to w_{i_1 j_1} \ldots w_{i_N j_N} c_{j_N \ldots j_1}, \\ \mathcal{P} : A^i_M &\to w_{ij} (A^j_{N-M+1})^T \end{aligned} \tag{2.22}$$

Since $\mathcal{P}^2 = e$, w is some representation of $\mathbb{Z}_2$. There is a special lattice site that has been chosen as the origin about which we invert the lattice. It is sensible for parity to be defined without any reference to such a special point. Hence we assume that any system invariant under parity also has lattice translation invariance which allows any site to be chosen as the origin. Note that the action of inversion $\mathcal{I}$ and the generator of translations $\mathcal{S}$ do not commute. They are related by

$$\mathcal{I}\mathcal{S}\mathcal{I} = \mathcal{S}^{-1} \tag{2.23}$$

The full symmetry group including translation invariance and parity, which we will call $G_\mathcal{P}$, generated by $\mathcal{S}$ and $\mathcal{P}$ is (for a finite chain with periodic boundary conditions)

$$G_\mathcal{P} = \langle \mathcal{P}, \mathcal{S} | \mathcal{P}^2 = \mathcal{S}^N = e, \mathcal{I}\mathcal{S}\mathcal{I} = \mathcal{S}^{-1} \rangle \cong \mathbb{Z}_N \rtimes \mathbb{Z}_2 \cong D_N. \tag{2.24}$$

For an infinite chain which we are interested in, we have

$$G_\mathcal{P} = \langle \mathcal{P}, \mathcal{S} | \mathcal{P}^2 = e, \mathcal{I}\mathcal{S}\mathcal{I} = \mathcal{S}^{-1} \rangle \cong \mathbb{Z} \rtimes \mathbb{Z}_2 \cong D_\infty. \tag{2.25}$$

If $G_\mathcal{P}$ is a symmetry of the Hamiltonian which is not broken by the ground state wavefunction $|\psi\rangle$, we have, under the action of $\mathcal{P}$,

$$\mathcal{P}|\psi\rangle = \alpha(P)^N |\psi\rangle. \tag{2.26}$$

The condition Eq. (2.26) can also be imposed on the level of the MPS matrices that describe $|\psi\rangle$:

$$w_{ij} (A^j)^T = \alpha(P) N^{-1} A^i N, \tag{2.27}$$

where, $\alpha(P) = \pm 1$ labels even and odd parity and N has the property $N^T = \beta(P)N = \pm N$. $\{\alpha(P), \beta(P)\}$ *label the 4 distinct SPT phases protected by* $G_\mathcal{P}$ [52].

With on-site symmetry

Let us consider invariance under the combination of an on-site symmetry G_{int} as described in Sec(2.3.3) with parity. If the actions of the two symmetry transformations commute on the physical level,

$$U(g)\mathcal{P}|\psi\rangle = \mathcal{P}U(g)|\psi\rangle, \tag{2.28}$$

i.e. $G = G_{int} \times G_{\mathcal{P}}$, this imposes constraints on the matrix N defined in Sec. 2.3.5 as [52].

$$N^{-1}V(g)N = \gamma_P(g)V^*(g). \tag{2.29}$$

Where, $\gamma_P(g)$ is a one-dimensional irrep of G_{int} that arises from the commutation of on-site and parity transformations [52] and $V(g)$ is the representation of G_{int} acting on the virtual space as discussed in Sec 2.3.3. Note that we can rephase $V(g) \mapsto \alpha(g)V(g)$ without changing anything at the physical level. However, Eq (2.29) is modified replacing $\gamma_P(g) \mapsto \gamma_P(g)/\alpha^2(g)$. Hence, the 1D irreps γ_P and γ_P/α^2 are equivalent labels for the same phase for all the 1D irreps α of G_{int}. *Different SPT phases of matter protected by* $G = G_{int} \times G_{\mathcal{P}}$ *are labeled by* $\{\omega, \chi(g), \alpha(P), \beta(P), \gamma_P(g)\}$ [52]. Where, as defined before $\omega \in H^2(G_{int}, U(1))$ with $\omega^2 = e$ and $\gamma_P \in \mathcal{G}/\mathcal{G}^2$ where $\mathcal{G}$ is the set of 1D representations of G_{int}.

The techniques used in this chapter can be extended easily to include time-reversal invariance. But, because our Hamiltoinian is not invariant under time reversal, we do not review the classification of SPT phases protected by time-reversal invariance and combinations with other symmetries here. We include the same in the Appendix (A.2.1) for the sake of completeness.

2.4 Using the parameters to understand the phases of the A_4 Hamiltonian

2.4.1 Details of the phase diagram

Armed with the family of parameters described in the last section, $\{\omega, \chi, \alpha, \beta, \gamma_P\}$, we now describe in detail the different phases of the Hamiltonian of Eq (2.3) seen in Fig. 2.1. The internal symmetry is A_4 which is a group of order 12 and can be enumerated by two generators with the presentation

$$A_4 : \langle a, x | a^3 = x^2 = (ax)^3 = e \rangle. \tag{2.30}$$

The 3D representation of these generators are

$$a = \begin{pmatrix} 0 & 1 & 0 \\ 0 & 0 & 1 \\ 1 & 0 & 0 \end{pmatrix}, \; x = \begin{pmatrix} 1 & 0 & 0 \\ 0 & -1 & 0 \\ 0 & 0 & -1 \end{pmatrix} \tag{2.31}$$

First we briefly outline the steps followed to numerically determine the phase diagram:

1. For every point in parameter space $\mu = [-3, 4]$, $\lambda = [-2, 2]$ of the Hamiltonian of Eq (2.3), we use the iTEBD algorithm [60] to compute the ground state.

2. We determine the residual symmetry $H \subset G$ of the full symmetry group $G = A_4 \times G_{\mathcal{P}}$ that leaves the ground state invariant. This includes checking the level of translation invariance, which may be broken down from one-site to two-site or beyond.

3. We determine the the labels (subset of $\{\omega, \chi(g)\alpha(P), \beta(P), \gamma_P(g)\}$) that characterizes the fractionalization of residual symmetry and measure their values using the appropriate MPS order parameters.

Several of these steps involve important numerical considerations. Full details of our implementation of these steps can be found in Sec 2.5.

We find that there are eight different phases in total. These phases, labeled "**A**" through "**H**" as indicated to match the phase diagram in Fig. 2.1, are characterized as follows:

1. Phase **A:** Parity and one-site translation only *i.e.* $H = G_{\mathcal{P}}$ (all internal symmetries are broken). This region is therefore classified by the values of $\{\alpha(P), \beta(P)\}$ and is found to have values

   - $\{\alpha(P) = -1, \beta(P) = -1\}$

2. **Phases B, C, and D:** No unbroken symmetries. The ground state in these three regions are invariant under the full symmetry group $G = A_4 \times G_{\mathcal{P}}$. The relevant labels are $\{\omega, \chi(g), \alpha(P), \beta(P)\}$ (Since all three 1D irreps of A_4 are equivalent under the relation $\gamma_P \sim \gamma_P/\chi^2$, $\gamma_P(g)$ is a trivial parameter). The MPS matrices in all three regions transform projectively *i.e.* these are non-trivial SPT phases with $\omega = -1$ where $H^2(A_4, U(1)) \cong \mathbb{Z}_2 \cong \{1, -1\}$. Also, $\alpha(P) = -1, \beta(P) = -1$ for all three phases. However, they can be distinguished by the values of χ, *i.e.* observing that the 1D irrep produced under the A_4 symmetry

transformation (Eq (2.9)) in the three regions corresponds to the three different 1D irreps of A_4 . The values of the set of parameters which characterize the regions are as follows.

- Phase **B**: $\{\omega = -1, \chi : \{a = e^{\frac{i2\pi}{3}}, x = 1\}, \alpha = -1, \beta = -1\}$
- Phase **C**: $\{\omega = -1, \chi : \{a = 1, x = 1\}, \alpha = -1, \beta = -1\}$
- Phase **D**: $\{\omega = -1, \chi : \{a = e^{-\frac{i2\pi}{3}}, x = 1\}, \alpha = -1, \beta = -1\}$

3. **Phase E:** Parity, $\mathbb{Z}_2$ and two-site translation. This region possess a hybrid parity $G_{\mathcal{P}}$, generated not by inversion alone but rather the combination of inversion and the order 2 element axa^2 of A_4. Additionally, there is an unbroken on-site $\mathbb{Z}_2$ actions with elements $\{e, x\}$. The relevant labels are $\{\chi(g), \alpha(P), \beta(P), \gamma_P(g)\}$ with values

   - $\{\chi : \{e = 1, x = 1\}, \alpha = 1, \beta = 1, \gamma_P = \{e = 1, x = 1\}\}$

4. **Phases F and G:** These regions possess the same parity and on-site A_4 symmetry as phases **B**, **C**, and **D**, but have translation invariance which is broken down to the two-site level. They are also distinct from the above phases because the MPS matrices transform under a linear representaion of A_4, and have a trivial representation of parity at the two site level. The relevant labels are parameters are $\{\omega, \chi(g), \alpha(P), \beta(P)\}$ with values

   - Phase **F**: $\{\omega = +1, \chi : \{a = e^{-\frac{i2\pi}{3}}, x = 1\}, \alpha = +1, \beta = +1\}$
   - Phase **G**: $\{\omega = +1, \chi : \{a = e^{+\frac{i2\pi}{3}}, x = 1\}, \alpha = +1, \beta = +1\}$

5. **Phase H:** In this final region, the on-site symmetry is broken down to a $\mathbb{Z}_2 \times \mathbb{Z}_2$ subgroup with elements $\{e, x, a^2xa, axa^2\}$. Parity and translation symmetry are both fully retained. It is therefore the only region in our sample phase diagram which requires all five labels $\{\omega, \chi, \alpha, \beta, \gamma_P\}$ to characterize. The values here are

   - $\{\omega = +1, \chi = \{1, -1, 1, -1\}, \alpha = +1, \beta = +1, \gamma_P = \{1, 1, 1, 1\}\}$

Note here that for compactness, the set of values given χ and γ refer to the four elements $\{e, x, a^2xa, axa^2\}$, respectively.

The diversity of phases seen in this phase diagram show the importance of carefully checking for both conventional symmetry-breaking phases and SPT phases. The phases present here also underscore the importance of considering the different possible instances of parity and translation invariance which can occur, since in addition to traditional one-site translation invariance and

inversion, one might find e.g. translation breaking without inversion breaking (phases **F** and **G**), or inversion which only exists when hybridized with an on-site symmetry (phase **E**).

2.5 Details of numerical extraction of phase diagram

For gapped 1D spin chains, the authors of Ref. [46, 54, 71] describe ways of numerically determining the SPT parameters and distinguishing different SPT orders. We build on the technique developed in Ref. [54] where the authors obtain the SPT labels using the representations of symmetry at the virtual level. The numerical characterization of the phase diagram of a general parametrized Hamiltonian $H(\lambda, \mu, \ldots)$ proceeds according to the following steps:

1. Identify the group of symmetries, G of the Hamiltonian.
2. For each point in parameter space $\{\lambda, \mu, \ldots\}$, obtain the ground state $|\psi(\lambda, \mu, \ldots)\rangle$ of the Hamiltonian $H(\lambda, \mu, \ldots)$ numerically as a MPS.
3. For each point in parameter space $\{\lambda, \mu, \ldots\}$, identify the subgroup of symmetries $H \subset G$ that leaves the ground state $|\psi(\lambda, \mu, \ldots)\rangle$ invariant.
4. Obtain the relevant virtual representations for the elements of the subgroup H, *i.e.* $\{\chi, V, \alpha(P), N\}$.
5. From the representations and their commutation relations, obtain all other labels that completely characterize the phase.

In general, this process results in calculating the full family $\{\chi, \omega, \alpha(P), \beta(P), \gamma(P)\}$ for each point in parameter space. However, in some cases, the elements of H are such that not all such parameters are necessary or even well-defined. For example, if the subgroup H does not contain the parity operator, then $\alpha(P), \beta(P)$ and $\gamma(P)$ do not exist. Similarly, if $H = \mathbb{Z}_3$, there is only one possible value of ω, and hence we do not need it to distinguish the phase.

2.5.1 Ground state preparation

Having constructed our Hamiltonian with an explicit symmetry group $G = A_4 \times \mathcal{P}$, the next step is to obtain the ground states. For this, we use the numerical "iTEBD" algorithm [60, 72, 73] to compute the ground states over a range of parameters, $\lambda \in [-2, 2]$ and $\mu \in [-3, 4]$ (this range is simply chosen

based on our results to include a large but not necessarily comprehensive sample of different SPT phases). The algorithm computes the ground state of a Hamiltonian H through the imaginary time evolution of an arbitrary initial state $|\psi\rangle$, since $|\psi\rangle$ can be expanded in the energy eigenbasis of Hamiltonian as $|\psi\rangle = \sum_i c_i |E_i\rangle$ and hence $e^{-\tau H}|\psi\rangle$ will suppress all such components except for the ground state $|E_0\rangle$ in the large-τ limit. Except where otherwise noted, data in this chapter were prepared with a random initial state represented as an MPS with bond dimension $\chi = 24$, and evolved according to a fixed sequence of timesteps which were chosen to be sufficient to converge the energy to the level of 10^{-8} at the most numerically "difficult" states. Within each phase, a random set of points have also been recomputed using states with a series of larger bond dimensions ($\chi = 36, 42$, and 60) and a longer sequence of imaginary timesteps, in order to verify that the observed characteristics are not numerical artifacts.

While the numerical details of the iTEBD algorithm have been extensively documented elsewhere, there is one salient point which must be remarked upon. For a Hamiltonian H with two-body interactions, the algorithm relies on a decomposition of the Hamiltonian into two sets of terms– those acting first on an even-numbered site (H_A) and those acting first on an odd-numbered site (H_B), so that $H = H_A + H_B$. As such the imaginary time evolution operator can be approximated by the Suzuki-Trotter decomposition [74, 75], which, to second order, gives

$$e^{-\tau H} \approx (e^{-\delta\tau H_A/2} e^{-\delta\tau H_B} e^{-\delta\tau H_A/2})^N, \tag{2.32}$$

with $\delta\tau = \tau/N$. The total operator can then be applied as a sequence of smaller operators, acting either on an even site first, or an odd site first. This distinction, then, requires the state to be represented with at least two sets of MPS matrices, A_A^j and A_B^j, even if the the resulting state is expected to possess a one-site translation invariance (which would generally allow it to be represented by only a single tensor A^j. This fact will have relevance in later sections, when the translational invariance of the MPS is explicitly discussed).

For now, however, let us simplify the discussion by considering a translationally invariant, infinite ground state, represented by the tensor A^j. Note that there is some gauge freedom allowed in the representation of an infinite MPS state–the tensors A^j and XAX^{-1} both represent the same one-site translationally invariant state, for example. This freedom allows us to make some choices about the structure of the representation which will prove useful in subsequent calculations. In particular, we can choose our MPS to be represented in the so-called "canonical form" [67, 73], in which the state satisfies the property,

$$A^j_{\alpha,\beta}(A^*)^j_{\alpha',\beta'}\delta^{\beta,\beta'} = \delta_{\alpha,\alpha'} \tag{2.33}$$

This condition can also be thought of in terms of the state's *transfer matrix* (see Fig. 2.4)– a common construction used in MPS formalism to compute things like expectation values:

$$T^{(\alpha\alpha')}_{(\beta\beta')} \equiv A^j_{\alpha,\beta}(A^*)^j_{\alpha',\beta'}. \tag{2.34}$$

Now consider the dominant eigenvector of T, which will be some vector $X_{(\beta,\beta')}$. Because the outgoing indices of T are a composite of smaller indices (β, β'), any eigenvector of this matrix can also be thought of as a (smaller) matrix in its own right, by interpreting $X_{(\beta,\beta')}$ as $X^{\beta}_{\beta'}$. The original vector $X_{(\beta,\beta')}$ is called the *vectorization* of the matrix $X^{\beta}_{\beta'}$. Now, the condition for canonical form can be rephrased as the requirement that the dominant eigenvector of the state's transfer matrix is a vectorization of the identity matrix, i.e.

$$(T)^{(\alpha\alpha')}_{(\beta\beta')}\delta^{(\beta\beta')} = \delta^{(\alpha\alpha')} \tag{2.35}$$

This property of a transfer matrix in canonical form (graphically depicted in Fig. 2.4) will be quite useful in subsequent calculations.

Because it represents a contraction of the physical indices of the tensors A^j, the transfer matrix can be thought of as containing the overlap of the state with itself at a single site. In other words, in an N-site periodic state with one-site translation invariance, the norm square of the state is given by taking a product of N transfer matrices (one for each site) and then tracing over them.

$$\langle\psi|\psi\rangle = Tr[T^N] \tag{2.36}$$

This fact in turn produces a relationship between the eigenvalues λ_j of the transfer matrix, and the norm of the state. Consider for example an infinite-length, translation-invariant state with unique largest eigenvalue λ_1, whose norm is given by $\lim_{N\to\infty} Tr[T^N] = \sum_j \lambda_j^N \approx \lambda_1^N$. This state is normalized if $|\lambda_1| = 1$. Hence in practice, computing the largest eigenvalue of the transfer matrix gives us a convenient way to ensure normalization.

A general iMPS computed via iTEBD will not necessarily be in exactly canonical form. In [73], Orus and Vidal have given an analytical prescription for placing an arbitrary iMPS in canonical form which could be used in principle. However, because this form is ultimately so useful, it is worthwhile to enforce it for the ground state representations at the time of their initialization. Successive Schmidt decompositions of a state after the application of unitary operators is equivalent to enforcing canonical form. Of course, when one com-

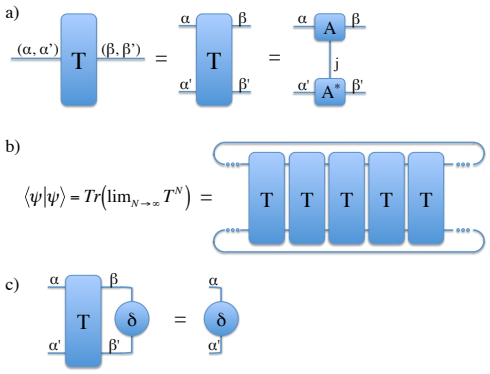

Figure 2.4: The transfer matrix of a translationally-invariant matrix product state, demonstrated in graphical tensor notation. In (a), the construction of the transfer matrix is shown as a contraction of two MPS matrices, with the virtual indices grouped to form a single matrix. In (b), the relationship between the transfer matrix and the norm square of the state is shown. Finally, in (c) we show graphically the behavior of a matrix product state in canonical form: such a state has a transfer matrix whose dominant eigenvector is a vectorized version of the identity matrix.

putes a ground state using imaginary time evolution, the operators which are used, of the form $e^{-\delta\tau H}$ (see Eq. 2.32), are not in general unitary. But for $\delta\tau$ very small, they will be quite close. Since a typical iTEBD algorithm ends with a sequence of very small time step evolutions, the resulting states are also typically "close" to canonical form [76]. To take this to its logical extension, it is a good practice to terminate every iTEBD algorithm with e.g. 100 steps of evolution in which we apply only the identity gate (which corresponds to the exact $\delta\tau = 0$ limit). Of course, this identity gate evolution is both explicitly unitary and incapable of changing the underlying state. In this way, one can ensure that the states computed via iTEBD algorithm are exactly in canonical form (up to numerical precision). To summarize, we have described how we obtain a ground state in MPS form in a canonical representation.

2.5.2 Symmetry detection and extraction of order parameters

States with one-site translation invariant representations

The general numerical scheme for extracting the topological order parameters from a numerical MPS was presented in [54], where it was principally used to study a specific class of SPT phases. We generalize their construction. We consider the situation first for on-site symmetries and assume that the infinite state possesses one-site translation invariance and is represented by a tensors A_j. The generalization to other symmetries and to different levels of translation invariance will be considered subsequently.

To check for symmetry and ultimately access the topological parameters, one first defines a "generalized" transfer matrix T_u, which extends the definition in Eq. 2.34 to include the action of some on-site operator u between the physical indices, i.e.

$$T_u \equiv A^j u_{j,j'} (A^*)^{j'}, \tag{2.37}$$

where, this time, we have suppressed the external indices of the matrix (See Fig. 2.5 for a graphical depiction). In the same manner that the original transfer matrix T represents the contribution of one site to the overlap $\langle\psi|\psi\rangle$, in this case the generalized transfer matrix T_u represents the contribution of one site to the expectation value $\langle\psi|U|\psi\rangle$, where $U = \bigotimes_j u_j$ represents the application of u to every site on the chain (see Fig. 2.5). And just as an iMPS is not normalized unless T has largest eigenvalue 1, so too is such state only symmetric under U if T_u has largest eigenvalue with unit modulus.

To study the SPT classification of a state, we thus begin by determining the symmetry. To check if the state is symmetric under the application of U, then we first construct T_u and compute the dominant eigenvector X and the associated eigenvalue λ_1. Note that, when the dimensions of T_u is large, it is numerically far easier to use some iterative procedure such as a power or Lanczos algorithm [77–79] to extract this, since only the largest eigenvalue is required and not the entire spectrum. If $|\lambda_1| < 1$, the state is not symmetric under U because $\langle\psi|U|\psi\rangle = lim_{N\to\infty} T(u)^N$ will vanish. If, however, the unique largest eigenvalue gives $|\lambda_1| = 1$, then we can proceed with the analysis.

Consider now a normalized iMPS in canonical form, which is invariant under a set of symmetries $u(g)$ at each site for g in some symmetry group $H \in G$. As per eq. 2.10 above, this invariance implies the existence of a set of matrices $V(g)$, which are generally projective representations, and $\chi(g)$, a one-dimensional representation. As shown in [54], one can extract both the projective and a 1-dimensional representation parameters directly from the dominant eigenvector and eigenvalue of the generalized transfer matrix. In

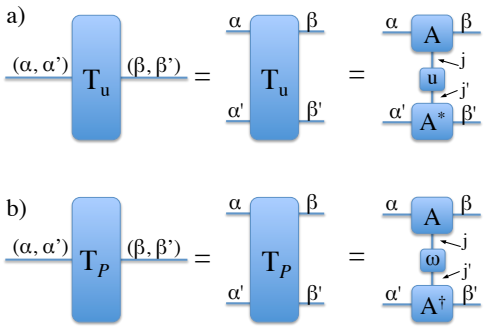

Figure 2.5: The notion of the transfer matrix can be generalized to include (a) on-site operation $U = \bigotimes_j u_j$, or (b) a parity operation $\mathcal{P}_\omega$. Generalizations to other symmetries are possible, but outside the scope of this work as they are not present in our model.

particular, if X is the dominant eigenvector (or more precisely, if $X^{\beta}_{\beta'}$ is a matrix and it's vectorization $X_{(\beta\beta')}$ is the dominant eigenvector), then $V = X^{-1}$. The one-dimensional rep $\chi(g)$ is simply equal to the dominant eigenvalue itself. In other words,

$$(T_u)^{(\alpha\alpha')}_{(\beta\beta')}(V^{-1})^{(\beta\beta')} = \chi \cdot (V^{-1})^{(\alpha\alpha')} \tag{2.38}$$

To see this, consider the left hand side of the equation (In many ways, this line of argument is clarified when represented by graphical notation; see also Fig. 2.5.2). Combining the definition of the generalized transfer matrix, Eq. 2.37, with the symmetry fractionalization condition in Eq. 2.10, we have

$$(T_u)^{(\alpha\alpha')}_{(\beta\beta')} = \chi \cdot (V^{-1})^{\alpha\rho} A^j_{\rho\sigma} V^{\sigma\beta} (A^\dagger)^j_{\alpha'\beta'} = \chi \cdot (V^{-1})^{\alpha\rho} T^{(\rho\alpha')}_{(\sigma\beta')} V^{\sigma\beta}. \tag{2.39}$$

When this is inserted in the left hand side of Eq. 2.38, the resulting cancellation of V and V^{-1} gives us

$$(T_u)^{(\alpha\alpha')}_{(\beta\beta')}(V^{-1})_{(\beta\beta')} = \chi \cdot (V^{-1})^{\alpha\rho} T^{(\rho\alpha')}_{(\sigma\beta')} \delta^{\sigma\beta'}. \tag{2.40}$$

Then, relabeling the dummy indices ρ and σ into α and β, we can appeal to the canonical form condition of Eq. 2.35 to see that

$$(T_u)^{(\alpha\alpha')}_{(\beta\beta')}(V^{-1})^{(\beta\beta')} = \chi \cdot (V^{-1})^{\alpha\alpha'}, \tag{2.41}$$

which proves that V^{-1} (vectorized) is an eigenvector with eigenvalue χ. Furthermore, because the state is normalized and because we required as a condition for symmetry that $|\chi| = 1$, this proves that V^{-1} is the dominant eigenvector, up to an overall phase factor in V. Hence, any procedure to numerically extract the dominant eigenvector and largest eigenvalue from the generalized transfer matrix is sufficient to extract both the 1D representation χ and the projective representation required to compute the projective parameters ω as defined above. Above, we have considered only on-site symmetries applied

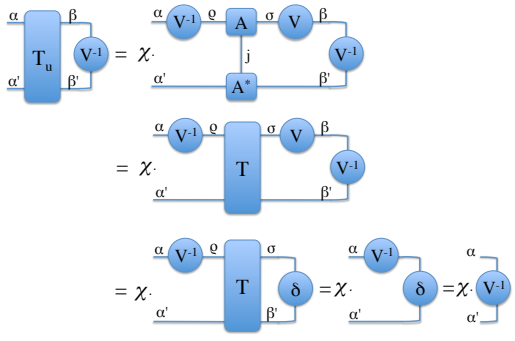

Figure 2.6: The projective representation V of a symmetry can be obtained from a state's generalized transfer matrix because the dominant eigenvector of said matrix will be the vectorization of, V^{-1}, so long as the original state is in canonical form. This relation is demonstrated graphically for the case of an on-site symmetry, but easily generalizes to the parity case.

globally to every site on the state[54]. To include other types of symmetries, one simply generalizes further the notion of the already-generalized transfer matrix. For example, the parity symmetry defined by Eq. 2.19 can be studied by means of the matrix

$$T_{\mathcal{P}} \equiv A^j w_{j,j'} (A^\dagger)^{j'}. \tag{2.42}$$

In comparison to Eq. 2.37, we have simply inserted the action of the inversion operator $\mathcal{I}$ by performing a transpose on the virtual indices of the second MPS tensor. In this way, the resulting generalized transfer matrix still represents a one-site portion of the overlap $\langle\psi|\mathcal{P}|\psi\rangle$. By the same arguments as above, and by analogy between Eq. 2.10 and Eq. 2.27, one can see that the quantities $\alpha(P)$ and N can be extracted from the dominant eigenvector and eigenvalue as before, with the latter used to compute the parity parameter $\beta(P)$ as described above.

States without one-site translationally invariant representations

Thus far, we have also assumed a state with one-site translation invariance. However, even when the ground state being studied *does* possess a one-site translational symmetry, the tensors in the MPS *representation* of this state may not, because the gauge freedom of an MPS is not itself constrained to be translationally invariant. For example, consider a set of translationally-invariant tensors $\{A^1, A^2, A^3 \dots\}$ and the gauge transformation

$$A^j \to \begin{cases} XA^jZ^{-1}, & j \text{ even} \\ \\ ZA^jX^{-1}, & j \text{ odd} \end{cases} \tag{2.43}$$

for X and Z of appropriate dimensions. Such a gauge transformation results in an MPS representation of the state whose tensors at even and odd sites may look dramatically different. But both sets of tensors (before and after the transformation) collectively represent the same translationally invariant state. Cases like this are of particular importance here because, as noted above, the iTEBD method (like other MPS ground-state preparation algorithms) necessarily results in an MPS representation with different tensors at even and odd sites, regardless of the translational symmetry of the physical state.

This feature does not affect our numerical calculation of the SPT order parameters ω and $\beta(P)$, which are obtained as eigenvectors of the generalized transfer matrices, but has important significance for the one-dimensional parameters $\chi, \alpha(P)$, and $\gamma(P)$. Consider, for example, a state which is represented by k sets of tensors $\{A^{j_1} ... A^{j_k}\}$, either because the underlying state has only a k-site translation symmetry, or perhaps simply because our particular numerical representation requires it. The symmetry condition of Eq. 2.10 must still hold on a k-site level; that is, we will have

$$u(g)^I_J A^J = \chi(g)^k V^{-1}(g) A^J V(g), \tag{2.44}$$

where $A^J = A^{j_1}A^{j_2}\cdots A^{j_k}$ is now a tensor representing the entire block of spins which are the unit cell of the translation invariance, and the composite indices I and J are equal to $(i_1 i_2 \cdots i_k)$ and $(j_1 j_2 \cdots j_k)$. Clearly if we now define a k-site generalized transfer matrix,

$$T_u^{(k)} \equiv A^J u_{I,J'} (A^*)^{J'} \tag{2.45}$$

then the arguments from the preceding section show that V^{-1} can still be found as the dominant eigenvector of $T_u^{(k)}$.

The largest eigenvalue, on the other hand, is now equal not to χ, but to χ^k. In the typical case of an iTEBD state, where $k = 2$, this is problematic because for many common symmetry groups, the values of $\chi(g)$ will be ± 1, so a numerical calculation which gives only χ^2 will be unable to distinguish between the different phases. More generally of course, a k-site representation will always leave us unable to distinguish the cases where χ is a k^{th} root of unity.

Of course, if the underlying state has a one-site translation invariance (despite being represented by tensors with only a two-site invariance), one expects that by use of some suitable gauge transformations it should be possible to transform the representation itself back into a translationally-invariant form. Here, we show how this can be done in practice. Suppose we have a translationally-invariant state with, say, a two-site representation $\{A^j, B^{j+1}\}$ and an even number of total spins, such that the state in question is given by either

$$|\psi\rangle = \sum_{j_1 \cdots} Tr[A^{j_1} B^{j_2} A^{j_3} \dots B^{j_N}] |j_1 j_2 \dots j_N\rangle \tag{2.46}$$

$$\text{or } |\psi\rangle = \sum_{j_1 \cdots} Tr[B^{j_1} A^{j_2} B^{j_3} \dots A^{j_N}] |j_1 j_2 \dots j_N\rangle \tag{2.47}$$

To recover a one-site representation, we first construct a new tensor of the form:

$$\tilde{A}^j = \begin{pmatrix} \mathbf{0} & B^j \\ A^j & \mathbf{0} \end{pmatrix}. \tag{2.48}$$

This new tensor in fact describes the same wavefunction $|\psi\rangle$ upto a change in normalization. This can be seen by considering the product:

$$\prod_j \tilde{A}_j = \begin{pmatrix} A^{j_1} B^{j_2} A^{j_3} B^{j_4} \cdots & \mathbf{0} \\ \mathbf{0} & B^{j_1} A^{j_2} B^{j_3} A^{j_4} \cdots \end{pmatrix}. \tag{2.49}$$

If we take $\tilde{A}^j$ to be the tensor specifying a new MPS and compute the coefficients, we will have

$$|\tilde{\psi}\rangle = \sum_{j_1 \cdots} Tr[\tilde{A}^{j_1} \dots \tilde{A}^{j_N}] |j_1 \dots j_N\rangle = \sum_{j_1 \cdots} Tr \left(\prod_j \tilde{A}_j \right) |j_1 \dots j_N\rangle \tag{2.50}$$

and thus, upon substituting Eq. 2.49, we find

$$|\tilde{\psi}\rangle = \sum_{j_1\cdots}(Tr[A^{j_1}B^{j_2}\cdots] + Tr[B^{j_1}A^{j_2}\cdots])|j_1\ldots\rangle = 2|\psi\rangle \tag{2.51}$$

In other words, the state described by the tensor $\tilde{A}^j$ is essentially identical to the state specified by the original tensors $\{A^j, B^{j+1}\}$. The only difference is that the correct product of tensors needed to give the coefficients of the state in Eq. 2.46 will always appear twice, differing only by an irrelevant one-site translation (because the underlying state has a one-site translation invariance to begin with, these two copies of the state are still equivalent).

Because the new tensor $\tilde{A}^j$ now contains two degenerate descriptions of the same state, it can be placed in a block diagonal form by appealing to the procedure given in Ref. [67] for block-diagonalizing an MPS representation (see also Appendix C in [80]). The resulting blocks will each independently represent the state, but with one-site translation invariance.

The procedure, briefly outlined, is as follows: first, one must ensure that the tensor $\tilde{A}^j$ is itself in the canonical form, in the sense that it satisfies Eq. 2.33. To do this, construct the transfer matrix for $\tilde{A}^j$ and compute the dominant eigenvector. This may result in a degenerate manifold of eigenvectors, but by properties of the transfer matrix, at least one of these will be the vectorization of some positive matrix X [81]. Since this X is invertible, we can then take $\tilde{A}^j \to X^{-1/2}\tilde{A}^j X^{1/2}$. By construction this new definition of $\tilde{A}^j$ will satisfy the canonical form.

From this, we once again construct a transfer matrix and compute its dominant eigenvector(s). At least one corresponds to a matrix Z which is not proportional to the identity matrix (up to numerical precision). Furthermore, since the vectorization of $Z^\dagger$ is also an eigenvector of the transfer matrix in canonical form, we can take $Z \to (Z + Z^\dagger)/2$ so that Z is Hermitian (unless $(Z + Z^\dagger)/2$ is itself proportional to the identity, in which case one can always choose instead $Z \to i(Z - Z^\dagger)/2$.) Finally, we compute the largest magnitude eigenvalue z_1 of this new matrix Z, so that we can construct a matrix $W = \mathbb{1} - (1/z_1)Z$ to be a matrix which is manifestly not full rank. Let P be a projector onto the support of W, and $P^\perp$ the projector onto its complement. We can now decompose $\tilde{A}^j$ around theses spaces, as

$$\tilde{A}^j = P\tilde{A}^j P + P^\perp\tilde{A}^j P^\perp + P\tilde{A}^j P^\perp + P^\perp\tilde{A}^j P. \tag{2.52}$$

The reason for the construction of the matrix W from a fixed point now becomes clear, as it has been shown that for such matrix W and its associated projector P, we have $\tilde{A}^j P = P\tilde{A}^j P$ [67]. Consequently, the final term in

Eq. 2.52, which represents one of two off-diagonal blocks in $\tilde{A}^j$, vanishes identically. This, in turn, ensures that the remaining off-diagonal block cannot mix with either of the diagonal blocks in any product $\tilde{A^{j_i}}\tilde{A^{j_{i+1}}}\cdots$. It therefore does not participate in the calculation of the coefficients of the corresponding states, and can be ignored.

The remaining terms, $P\tilde{A}^jP$ and $P^\perp\tilde{A}^jP^\perp$, represent the relevant blocks along the diagonal of the tensor. We remark that in principle, one may need to carry out the above procedure iteratively for each such block ($P\tilde{A}^jP$ and $P^\perp\tilde{A}^jP^\perp$) to see if further block reduction is possible. But in practice, for the two-site iTEBD ansatz, a single iteration should suffice. Then, by construction of $\tilde{A}^j$, each will be an equivalent representation of the same state, and each can represent the state with only a one-site translation invariance. In other words, if we simply treat $P\tilde{A}^jP$ as the tensor representing the state, we can use all the procedures in the preceding section to directly compute the entire family of SPT parameters.

An alternative method for extracting the one-dimensional parameters when their values are k^{th} roots of unity would be to compute the ground state with a version of the iTEBD algorithm designed to act on an n-site unit cell, where n does not divide k. In this case, the dominant eigenvalue of the generalized transfer matrix will be χ^n, from which χ can now be calculated without ambiguity. Such generalized iTEBD algorithms have been employed successfully (see for example [82]), but may be less numerically stable, and cannot be used for a general state unless one is sure that n is commensurate with the underlying translation invariance of the state. Nevertheless, both methods are possible in practice, and we have used both to cross-check one another in the results presented in this chapter.

States with broken translation invariance

Finally, it may also be the case that a state lacks a one-site translationally invariant representation precisely because the ground state is not one-site translationally invariant. When this occurs, one can still compute topological order parameters for on-site symmetries, but only once they and the associated symmetries have been suitably redefined to be consistent with the translational invariance. In other words, if the state has a k-site translation invariance and is represented by the k tensors $\{A^{j_1}A^{j_2}\ldots A^{j_k}\}$, one combines the tensors in the same manner contemplated above, forming a new tensor $A^J = A^{j_1}A^{j_2}\cdots A^{j_k}$ with an enlarged physical index which is given by the composite index $J = (j_1 j_2 \ldots j_k)$. We then also re-interpret the on-site symmetry operation to be $u_J^I = u_{j_1}^{i_1} \otimes u_{j_2}^{i_2} \otimes \ldots u_{j_k}^{i_k}$ under the same convention. Once again, with the tensors merged so they continue to represent an individ-

ual "unit cell" of the state, then the relation of Eq. 2.10 will still hold, and we can compute the projective representations of the symmetry from the dominant eigenvalue of the transfer matrix. Unlike the situation described above, however, where the dominant eigenvalue did not give the one-dimensional representation χ (but rather χ^k), in this case the eigenvalue for the merged cell still gives an order parameter. Indeed, there is no longer a physical meaning to the k^{th} root of the eigenvalue, because one-site translation is no longer a symmetry.

For such states, it is also essential to carefully verify the level of any residual translation symmetry. As discussed above, the traditional iTEBD algorithm assumes a two-site invariant representation of the state; hence, if this algorithm produces a state which appears to have translation symmetry which is broken on the one-site level but present at a two-site level, it cannot be assumed that two-site translation is a symmetry of the true ground state; such symmetry may instead have been forced by the algorithm. In this work, whenever one-site translation symmetry is broken, we recompute the ground state using a version of iTEBD with a larger (say, four-site) unit cell. If the two-site translation invariance is still present after such a test, it can then be safely assumed to be a genuine property of the true ground state, and not a property forced by the numerical ansatz. In general, an algorithm with an k-site ansatz cannot by itself confirm translation invariance at the k-site level.

2.5.3 Obtaining the SPT labels $\{\omega, \beta(P), \gamma(g)\}$

It is clear how the one-dimensional representations χ and $\alpha(P)$ can be used by themselves to label a phase, since each is a single number. Now, however we must discuss how to extract similar numerical labels from the projective representations and other matrices obtained above (V, N, etc). Hence, we must define a procedure to obtain an order parameter from these matrices. A good order parameter that gives us an SPT label has to satisfy the following conditions:

- It should be sensitive to the fractionalization of the symmetry at the virtual level.
- It should be invariant under the allowed gauge transformations of MPS states $V \mapsto XVX^{-1}$, $V \mapsto e^{i\theta}V$ where V is some symmetry acting on the virtual level.

Order parameter to detect $\omega \in H^2(G_{int}, U(1))$

The authors of [54] show that tracing over products of elements of the form $V(g_1)V(g_2)V^\dagger(g_1)V^\dagger(g_2)$ satisfies both the above requirements and also gives us the information to extract the class of ω. We will now consider $G_{int} = A_4$ and its subgroups ($H = \mathbb{Z}_2 \times \mathbb{Z}_2, \mathbb{Z}_2, \mathbb{Z}_3$ and the trivial group) for which $H^2(G_{int}, U(1)) = \mathbb{Z}_2$ ($H = A_4, \mathbb{Z}_2 \times \mathbb{Z}_2$) or the trivial group (everything else). For groups which have $H^2(G_{int}, U(1)) = \mathbb{Z}_2$, we will list order parameters which picks the value ± 1 depending on whether the representation is linear or projective indicating if the SPT phase of matter is trivial or non-trivial. (Note: as defined before, D refers to the bond dimension and $V(g)$ is the representation of on-site symmetry at the virtual level (2.10))

1.
   - $G_{int} = A_4 = \langle a, x | a^3 = x^2 = (ax)^3 = e \rangle$
   - $H^2(A_4, U(1)) = \mathbb{Z}_2$
   - $\omega = \frac{1}{D} Tr\left[(V(a)V(x)V^\dagger(a)V^\dagger(x))^2\right] = \pm 1$
2.
   - $G_{int} = \mathbb{Z}_2 \times \mathbb{Z}_2 = \langle x_1, x_2 | x_1^2 = x_2^2 = (x_1 x_2)^2 = e \rangle$
   - $H^2(\mathbb{Z}_2 \times \mathbb{Z}_2, U(1)) = \mathbb{Z}_2$
   - $\omega = \frac{1}{D} Tr\left[V(x_1)V(x_2)V^\dagger(x_1)V^\dagger(x_2)\right] = \pm 1$
3.
   - $G_{int} = \mathbb{Z}_3$ or $\mathbb{Z}_2$ or the trivial group
   - $H^2(G, U(1)) =$ trivial group
   - $\omega = 1$ (no projective representations)

Order parameter to detect $\beta(P)$ and $\gamma(g)$

It was shown in [54] that $\beta(P)$ can be obtained as

$$\beta(P) = \frac{1}{D} Tr\left[NN^*\right] \tag{2.53}$$

From Eq (2.29) we can see that $\gamma(g)$ that results from the commutation of on-site and parity can be obtained as

$$\gamma(g) = \frac{1}{D} Tr\left[N^{-1} V(g) N V^T(g)\right] \tag{2.54}$$

Here, however, an important technical point arises. Although eq (2.54) has a similar form to the equations used to compute ω and β, it differs in an important respect. Recall that, as calculated above, the matrices V and N are obtained only up to arbitrary overall phase factors. These phases are

irrelevant to the calculation of ω and β, as both V and V^* appear equally in the equations which define them. In Eq. 2.54, however, the matrix V^T will fail in general to cancel the phase contributed by V.

Since the $V(g)$ can carry a different phase for each g, we must find a way to self-consistently fix the phase factors of each. In principle, this can always be done by appealing to the properties of projective representations. The extracted matrices V should satisfy a set of relationships

$$V(g_1)V(g_2) = \omega(g_1, g_2)V(g_1 g_2), \tag{2.55}$$

with the phases $\omega(i, j)$ forming the "factor system" of the representation. Since the matrices which we numerically extract by the above procedure do not automatically satisfy this relationship, let us label them $\tilde{V}$, with $\tilde{V}(g) = \theta_g V(g)$ for some phase factor θ_g. From this, one can conclude that the numerical matrices obey a similar relation:

$$\tilde{V}(g_1)\tilde{V}(g_2) = \frac{\theta_{g_1 g_2}}{\theta_{g_1}\theta_{g_2}}\omega(g_1, g_2)\tilde{V}(g_1 g_2). \tag{2.56}$$

By analogy to Eq. 2.55, let us define

$$\tilde{\omega}(g_1, g_2) = \frac{\theta_{g_1 g_2}}{\theta_{g_1}\theta_{g_2}}\omega(g_1, g_2). \tag{2.57}$$

Note that these phases $\tilde{\omega}(g_1, g_2)$ can be computed numerically from

$$(1/D)Tr[\tilde{V}(g_1)\tilde{V}(g_2)\tilde{V}(g_1 g_2)^{-1}]. \tag{2.58}$$

Furthermore, since parity is assumed to be a symmetry of the state in question (if it is not, then the concept of a γ parameter is undefined and the phase factors θ are irrelevant), then we must have $\omega(g_1 g_2)^2 = 1$ [52]. Inverting Eq. 2.57 and applying this condition tells us that

$$\theta_{g_1}^2 \theta_{g_2}^2 \tilde{\omega}(g_1, g_2)^2 = \theta_{g_1 g_2}^2. \tag{2.59}$$

Since the $\tilde{\omega}$ are known, this set of equations, which run over all the group elements g, are sufficient to solve for the phases θ. In fact, when V is unitary, it is clear from the definition of γ in Eq. 2.54 that only θ^2, and not θ itself, is needed to correct for the spurious phase factors, which further simplifies the system of equations which must be solved.

In practice, another convenient way to fix these phase factors is by interpreting the projective representations of the group, $\tilde{V}$ as linear representations of the covering group (or at least, one of the covering groups). For example,

in the case of $\mathbb{Z}_2 \times \mathbb{Z}_2$, the quaternion group $\mathbb{Q}_8$ is a covering group. Hence the elements of the projective representation of $\mathbb{Z}_2 \times \mathbb{Z}_2$, $V(g)$ can have their overall phases fixed so that they obey the structure of this group; in particular, for the representation of the identity element we must have $V(e)^2 = \mathbb{1}$, and for all others, $V(g)^2 = -\mathbb{1}$.

2.6 Summary and outlook

In this chapter, we have studied the phase diagram of a quantum spin-1 lattice with an on-site A_4 symmetry along with invariance under lattice translation and inversion. Using numerical methods, we obtain the ground state of the Hamiltonian for a range of parameters and using appropriate matrix product state order parameters, we study the phase diagram. In the parameter range we study, we detect 8 gapped phases characterized by a combination of symmetry breaking and symmetry fractionalization. In a recent paper [63], the authors study continuous phase transitions between two SPT phases and determine that the central charge of the conformal field theory (CFT) that describes that system at the phase boundary has a central charge $c \geq 1$. In our phase diagram, we observe that the phase boundaries separating phases **B** and **C** and also **C** and **D** by continuous phase transitions are characterized by a CFT with $c \approx 1.35$ which is consistent with $c \geq 1$. However, there is a distinction that must be noted. The authors of Ref [63] state their result for phase transitions between two distinct SPT phases protected by on-site symmetries *i.e.* when two phases have linear and projective representations in the virtual space. For our case, the phases **B**, **C** and **D** are distinct because of the presence of translation invariance in addition to the internal A_4 symmetry. Specifically, the ground states belonging to three phases are invariant under A_4 transformations up to $U(1)$ factors that corresponds to the three 1D representations of A_4 rather than projective representations. In fact, all three phases have non-trivial projective representations in the virtual space. Furthermore, the authors of Ref [61] conjecture that there can exist no continuous phase transitions between non-trivial SPT phases when the internal symmetry is discrete at all length scales. The phase transitions mentioned above appear to be counter examples. However, at the moment we do not know whether the discrete symmetry in our model is enhanced to a continuous one at the transitions between the A_4 SPT phases. It seems that the transitions seen in this model are not the result of fine-tuning, as they appear in a finite range of the parameter μ. These observations suggest that it is interesting to study the nature of phase transitions and the physics involved in the phase boundary when the protecting symmetry has both internal and on-site symmetries.

Chapter 3

Unwinding symmetry protected topological phases.

The contents of this chapter are published in Ref.[83] completed in collaboration with Juven Wang and Tzu-Chieh Wei.

3.1 Introduction and summary of main results

Gapped phases of quantum matter can be thought of as equivalence classes of physical systems, whose dynamics are governed by local Hamiltonians with a spectral gap. Two gapped Hamiltonians are said to be equivalent, i.e., the physical systems described by them belong to the same phase iff they can be interpolated without closing the spectral gap. The presence of global symmetries, which is natural in many condensed matter systems adds an additional degree of complexity and results in an increase in the number of possible fine-grained phases. A Hamiltonian that belongs to the trivial phase within the space of gapped Hamiltonians without any symmetry constraint may become non-trivial in the space of *symmetric* gapped Hamiltonians. One well known mechanism by which phases can appear due to the presence of symmetries is when the global symmetry is *spontaneously broken* á la Ginzburg and Landau. Interestingly, even when symmetry is unbroken, it was recently discovered that we can have different phases that cannot be connected without a phase transition. Such phases are called symmetry-protected-topological (SPT) phases which are the focus of our current study.

There has been a great deal of interest in recent years in characterizing and classifying SPT phases in various spatial dimensions. This is in part due to the successful prediction and experimental detection of topological insulators and in part due to the rich theoretical structure that has been uncovered

in understanding these phases (see [84–88] for reviews). Let us review some important facts about non-trivial SPT phases with a global symmetry G:

Fact 1: The ground state of any Hamiltonian describing a non-trivial SPT phase cannot be mapped to a trivial state (product state for bosons, slater determinant state for fermions) using a finite-depth unitary circuit (FDUC) with each layer being invariant under G.

An FDUC is a unitary operator that can be written as the product of a finite number of ultra-local unitary operators of the form $\bigotimes_i u_i$ where each u_i operates on a disjoint Hilbert space associated to a finite number of lattice points close to the site i. Clearly, any FDUC can only produce short-range entanglement. Fact 1 is an alternative way of phrasing the fact that the Hamiltonian cannot be connected to a trivial one via a path of gapped Hamiltonians that are invariant under G. We can ask important questions about the precise conditions under which a non-trivial SPT phase can or cannot be unwound to a trivial one. For instance,

Q1: How much symmetry needs to be broken to be able to map the ground state of a non-trivial SPT phase to a product state using an FDUC?

To answer this, let us consider the famous example of the AKLT model [89], which is invariant under an on-site action of the group $SO(3)$ and belongs to the so-called Haldane phase. It is known that certain essential features of the Haldane phase, such as the emergent fractionalized boundary modes are present even if $SO(3)$ is explicitly broken down, using weak perturbations, to its Abelian subgroup, $\mathbb{Z}_2 \times \mathbb{Z}_2$ comprising of π rotations about the x, y and z axes [90, 91]. However, if the symmetry is broken down further to $\mathbb{Z}_2$ (leaving behind no other accidental symmetries like inversion), generated by π rotations only about one of the axes, then the phase becomes trivial! This means that we cannot use a $\mathbb{Z}_2 \times \mathbb{Z}_2$ invariant path to unwind the AKLT gound state but we can use a $\mathbb{Z}_2$ invariant one. This above result can be understood within the group-cohomology classification framework which posits that in d spatial dimensions, bosonic SPT phases are classified by the elements of the cohomology group $H^{d+1}(G, U(1))$. The 1+1 D AKLT model is non-trivial in the sense that it corresponds to the non-trivial element of $H^2(SO(3), U(1)) \cong \mathbb{Z}_2$. Now, upon restricting the group $SO(3)$ to $\mathbb{Z}_2 \times \mathbb{Z}_2$ by introducing symmetry-breaking perturbations to the AKLT Hamiltonian, it turns out that the system still belongs to a non-trivial SPT phase, now labeled by the non-trivial element of $H^2(\mathbb{Z}_2 \times \mathbb{Z}_2, U(1)) \cong \mathbb{Z}_2$. However, since $H^2(\mathbb{Z}_2, U(1)) \cong 1$, upon further breaking the symmetry down to $\mathbb{Z}_2$, we are only left with the trivial SPT phase. In summary, the answer to $Q1$ is:

An SPT phase with global symmetry G classified by $H^{d+1}(G, U(1))$ can be trivialized by breaking G to $K \subset G$ such that $H^{d+1}(K, U(1)) \cong 1$. As a

corollary, a guaranteed way to trivialize any SPT phase is by breaking all symmetries i.e. $K \cong 1$. In this chapter, we explore a second question which is, in some sense converse to $Q1$:

Q2: Instead of breaking the symmetry, can we find a way to unwind an SPT phase by extending the global symmetry?

We demonstrate that the answer to the above quesion is in the affirmative. The theoretical justification is established in a recent work [92] where the authors provide a new perspective on another fact about SPT phases:

Fact 2: The symmetry action on the boundary of a non-trivial SPT phase suffers from an 't Hooft anomaly. This presents an obstruction to gauging the symmetry and also producing a short-range-entangled symmetric gapped Hamiltonian for the boundary degrees of freedom. However, if the symmetry on the boundary is broken, the boundary Hamiltonian can be short-range entangled and gapped.

The authors of [92] show that the boundary anomaly can be trivialized by suitably extending the global symmetry $G \to \tilde{G}$ and dynamically gauging the extra part, $\tilde{G}/G$. This produces a symmetric gapped Hamiltonian at the boundary. Furthermore, the presence of emergent gauge degrees of freedom leads to long-range entanglement. This result helps us answer $Q2$:

The ground state of a non-trivial SPT phase can be mapped to a trivial state using a finite-depth unitary circuit in which each layer is invariant under the extended symmetry $\tilde{G}$ which trivializes the boundary anomaly.

The rest of the chapter is organized as follows. In Sec. 3.3 we discuss unwinding of nontrivial bosonic SPT phases, including representative states in the Haldane phase under different symmetry considerations and the cluster state. We provide a general picture for unwinding nontrivial (1+1)D SPT phases protected by onsite symmetry. In Sec 3.4 we turn to unwinding nontrivial fermionic SPT phases. Five of the ten Altland-Zirnbauer symmetry classes in (1+1)D have a non-trivial classification in the free-fermionic limit and some of these are reduced in the presence of interactions. These classes are D, DIII, BDI, AIII and CII. We show that representative models of non-trivial SRE phases belonging to all of these classes can be constructed by stacking Kitaev's Majorana chains [93] (henceforth referred to as the Kitaev chain). We show that some of these non-trivial fermionic models that can be understood as bosonic SPT phases can be unwound by a suitable symmetry extension. In Sec. 3.5, we summarize and make some concluding remarks.

We remark on the notation of symmetry groups. We use the 'mathcal' convention for symmetry groups that contains the fermionic parity operator $(-1)^{N_f}$ in the group center. For example, the group of time reversal symmetry generated by $\mathcal{T}$ such that $\mathcal{T}^2 = (-1)^{N_f}$ is denoted as $\mathcal{Z}_4^T =$

$\{1, \mathcal{T}, (-1)^{Nf}, (-1)^{Nf}\mathcal{T}\}$. On the other hand, the group of time reversal symmetry generated by $\mathcal{T}$ such that $\mathcal{T}^2 = 1$ is denoted as $\mathbb{Z}_2^T = \{1, \mathcal{T}\}$.

3.2 Two known roads to unwinding SPT phases and a third one

In this section, we review two known ways of mapping (using a FDUC) a non-trivial SPT state to a trivial one– symmetry breaking and inversion. We then introduce the third way– symmetry extension which will form the subject matter for the rest of the chapter. We use a representative caricature of an SPT state shown in Fig. 3.1 formed by considering two qubits per unit site and maximally entangling the neighboring qubits on different sites.

$$|\psi\rangle = \prod_k \left(\frac{|\uparrow\rangle_{B,k}|\downarrow\rangle_{A,k+1} + |\downarrow\rangle_{B,k}|\uparrow\rangle_{A,k+1}}{\sqrt{2}} \right) \tag{3.1}$$

This state represents a non-trivial SPT ground state protected symmetry group $\mathbb{Z}_2 \times \mathbb{Z}_2$ generated by the two commuting operators, $\prod_k \sigma^x_{A,k}\sigma^x_{B,k}$ and $\prod_k i\sigma^z_{A,k} i\sigma^z_{B,k}$ in that it cannot be mapped to a trivial product state using a FDUC where each layer commutes with the symmetry generators. We will return to this state and also write down its zero correlation length fixed-point Hamiltonian explicitly in Sec. 3.3. We now proceed to trivializing the state.

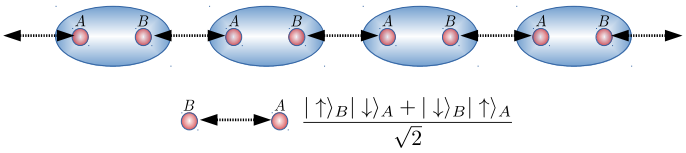

Figure 3.1: A representative SPT state.

3.2.1 Explicit symmetry breaking

Consider the 2-layer FDUC, $\mathcal{W} = \mathcal{W}_2\mathcal{W}_1$

$$\mathcal{W}_1 = \prod_k \left[|\uparrow\rangle\langle\uparrow|_{B,k} \otimes \sigma^x_{A,k+1} + |\downarrow\rangle\langle\downarrow|_{B,k} \otimes \mathbb{1}_{A,k+1} \right] \tag{3.2}$$

$$\mathcal{W}_2 = \prod_k \left[|\uparrow\rangle\langle\uparrow|_{B,k} \otimes \sigma^x_{A,k} + |\downarrow\rangle\langle\downarrow|_{B,k} \otimes \mathbb{1}_{A,k} \right] \tag{3.3}$$

Applying $\mathcal{W}$ to $|\psi\rangle$ leaves us with the trivial product state, $|\psi_0\rangle$ as shown in Fig. 3.2.

$$\mathcal{W}|\psi\rangle = |\psi_0\rangle = \prod_k \left(\frac{|\uparrow\rangle_A|\downarrow\rangle_B + |\downarrow\rangle_A|\uparrow\rangle_B}{\sqrt{2}} \right)_k \tag{3.4}$$

However, $\mathcal{W}_1$ and $\mathcal{W}_2$ do not commute with the symmetry operators $\prod_k \sigma^x_{A,k}\sigma^x_{B,k}$ and $\prod_k i\sigma^z_{A,k}i\sigma^z_{B,k}$ and hence this is a case of unwinding by explicit symmetry-breaking.

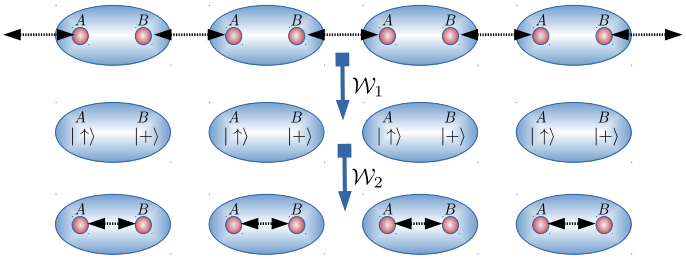

Figure 3.2: Unwinding by explicit symmetry-breaking.

3.2.2 Inversion

SPT phases are said to be invertible. This means that for every non-trivial SPT phase, we can find its inverse phase, which, if stacked on the original SPT phase can be unwound to a trivial one. This follows from the fact that SRE phases have an Abelian group structure with respect to stacking. If a phase, labeled by an element α is stacked on another phase, labeled by β, the net system is a phase labeled by $\alpha + \beta$. The non-trivial SPT state we are considering has a $\mathbb{Z}_2$ classification from group-cohomology (see sec (3.3)). This means that the non-trivial phase is its own inverse and by stacking two layers of the system, we should be able to map it to a trivial state using a FDUC that commutes with the $\mathbb{Z}_2 \times \mathbb{Z}_2$ symmetry generators at each layer. Let us check this explicitly.

First, let us consider the ground state of two stacked SPT phases.

$$|\tilde{\psi}\rangle \quad = \quad |\psi\rangle_1 \otimes |\psi\rangle_2 = \prod_k \prod_{\alpha=1,2} \left(\frac{|\uparrow\rangle_{B,k}|\downarrow\rangle_{A,k+1} + |\downarrow\rangle_{B,k}|\uparrow\rangle_{A,k+1}}{\sqrt{2}} \right)_\alpha$$

We can use the following two-layer FDUC to map this state to two layers

of the trivial state of Eq. 3.4.

$$\mathcal{W}_1 = \prod_k \frac{1}{2}\left(\mathbb{1} + \boldsymbol{\sigma}_{B,1,k}.\boldsymbol{\sigma}_{A,2,k+1}\right) \tag{3.5}$$

$$\mathcal{W}_2 = \prod_k \frac{1}{2}\left(\mathbb{1} + \boldsymbol{\sigma}_{A,1,k}.\boldsymbol{\sigma}_{B,2,k}\right) \tag{3.6}$$

$$\mathcal{W}|\tilde{\psi}\rangle = \prod_k \prod_{\alpha=1,2} \left(\frac{|\uparrow\rangle_{B,k}|\downarrow\rangle_{A,k} + |\downarrow\rangle_{B,k}|\uparrow\rangle_{A,k}}{\sqrt{2}} \right)_\alpha, \tag{3.7}$$

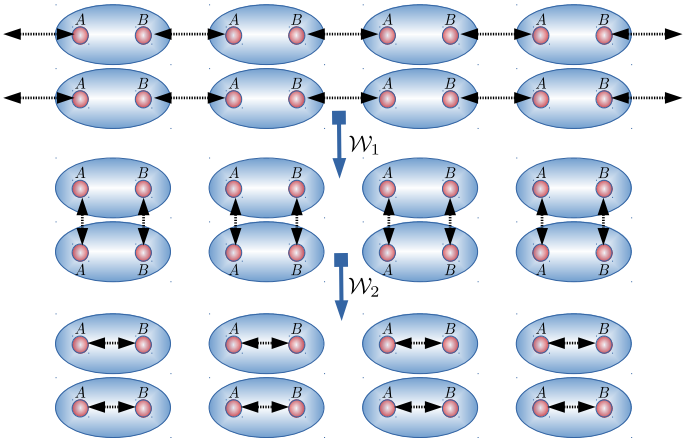

Figure 3.3: Unwinding by inversion.

where $\mathcal{W} = \mathcal{W}_2\mathcal{W}_1$. The operator $\frac{1}{2}\left(\mathbb{1} + \boldsymbol{\sigma}_A.\boldsymbol{\sigma}_B\right)$ is a swap operator that exchanges the basis states $|\uparrow\rangle$, $|\downarrow\rangle$ on two sites, A and B and is easily checked to commute with the $\mathbb{Z}_2 \times \mathbb{Z}_2$ symmetry generators. Thus, we have unwound the SPT phase without breaking symmetry but by stacking an 'inverse phase'.

3.2.3 Symmetry extension

Let us now consider coupling the original SPT state to a product state of dimers:

$$|\tilde{\psi}\rangle = |\psi\rangle \otimes \prod_{\text{odd } k} \frac{(|\downarrow\rangle_k|\uparrow\rangle_{k+1} + |\uparrow\rangle_k|\downarrow\rangle_{k+1})_C}{\sqrt{2}} \tag{3.8}$$

This state can be unwound by the application of the following FDUC:

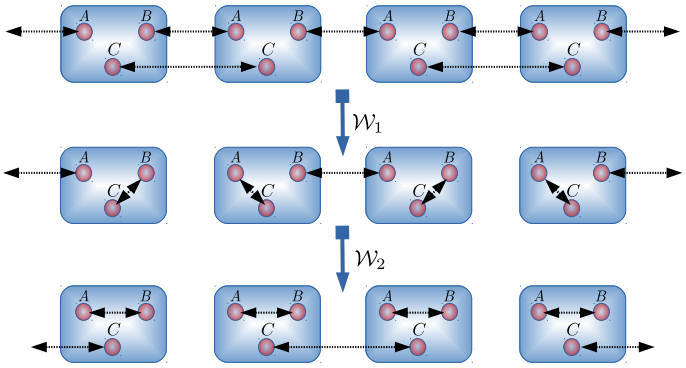

Figure 3.4: Unwinding by symmetry extension.

$$\mathcal{W} = \mathcal{W}_1\mathcal{W}_2 \tag{3.9}$$

$$\mathcal{W}_1 = \prod_{\text{odd } k} \frac{1}{2}\left(\mathbb{1} + \boldsymbol{\sigma}_{C,k}.\boldsymbol{\sigma}_{A,k+1}\right) \tag{3.10}$$

$$\mathcal{W}_2 = \prod_{\text{odd } k} \frac{1}{2}\left(\mathbb{1} + \boldsymbol{\sigma}_{C,k}.\boldsymbol{\sigma}_{A,k}\right) \prod_{\text{even } k} \frac{1}{2}\left(\mathbb{1} + \boldsymbol{\sigma}_{C,k}.\boldsymbol{\sigma}_{B,k}\right) \tag{3.11}$$

$$\mathcal{W}|\tilde{\psi}\rangle = \prod_{k}\left(\frac{|\uparrow\rangle_{B,k}|\downarrow\rangle_{A,k+1} + |\downarrow\rangle_{B,k}|\uparrow\rangle_{A,k+1}}{\sqrt{2}}\right) \prod_{\text{even } k} \frac{(|\downarrow\rangle_k|\uparrow\rangle_{k+1} + |\uparrow\rangle_k|\downarrow\rangle_{k+1})_C}{\sqrt{2}}$$

However, notice that the extended state, as well as the layers of $\mathcal{W}$ is invariant under the larger symmetry group, generated by the operators $\prod_k \sigma^x_{A,k}\sigma^x_{B,k}\sigma^x_{C,k}$ and $\prod_k i\sigma^z_{A,k}i\sigma^z_{B,k}i\sigma^z_{C,k}$ which do not commute with each other. These generators are a faithful representation of the dihedral group of 8 elements, $\mathbb{D}_8$. This is an example of unwinding by extension which we will explore. The relationship between the original symmetry group, $\mathbb{Z}_2 \times \mathbb{Z}_2$ to the extended one, $\mathbb{D}_8$ as well as a number of other details and generalities will be made clear in the following sections.

3.3 Unwinding bosonic SPT phases

In this section, we demonstrate how fixed-point bosonic SPT states and their parent Hamiltonians can be trivialized by symmetry extension. We begin with a short review of the group cohomology classification of bosonic SPT phases, first in 1+1 D and then in general dimensions. We also review key results from the paper by Wang, Wen and Witten [92] on how the boundary 't Hooft anomaly can be trivialized using symmetry extension to produce symmetric gapped boundary. We then demonstrate our trivialization procedure

for (1+1)D bulk using the same symmetry-extension procedure on a few specific examples of well known bosonic SPT phases, and we also state a general picture for the case of arbitrary on-site finite unitary symmetry. Note that everywhere in this chapter, unless stated otherwise, we consider one dimensional systems of length L assumed to be in the thermodynamic limit ($L >> 1$) with lattice constant set to 1 and employ periodic boundary conditions.

3.3.1 A quick recap of the classification of bosonic SPT phases in 1+1D and beyond

We start with a quick recap of the classification of bosonic SPT phases in (1+1)D following Ref [52]. Let us first recall that SPT phases are gapped phases of matter with a unique ground state. In (1+1)D, this allows us to represent any such ground state faithfully as a matrix product state (MPS) with a sufficiently large but finite bond dimension χ that does not scale with the system size [94, 95]. Let us focus on a spin chain with an on-site Hilbert space of dimension J and choose some basis appropriately labeled $|i\rangle = |1\rangle, |2\rangle, \ldots, |J\rangle$. For convenience of notation, let us also assume lattice translation invariance. An MPS representation of a gapped ground state of such a system can be written using J matrices of size $\chi \times \chi$, $A_1, \ldots, A_J$ as follows

$$|\psi\rangle = \sum_{i_1=1}^{J} \ldots \sum_{i_L=1}^{J} Tr\left[A_{i_1} A_{i_2} \ldots A_{i_L}\right] |i_1 \ldots i_L\rangle. \tag{3.12}$$

First, note that changing $A_i \mapsto M A_i M^\dagger$ with any unitary M leaves $|\psi\rangle$ invariant and hence is a redundancy in the MPS representation. Let us now consider $|\psi\rangle$, a unique ground state which invariant under the group of symmetry operations, $g \in G$ of Hamiltonian, $g : |\psi\rangle \mapsto |\psi\rangle$. We can re-express the invariance condition of $|\psi\rangle$ as a condition on the set of matrices A_i. The different inequivalent ways of this symmetry action on the matrices A_i effectively give us a classification of different SPT phases. Let us demonstrate this using a few examples starting with time reversal symmetry.

Consider the action of time-reversal symmetry with an anti-unitary representation, $\mathcal{T}$ such that $\mathcal{T}^2 = 1$. Any time-reversal symmetry operator can be written using an on-site unitary operator, U^T combined with complex-conjugation, $\mathcal{K}$,

$$\mathcal{T} = \left[\bigotimes_{i=1}^{L} U^T\right] \mathcal{K}, \tag{3.13}$$

The invariance condition $\mathcal{T}|\psi\rangle = |\psi\rangle$ can translated to the matrices A_k as

follows

$$\sum_{k=1}^{J} U_{ik}^{T} A_k^* = V A_i V^\dagger. \tag{3.14}$$

The condition $\mathcal{T}^2 = 1$ imposes the condition $V^*V = \pm\mathbb{1}$ and thus divides the *virtual space* (sometimes also called the *bond space*) symmetry representation V into two classes labeled by $\pm$. This gives us the $\mathbb{Z}_2$ classification of $\mathcal{T}$ invariant spin-chains.

Let us now consider the case of internal unitary symmetries, which is described by an on-site unitary representation of the elements of some group G, $\bigotimes_{i=1}^{L} U(g)$. The invariance condition, $\bigotimes_{i=1}^{L} U(g)|\psi\rangle = |\psi\rangle$ can be translated to the level of A_k matrices as follows

$$\sum_{k=1}^{J} U(g)_{ik} A_k = V(g) A_i V^\dagger(g). \tag{3.15}$$

Firstly, note that re-phasing the representation of G on the virtual dimension $V(g)$ by a 1D representation, $\beta_1(g)$ as follows is a gauge freedom that leaves Eq. 3.15 invariant

$$V(g) \mapsto \beta_1(g) V(g). \tag{3.16}$$

Group theoretic constraints on $U(g)$ further impose conditions on $V(g)$. The composition rule $U(g)U(h) = U(gh)$ requires $V(g)$ only closes up to a $U(1)$ factor

$$V(g)V(h) = \omega_2(g,h) V(gh), \tag{3.17}$$

where $\omega_2(g,h)$ is a $U(1)$ phase factor dependent on g and h. This means that $V(g)$ are *projective representations* of G. Furthermore, associativity imposes the following *cocycle* constraint on the phases ω_2

$$\omega_2(g,h)\omega_2(gh,l)\omega_2^{-1}(g,hl)\omega_2^{-1}(h,l) \equiv (\delta\omega_2)(g,h,l) = \mathbb{1}. \tag{3.18}$$

Eq. (3.16) defines the following *coboundary* equivalence relation

$$\omega_2(g,h) \sim \omega_2(g,h)\beta_1(g)\beta_1(h)\beta_1^{-1}(gh) \equiv \omega_2(g,h)(\delta\beta_1)(g,h). \tag{3.19}$$

The different SPT phases in 1+1 D with symmetry group G are classified by the different equivalence classes of ω_2 with the equivalence relation of Eq. 3.19 subject to the condition of Eq. 3.18. These classes are labeled by the elements of the second cohomology group of G with $U(1)$ coefficients, $H^2(G, U(1))$.

A natural generalization of the $H^2(G, U(1))$ classification of bosonic SPT phases in 1+1 dimensions to d+1 dimensions is replacing $H^2(G, U(1))$ by

$H^{d+1}(G, U(1))$ [96] which labels equivalence classes of $d+1$ cocycles, $\omega_{d+1}(\{g_i\})$ subject to generalizations of Eqs.3.18,3.19. This classification is known to capture a large class of bosonic SPT phases although exceptions are known to exist [97–99]. One important feature of bosonic SPT phases classified by group cohomology is the presence of an 't Hooft anomaly on the boundary [100, 101] which has several consequences. First, it presents an obstruction to gauging the symmetry on the boundary by forcing it to have a non on-site representation [102]. Second, it forbids the boundary from being symmetric, gapped and short-range-entangled (see [103] for a nice proof-by-contradiction). However, it has been known that the boundary can be gapped by breaking symmetry (spontaneously or explicitly), or, more interestingly, when accompanied by surface topological order with long-range-entanglement [104–109]. Ref.[92] puts the latter route to gapping symmetric boundary for bosonic phases classified by group cohomology in a systematic footing by *symmetry extension* which we briefly review below.

Consider a bosonic SPT phase with a boundary 't Hooft anomaly classified by a $(d+1)$ cocycle $\omega_{d+1}(\{g_i\})$ belonging to a non-trivial class of $H^{d+1}(G, U(1))$ meaning $\omega_{d+1}(\{g_i\}) \neq \delta\beta_d(\{g_i\})$. It was shown in [92] that given the above data, there exists a group extension $\tilde{G}$ which fits into the following *short exact sequence*.

$$1 \longrightarrow K \xrightarrow{i} \tilde{G} \xrightarrow{s} G \longrightarrow 1. \tag{3.20}$$

As usual, i is an injective map and s is a surjective map (see [110] for an introduction to short exact sequences and group extensions). The short exact sequence is such that if we consider the cocycle for the bigger group, $\tilde{G}$, as defined via *pullback* of the surjective map s, then it belongs to the trivial class:

$$\omega_{d+1}(\{\tilde{g}_i\}) = s^*\omega_{d+1}(\{g_i\}) = \omega_{d+1}(\{s(\tilde{g}_i)\}) = \delta\beta_d(\{\tilde{g}_i\}). \tag{3.21}$$

This fact was used in [92] to produce gapped boundaries by considering a $\tilde{G}$ invariant boundary theory but with the extra symmetry K, being dynamically gauged, leaving the true global symmetry to be $\tilde{G}/K \cong G$.

Another consequence of the above result, which is the focus of this chapter, is that if we extend the symmetry G to $\tilde{G}$ as prescribed by the short exact sequence (3.20), we can unwind the non-trivial G SPT to a trivial one in a $\tilde{G}$ invariant path in Hamiltonian space. The rest of the chapter is concerned with demonstrating this by constructing a $\tilde{G}$ invariant FDUC to map a non-trivial G SPT state to a trivial one for various symmetries. For each case, we state the extension used and demonstrate unwinding but do not explain how the extension is arrived at. We relegate the reader to [92] for those technical

details.

3.3.2 Unwinding an AKLT-like spin chain

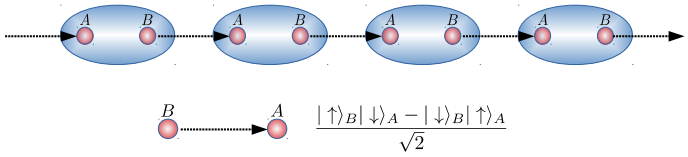

Figure 3.5: The AKLT-like model.

The Affleck-Kennedy-Lieb-Tasaki model [45] is a chain of spin-1 particles with the following Hamiltonian

$$H_{AKLT} = \sum_j \left[\boldsymbol{S}_j \cdot \boldsymbol{S}_{j+1} + \frac{1}{3} \left(\boldsymbol{S}_j \cdot \boldsymbol{S}_{j+1} \right)^2 \right], \tag{3.22}$$

where S^α are the spin-1 generators of the $SU(2)$ algebra. This Hamiltonian has a unique MPS ground state which can be written in the basis of the S^z operator, $|+1\rangle, |-1\rangle, |0\rangle$ as follows

$$\begin{aligned} |\psi\rangle &= \sum_{i_1=\pm1,0} \dots \sum_{i_L=\pm1,0} Tr\left[M_{i_1} M_{i_2} \dots M_{i_L}\right] |i_1 \dots i_L\rangle. \\ M_{\pm1} &= \pm\sqrt{\frac{2}{3}} \left(\frac{\sigma^x \pm i\sigma^y}{2} \right), \quad M_0 = \frac{-1}{\sqrt{3}} \sigma^z. \end{aligned} \tag{3.23}$$

This ground state can also be interpreted as a valence-bond-solid state by first starting with two spin-$\frac{1}{2}$'s per unit site, entangling neighboring spins to form $SU(2)$ singlets and then projecting each site onto the spin-1 sector of the Clebsch-Gordan decomposition $\frac{1}{2} \otimes \frac{1}{2} \cong 1 \oplus 0$.

We now consider a simplified version of the AKLT model shown in Fig.3.5, whose ground state, $|G\rangle$ is the same as $|\psi\rangle$ of Eq. 3.23 except for the projection onto the spin-1 sector on each site. This leaves us with a 4 dimensional local Hilbert space coming from the two spin halves, which we will call A and B, that still transforms as a faithful $1 \oplus 0$ representation of $SO(3)$. We can also write a parent commuting-projector Hamiltonian H, that has $|G\rangle$ as its unique

ground state:

$$|G\rangle = \prod_k |\psi\rangle_{Bk,Ak+1} = \prod_k \frac{(|\uparrow\rangle_{B,k}|\downarrow\rangle_{A,k+1} - |\downarrow\rangle_{B,k}|\uparrow\rangle_{A,k+1})}{\sqrt{2}}, \quad (3.24)$$

$$H = -\sum_k |\psi\rangle\langle\psi|_{Bk,Ak+1}. \quad (3.25)$$

This model has all the appealing features of the AKLT model like fractionalized boundary spins, unique ground state with periodic bounary conditions and a spectral gap, with the added advantage of being exactly solvable. We now unwind this model by interpreting it as two different non-trivial SPT phases protected by two different global symmetries.

As an $SO(3)$-invariant SPT phase

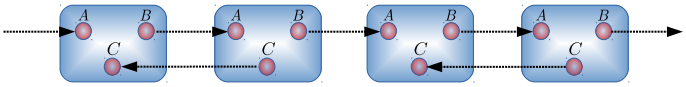

Figure 3.6: The AKLT-like model with extension.

If we disregard all other symmetries except for $SO(3)$ with the following on-site unitary representation

$$U(\theta) = \prod_k \exp\left[i\theta \frac{\boldsymbol{n}\cdot\boldsymbol{\sigma}}{2}\right]_{A,k} \exp\left[i\theta \frac{\boldsymbol{n}\cdot\boldsymbol{\sigma}}{2}\right]_{B,k}, \quad (3.26)$$

we can interpret the model (3.24) as a non-trivial SPT phase protected by $SO(3)$ which has a $H^2(SO(3), U(1)) \cong \mathbb{Z}_2$ classification. We now use the following extension to unwind the model:

$$1 \longrightarrow \mathbb{Z}_2 \xrightarrow{i} SU(2) \xrightarrow{s} SO(3) \longrightarrow 1. \quad (3.27)$$

In order to make the system transform faithfully under $SU(2)$, we introduce an additional spin-$\frac{1}{2}$ particle at each site, which we will label C as shown in Fig.(3.6). We extend H with a trivial $SU(2)$ invariant Hamiltonian such that the ground state of the additional spins is a product of dimers of $SU(2)$

singlets:

$$|\tilde{G}\rangle = |G\rangle \otimes \prod_{\text{odd } k} -|\psi\rangle_{Ck,Ck+1} = |G\rangle \otimes \prod_{\text{odd } k} \left(\frac{|\downarrow\rangle_k|\uparrow\rangle_{k+1} - |\uparrow\rangle_k|\downarrow\rangle_{k+1}}{\sqrt{2}} \right)_C ,$$
$$\tilde{H} = H - \sum_{\text{odd } k} |\psi\rangle\langle\psi|_{Ck,Ck+1}.$$

The on-site Hilbert space now transforms as the $\frac{1}{2} \otimes \frac{1}{2} \otimes \frac{1}{2} \cong \frac{3}{2} \oplus \frac{1}{2} \oplus \frac{1}{2}$ representation, which is faithful to $SU(2)$. It can be checked that the symmetry representation commutes with the extended Hamiltonain $\tilde{H}$ and leaves the ground state $|\tilde{G}\rangle$ invariant:

$$\tilde{U}(\theta) = \prod_k \exp\left[i\theta \frac{\boldsymbol{n}\cdot\boldsymbol{\sigma}}{2}\right]_{k,A} \exp\left[i\theta \frac{\boldsymbol{n}\cdot\boldsymbol{\sigma}}{2}\right]_{k,B} \exp\left[i\theta \frac{\boldsymbol{n}\cdot\boldsymbol{\sigma}}{2}\right]_{k,C}. \quad (3.28)$$

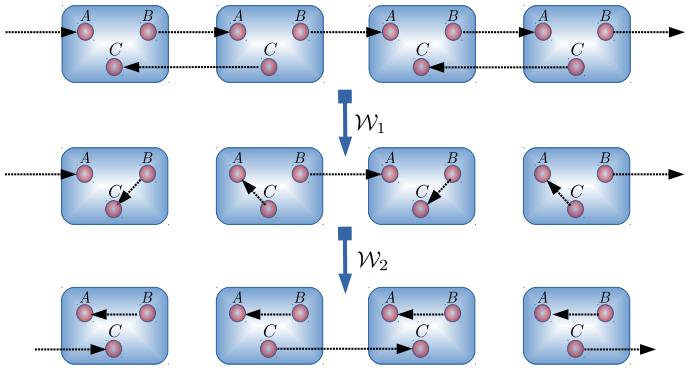

Figure 3.7: Unwinding of the AKLT-like model.

We use the two-layer FDUC $\mathcal{W} = \mathcal{W}_2\mathcal{W}_1$ constructed using a series of entanglement swap operations to trivialize the system as shown in Fig.3.7

$$\mathcal{W}_1 = \prod_{\text{odd } k} \mathcal{S}_{Ck,Ak+1}, \quad (3.29)$$
$$\mathcal{W}_2 = \prod_{\text{odd } k} (\mathcal{S}_{C,A})_k \prod_{\text{even } k} (\mathcal{S}_{C,B})_k, \quad (3.30)$$
$$\mathcal{S}_{AB} = \sum_{\alpha=\uparrow,\downarrow} \sum_{\beta=\uparrow,\downarrow} |\alpha\rangle\langle\beta|_A|\beta\rangle\langle\alpha|_B = \frac{1}{2}\left(\mathbb{1} + \boldsymbol{\sigma}_A.\boldsymbol{\sigma}_B\right). \quad (3.31)$$

Each 2-qubit swap operator, $\mathcal{S}_{AB}$ is manifestly $SU(2)$ invariant and, as a result, so are $\mathcal{W}_1$ and $\mathcal{W}_2$. $\mathcal{W}$ maps $|\tilde{G}\rangle$ and $\tilde{H}$ to the following trivial ground state,

$|G_0\rangle$ and Hamiltonian H_0 thereby unwind the SPT phase.

$$\mathcal{W}|\tilde{G}\rangle = \prod_k -|\psi\rangle_{Ak,Bk} \otimes \prod_{\text{even } k} |\psi\rangle_{Ck,Ck+1} = |G_0\rangle, \tag{3.32}$$

$$\mathcal{W}\tilde{H}\mathcal{W}^\dagger = -\sum_k |\psi\rangle\langle\psi|_{Ak,Bk} - \sum_{\text{even } k} |\psi\rangle\langle\psi|_{Ck,Ck+1} = H_0. \tag{3.33}$$

As a time-reversal $\mathbb{Z}_2^T$-invariant SPT phase

Let us now take the same model but consider it as an SPT protected by the anti-unitary time reversal symmetry, $\mathbb{Z}_2^T$ generated by

$$\mathcal{T} = \prod_k \exp\left[\frac{i\pi\sigma_y}{2}\right]_{k,A} \exp\left[\frac{i\pi\sigma_y}{2}\right]_{k,B} \mathcal{K}, \tag{3.34}$$

where, $\mathcal{K}$ is the complex conjugation operation, and disregarding all other symmetries. Since each site contains two spin-1/2 particles (A and B), it is clear that the time-reversal operator squares to identity locally, i.e. $\mathcal{T}^2 = \mathbb{1}$.

We now use the following extension to trivialize the model

$$1 \longrightarrow \mathbb{Z}_2 \xrightarrow{i} \mathbb{Z}_4^T \xrightarrow{s} \mathbb{Z}_2^T \longrightarrow 1. \tag{3.35}$$

It turns out that we can repurpose the unwinding procedure involving $SO(3)$ to $SU(2)$ extension to also define a $\mathbb{Z}_2^T$ to $\mathbb{Z}_4^T$ extension, with the $\mathbb{Z}_4^T$ being generated by

$$\tilde{\mathcal{T}} = \prod_k \exp\left[\frac{i\pi\sigma_y}{2}\right]_{k,A} \exp\left[\frac{i\pi\sigma_y}{2}\right]_{k,B} \exp\left[\frac{i\pi\sigma_y}{2}\right]_{k,C} \mathcal{K}. \tag{3.36}$$

It can be checked that, because of the extra spin-1/2 particle on each site, $\tilde{\mathcal{T}}^2 = -1$ locally on each site, which means $\tilde{\mathcal{T}}$ is an order-4 group element and generates the $\mathbb{Z}_4^T$ symmetry that we seek. It can easily be checked that $\tilde{H}$ and $|\tilde{G}\rangle$ are invariant under $\tilde{\mathcal{T}}$ as are $\mathcal{W}_1$ and $\mathcal{W}_2$. Thus, using the FDUC $\mathcal{W} = \mathcal{W}_2\mathcal{W}_1$, we obtain the trivial Hamiltonian and ground state just as before.

To summarize, we have demonstrated how we can trivialize the AKLT-like model by symmetry extension. When viewed as an SPT phase protected by $SO(3)$, it can be trivialized using extension (3.27) and when viewed as an SPT phase protected by time-reversal symmetry, it can be trivialized using extension (3.35).

For completeness, let us consider a simpler demonstration that this SPT phase can be trivialized by symmetry extension– instead of unwinding the

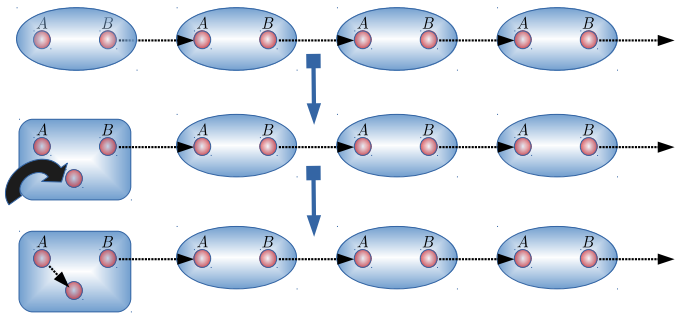

Figure 3.8: Gapping out the boundary modes by symmetry extension.

entire chain to a trivial one, we might be interested in simply gapping out the degenerate boundary spins by extending symmetry just on the boundary. This is very easy to do as shown in [92]. Consider an open chain as shown in Fig. 3.8 with a dangling spin 1/2 at each end giving rise to a 4-fold degeneracy. We can introduce additional spins that extends the symmetry on the boundary to $SU(2)$ and then tune in $SU(2)$ invariant boundary interaction terms, $h = -|\psi\rangle\langle\psi|$ where $|\psi\rangle$ is the $SU(2)$ singlet, that favors entangling the two dangling spins into a singlet in the ground state thus lifting the degeneracy. This also applies to the interpretation of the boundary modes coming from time-reversal symmetry. Such a boundary gapping can be done for all the examples below but we will not mention it. We will focus on unwinding the entire system.

3.3.3 Unwinding the Cluster state

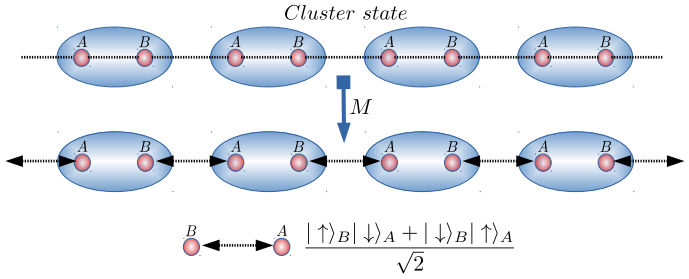

Figure 3.9: The cluster state before and after change of basis.

We now consider another famous model of an SPT phase, the cluster state

$|\psi_C\rangle$ and the Hamiltonian it is the ground state of, H_c:

$$|\psi_c\rangle = \prod_k CZ_{k,k+1} \prod_j |+\rangle_j, \tag{3.37}$$

$$H_c = -\sum_k \sigma^z_{k-1}\sigma^x_k\sigma^z_{k+1}, \tag{3.38}$$

where, $|+\rangle$ is the positive eigenstate of σ^x and CZ_{ab} is the two-qubit operator

$$CZ_{ab} = \frac{1}{2}\left(\mathbb{1} + \sigma^z_a + \sigma^z_b - \sigma^z_a\sigma^z_b\right) \tag{3.39}$$

The cluster state [111] was introduced as a resource state for measurement-based quantum computation (MBQC) [112, 113]. This model was later on understood to be a non-trivial SPT phase protected by a unitary on-site $\mathbb{Z}_2\times\mathbb{Z}_2$ symmetry [114, 115], generated by the following two operators

$$U(x) \equiv \prod_{\text{odd } k} \sigma^x_k,\ U(z) \equiv \prod_{\text{even } k} \sigma^x_k. \tag{3.40}$$

We also comment that the short-range entanglement structure that facilitates quantum computation is now understood as arising from the non-trivial SPT nature and the study of the utility of SPT phases for MBQC is a field of active research (See[32, 34, 35, 116]).

For our purpose, it will be helpful to apply an on-site change-of-basis to change the cluster state into a more convenient form. First, let us collect two spins together and label them A and B to form a four dimensional local Hilbert space as shown in Fig.(3.9). The symmetry generators can now be rewritten as

$$U(x) = \prod_k \sigma^x_{A,k},\ U(z) = \prod_k \sigma^x_{B,k}. \tag{3.41}$$

Next, we apply the on-site change of basis, M defined as below to obtain

the new form of the Hamiltonian, ground state and symmetry generators

$$
\begin{aligned}
M &= \prod_k \exp\left[\frac{-i\pi\sigma^y}{4}\right]_{A,k} [CZ_{AB}]_k\,, && (3.42)\\
MU(x)M^\dagger &\equiv V(x) = \prod_k \sigma^x_{A,k}\ \sigma^x_{B,k}, && (3.43)\\
MU(z)M^\dagger &\equiv V(z) = \prod_k i\sigma^z_{A,k}\ i\sigma^z_{B,k}, && (3.44)\\
MH_CM^\dagger &\equiv H_{\mathcal{C}} = \sum_k \left(\sigma^z_{B,i}\sigma^z_{A,i+1} - \sigma^x_{B,i}\sigma^x_{A,i+1}\right), && (3.45)\\
M|\psi_C\rangle M^\dagger &\equiv |\phi_{\mathcal{C}}\rangle = \prod_k |\phi\rangle_{Bk,Ak+1} = \prod_k \frac{(|\uparrow\rangle_{B,k}|\downarrow\rangle_{A,k+1} + |\downarrow\rangle_{B,k}|\uparrow\rangle_{A,k+1})}{\sqrt{2}}.
\end{aligned}
$$

This is the same state that was briefly studied in Sec. 3.2. We now use the following symmetry extension to unwind this phase:

$$1 \longrightarrow \mathbb{Z}_2 \xrightarrow{i} \mathbb{D}_8 \xrightarrow{s} \mathbb{Z}_2 \times \mathbb{Z}_2 \longrightarrow 1. \tag{3.46}$$

$\mathbb{D}_8$ is the order 8 dihedral group generated by two elements with the following presentation

$$\mathbb{D}_8 = \langle a, x | a^4 = x^2 = 1, xax = a^{-1}\rangle. \tag{3.47}$$

To achieve this, like before, we introduce a third qubit at each site, which we call C and whose dynamics is governed by a dimerizing Hamiltonian that belongs to the trivial phase. The new ground state and Hamiltonian are as follows,

$$
\begin{aligned}
|\tilde{\phi}_{\mathcal{C}}\rangle &= |\phi_{\mathcal{C}}\rangle \otimes \prod_{\text{odd } k} |\phi\rangle_{Ck,Ck+1} = |G\rangle \otimes \prod_{\text{odd } k} \frac{(|\downarrow\rangle_k|\uparrow\rangle_{k+1} + |\uparrow\rangle_k|\downarrow\rangle_{k+1})_C}{\sqrt{2}},\\
\tilde{H}_{\mathcal{C}} &= H_{\mathcal{C}} + \sum_{\text{odd } k} \left(\sigma^z_{C,i}\sigma^z_{C,i+1} - \sigma^x_{C,i}\sigma^x_{C,i+1}\right). && (3.48)
\end{aligned}
$$

The symmetries of this model are generated by

$$\tilde{V}(x) = \prod_k \sigma^x_{A,k}\ \sigma^x_{B,k}\ \sigma^x_{C,k}, \quad \tilde{V}(z) = \prod_k i\sigma^z_{A,k}\ i\sigma^z_{B,k}\ i\sigma^z_{C,k}. \tag{3.49}$$

It can be checked that these generators satisfy the presentation of Eq.3.47 and are a faithful representation of $\mathbb{D}_8$. With this, just like before, we can use a FDUC that commutes with this extended symmetry to unwind the system. In fact, we can use the exact same FDUC, $\mathcal{W} = \mathcal{W}_2\mathcal{W}_1$ used in the previous

section to do the job.

$$\mathcal{W}_1 = \prod_{\text{odd } k} \mathcal{S}_{Ck,Ak+1}, \tag{3.50}$$

$$\mathcal{W}_2 = \prod_{\text{odd } k} (\mathcal{S}_{C,A})_k \prod_{\text{even } k} (\mathcal{S}_{C,B})_k, \tag{3.51}$$

$$\mathcal{S}_{AB} = \frac{1}{2}\left(\mathbb{1} + \boldsymbol{\sigma}_A.\boldsymbol{\sigma}_B\right). \tag{3.52}$$

Using this, we get the following trivial ground state and Hamiltonian

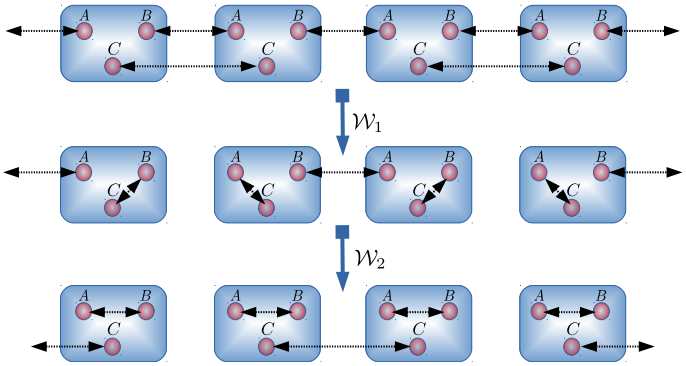

Figure 3.10: Unwinding the cluster state.

$$\mathcal{W}|\tilde{\phi}_{\mathcal{C}}\rangle = |\phi_0\rangle = \prod_k |\phi\rangle_{Ak,Bk} \otimes \prod_{\text{even } k} |\phi\rangle_{Ck,Ck+1}, \tag{3.53}$$

$$\mathcal{W}\tilde{H}_{\mathcal{C}}\mathcal{W}^\dagger = H_0 = \sum_k \left(\sigma^z_{A,k}\sigma^z_{B,k} - \sigma^x_{A,k}\sigma^x_{B,k}\right) + \sum_{\text{even } k} \left(\sigma^z_{C,k}\sigma^z_{C,k+1} - \sigma^x_{C,k}\sigma^x_{C,k+1}\right).$$

3.3.4 General picture for finite on-site unitary symmetries: proof based on Schur cover

We now describe a general procedure to unwind fixed-point states of SPT phases with any on-site unitary symmetry of a finite group, G classified by $\omega \in H^2(G, U(1))$. To construct the on-site Hilbert space, we consider one spin that transforms as a projective representation belonging to class ω and another that transforms as ω^*, the inverse of ω in the group $H^2(G, U(1))$. To be more precise, let $|i_\omega\rangle = |1_\omega\rangle \ldots |J_\omega\rangle$ be the basis states for some faithful J dimensional projective represenation of G belonging to class $\omega \in H^2(G, U(1))$.

Under group transformations, we have

$$g : |i_\omega\rangle \mapsto \sum_{i'=1}^{J} V(g)_{ii'}|i'_\omega\rangle, \tag{3.54}$$

$$V(g)V(h) = \omega(g,h)V(gh), \tag{3.55}$$

where $\omega(g,h)$ is a $U(1)$ phase factor. Now consider another spin of the same dimension J that transforms as ω^*, with basis states $|i_{\omega^*}\rangle = |1_{\omega^*}\rangle \ldots |J_{\omega^*}\rangle$ and the transformation property,

$$g : |i_{\omega^*}\rangle \mapsto \sum_{i'=1}^{J} V^*(g)_{ii'}|i'_{\omega^*}\rangle, \tag{3.56}$$

$$V^*(g)V^*(h) = \omega^*(g,h)V^*(gh). \tag{3.57}$$

If we consider a physical site to contain both spins, the representation of the symmetry that acts on the site, $U(g) \equiv V(g) \otimes V^*(g)$ can be checked to be a *linear* representation of G by observing that $U(g)U(h) = U(gh)$. To construct a non-trivial SPT state, we maximally entangle neighboring spins from different sites to form a symmetric state $|\chi_\omega\rangle$ as shown in Fig. (3.11),

$$|\chi_\omega\rangle_{BA} = \frac{1}{\sqrt{J}} \sum_{i=1}^{J} |i_{\omega^*}\rangle_B |i_\omega\rangle_A. \tag{3.58}$$

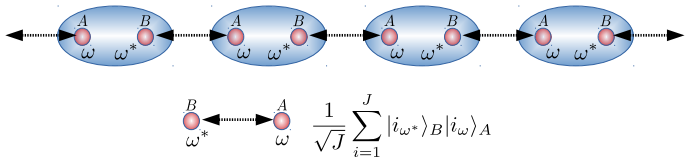

Figure 3.11: SPT state with finite on-site symmetry.

Using this, we can write down the following ground state and parent Hamiltonian

$$|\psi_\omega\rangle = \prod_k |\chi_\omega\rangle_{kk+1}, \tag{3.59}$$

$$H = -\sum_k |\chi_\omega\rangle\langle\chi_\omega|_{kk+1}. \tag{3.60}$$

For general dimensions, it is a difficult task to find the symmetry extension

that will trivialize the SPT phase. However, in 1+1 D, we use the following theorem [117, 118]

Theorem: Every finite group G has associated to it at least one finite group $\tilde{G}$, called a Schur cover, with the property that every projective representation of G can be lifted to an ordinary representation of $\tilde{G}$.

The Schur cover, $\tilde{G}$ is precisely the extension we need to trivialize the system, as we now show. Consider an extension to the original system by introducing an ancillary degree of freedom, which we label C which transform as ω and ω^* projective representations on alternating sites. With this extension, each site transforms as a projective representation under either the following two representations,

$$\tilde{U}_\omega(g) \equiv V(g) \otimes V^*(g) \otimes V(g) \quad \text{or} \quad \tilde{U}_{\omega^*}(g) \equiv V(g) \otimes V^*(g) \otimes V^*(g), \tag{3.61}$$

both of which, from the theorem above is a faithful representation of the Schur cover, $\tilde{G}$. Let us also write down the ground state and Hamiltonian for the extended system

$$|\tilde{\psi}\rangle = |\psi\rangle \prod_{\text{odd } k} |\chi_{\omega^*}\rangle_{CkCk+1}, \tag{3.62}$$

$$\tilde{H} = H - \sum_{\text{odd } k} |\chi_{\omega^*}\rangle\langle\chi_{\omega^*}|_{CkCk+1}. \tag{3.63}$$

To trivialize the extended system, we use the following swap operator

$$\mathcal{S}^\omega_{AB} \equiv \sum_{i=1}^{J}\sum_{j=1}^{J} |i_\omega\rangle\langle j_\omega|_A \otimes |j_\omega\rangle\langle i_\omega|_B. \tag{3.64}$$

Finally, we define the following FDUC $\mathcal{W} = \mathcal{W}_2\mathcal{W}_1$ to trivialize the system as shown in Fig (3.12),

$$\mathcal{W}_1 = \prod_{\text{odd } k} \mathcal{S}^\omega_{C,k,A,k+1}, \tag{3.65}$$

$$\mathcal{W}_2 = \prod_{\text{odd } k} \mathcal{S}^\omega_{A,k,C,k} \prod_{\text{even } k} \mathcal{S}^{\omega^*}_{B,k,C,k}. \tag{3.66}$$

$$\tag{3.67}$$

Applying $\mathcal{W}$, we end up with the following trivial ground state and Hamil-

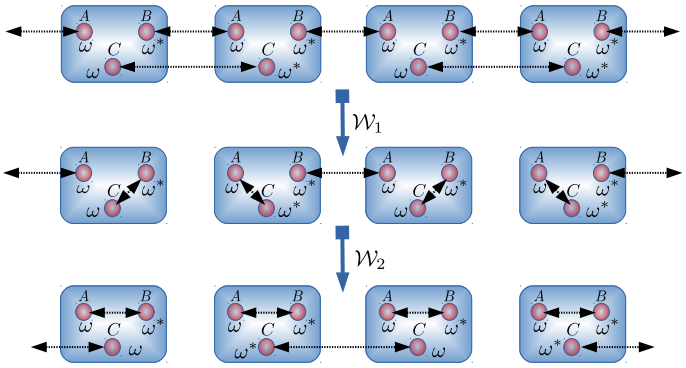

Figure 3.12: Unwinding SPT state with finite on-site symmetry.

tonian

$$\mathcal{W}|\tilde{\psi}\rangle = \prod_k |\chi_{\omega^*}\rangle_{AkBk} \prod_{\text{even } k} |\chi_{\omega}\rangle_{CkCk+1}, \tag{3.68}$$

$$\mathcal{W}\tilde{H}\mathcal{W}^\dagger = -\sum_k |\chi_{\omega^*}\rangle\langle\chi_{\omega^*}|_{AkBk} - \sum_{\text{even } k} |\chi_{\omega}\rangle\langle\chi_{\omega}|_{CkCk+1}. \tag{3.69}$$

3.4 Unwinding fermionic SPT phases

3.4.1 Realizing fermionic SPT phases by stacking Kitaev chains

In this section, we present model Hamiltonians using layers of the so-called Kitaev Majorana chain, which realize short-range-entangled fermionic phases corresponding to the five Altland-Zirnbauer classes that have a non-trivial classification in the free limit in 1+1 d. These classes are D, DIII, BDI, AIII and CII. To connect with the classification in the presence of interactions, we consider particular global symmetries of D, DIII, BDI, AIII and CII – $\mathcal{Z}_2^f$, $\mathcal{Z}_4^T$, $\mathbb{Z}_2^T \times \mathcal{Z}_2^f$, $\mathcal{U}(1) \times \mathbb{Z}_2^T$, $\frac{(\mathcal{U}(1)\times\mathcal{Z}_4^C)}{\mathcal{Z}_2^f} \times \mathbb{Z}_2^T$-symmetries. In the next section, we will demonstrate how a subset of these fermionic phases, which can be interpreted as bosonic SPT phases, can be trivialized by symmetry extension.

A note about the notation used in describing global symmetries in fermionic systems– any Hamiltonian describing the dynamics of fermions commutes with the fermion parity operator, $\hat{P}_f = (-1)^{\hat{N}_f}$. While this can be thought of as a symmetry, which we will call $\mathcal{Z}_2^f$, it is important to note that it can never be explicitly broken. One way to understand this is that this 'symmetry' is imposed by the condition of locality on the Hamiltonian. If we explicitly break

$\mathcal{Z}_2^f$ by adding a term to the Hamiltonian that does not commute with $\hat{P}_f$ like $\delta H = \sum_k \psi_k^\dagger + \psi_k$, the local terms in the Hamiltonian that are far-separated no longer commute rendering the Hamiltonian non-local. Hence, the $\mathcal{Z}_2^f$ symmetry is sometimes implicitly assumed when defining global symmetries in the literature. In this chapter however, we choose to list $\mathcal{Z}_2^f$ explicitly for clarity to avoid any potential confusion. Furthermore, whenever $\mathcal{Z}_2^f$ is part of a symmetry group, we indicate it using a 'mathcal' font.

Class D ($\mathcal{Z}_2^f$-symmetry)

Let us start with the Hamitonian for the Kitaev chain [93] which is a model of spinless fermions (on-site Hilbert space of a single fermionic mode) on a one-dimensional chain as shown in Fig. 3.13:

$$H_{\mathrm{D}} = i \sum_k d_k c_{k+1}. \tag{3.70}$$

c_i and d_i are Majorana operators which are defined in terms of creation and annihilation operators of the fermion mode, $\psi_i, \psi_i^\dagger$ as follows

$$c_i = \psi_i^\dagger + \psi_i, \quad d_i = i\left(\psi_i^\dagger - \psi_i\right). \tag{3.71}$$

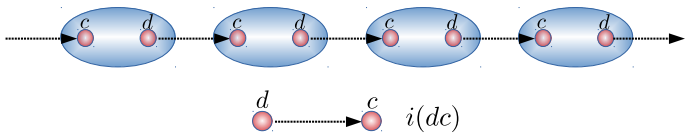

Figure 3.13: The Kitaev chain.

If no other symmetries except $\mathcal{Z}_2^f$ is taken into consideration, this model of free fermions belongs to class D. SRE phases of this class has a $\mathbb{Z}_2$ classification in the non-interacting limit [119, 120] and H_D is a representative of the non-trivial phase. Since this phase is stable to interactions [121, 122], *H_D is a representative of a non-trivial phase of interacting fermions with no symmetries other than $\mathcal{Z}_2^f$*. For completeness, we also mention a representative of the trivial phase with the same symmetries shown in Fig .3.14.

$$H_D^0 = i \sum_k c_k d_k. \tag{3.72}$$

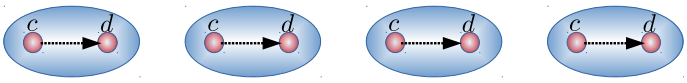

Figure 3.14: The trivial Majorana chain.

Class DIII ($\mathcal{Z}_4^T$-symmetry)

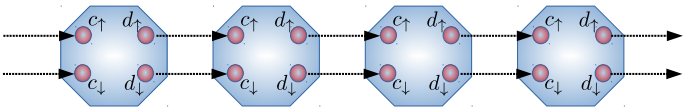

Figure 3.15: Non-trivial DIII chain.

We now consider a Hamiltonian with two species of fermions per unit site, which we will label as $\uparrow$ and $\downarrow$, constructed using two layers of Kitaev chains as shown,

$$H_{\rm DIII} \;=\; i\sum_k \sum_{\sigma=\uparrow,\downarrow} d_{\sigma,k}\; c_{\sigma,k+1}. \tag{3.73}$$

This Hamiltonian commutes with the anti-unitary time-reversal operator $\mathcal{T}$,

$$\mathcal{T} \;=\; \prod_k e^{-\frac{\pi}{4}\left(c_\uparrow c_\downarrow + d_\uparrow d_\downarrow\right)_k}\; \mathcal{K} = \prod_k \frac{(1-c_\uparrow c_\downarrow)_k}{\sqrt{2}} \frac{(1-d_\uparrow d_\downarrow)_k}{\sqrt{2}}\; \mathcal{K}, \tag{3.74}$$

$$\mathcal{T}^2 \;=\; \prod_k \left(ic_{\uparrow,k}d_{\uparrow,k}\right)\left(ic_{\downarrow,k}d_{\downarrow,k}\right) = \hat{P}_f, \tag{3.75}$$

where $\hat{P}_f$ is the fermion parity and $\mathcal{K}$ denotes complex conjugation which has the following action

$$\mathcal{K}i\mathcal{K} \;=\; -i, \quad \mathcal{K}c_\alpha\mathcal{K} = c_\alpha, \quad \mathcal{K}d_\alpha\mathcal{K} = -d_\alpha. \tag{3.76}$$

We denote this symmetry group as $\mathcal{Z}_4^T$ and should be distinguished from $\mathbb{Z}_4^T$ defined in the previous section. The action of $\mathcal{T}$ can be seen in a more conventional form on creation and annihilation operators defined in the usual

way.

$$\psi_{\sigma,k} = \frac{1}{2}\left(c_\sigma + id_\sigma\right)_k, \quad \psi^\dagger_{\sigma,k} = \frac{1}{2}\left(c_\sigma - id_\sigma\right)_k, \tag{3.77}$$

$$\mathcal{T} = \prod_k \left(e^{-i\frac{\pi}{2}\sigma^y_{\alpha\beta}\psi^\dagger_\alpha\psi_\beta}\right)_k \mathcal{K} = \prod_k \left(e^{-i\pi\hat{S}_y}\right)_k \mathcal{K}, \tag{3.78}$$

$$\mathcal{T}\psi_{\alpha,k}\mathcal{T}^{-1} = i\sigma^y_{\alpha,\beta}\ \psi_{\beta,k}. \tag{3.79}$$

With the symmetry $\mathcal{G} = \mathcal{Z}_4^T$, this free fermion model belongs to class DIII. SRE phases of this class has a $\mathbb{Z}_2$ classification in the non-interacting limit [119, 120] and H_{DIII} is a representative of the non-trivial phase. Since this phase is stable to $\mathcal{T}$ invariant interactions [121, 122], *H_{DIII} is a representative of a non-trivial phase of interacting fermions with $\mathcal{G} = \mathcal{Z}_4^T$ symmetry.* For completion, we also mention a representative of the trivial phase with the same symmetries

$$H^0_{\text{DIII}} = i\sum_k \sum_{\sigma=\uparrow,\downarrow} c_{\sigma,k}\ d_{\sigma,k}, \tag{3.80}$$

which is simply two copies of the trivial Hamiltonian (3.72).

Class BDI ($\mathbb{Z}_2^T \times \mathcal{Z}_2^f$-symmetry)

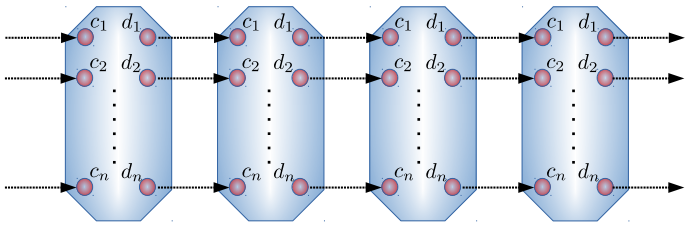

Figure 3.16: Stacked Kitaev chains.

Let us once again consider the Kitaev chain Hamiltonian of Eq. 3.70. It can be checked that the Hamiltonian is invariant under an anti-unitary time-reversal operation that only involves complex conjugation, $\mathcal{T} = \mathcal{K}$ which satisfies $\mathcal{T}^2 = 1$ and we call the group $\mathbb{Z}_2^T$. The full symmetry group is $\mathcal{G} = \mathbb{Z}_2^T \times \mathcal{Z}_2^f$. With this symmetry being considered, the free-fermion Kitaev Hamiltonian (3.70) belongs to class BDI. SRE phases of this class has a $\mathbb{Z}$ classification in the non-interacting limit [119, 120]. We can think of the Kitaev chain to be a *generating* Hamiltonian for all the non-trivial phases in

this class by stacking as shown in Fig. 3.16. Let us list representatives of each non-interacting phase labeled by $n \in \mathbb{Z}$:

$$H^{(n)}_{\text{BDI}} = i \sum_{\alpha=1}^{|n|} \sum_{k} d_{\alpha,k}\ c_{\alpha,k+1} \quad \forall n \in \mathbb{Z}^+, \tag{3.81}$$

$$H^{(n)}_{\text{BDI}} = i \sum_{\alpha=1}^{|n|} \sum_{k} c_{\alpha,k}\ d_{\alpha,k+1} \quad \forall n \in \mathbb{Z}^-, \tag{3.82}$$

$$H^{(0)}_{\text{BDI}} = i \sum_{k} c_k d_k. \tag{3.83}$$

In the presence of interactions, it was shown in [123] that the $n = 8$ Hamiltonian can be smoothly deformed to eight copies of $H^{(0)}_{\text{BDI}}$ without closing the gap. This means that in the presence of interactions, the SPT phases for this global symmetry has a $\mathbb{Z}_8$ classification whose representatives are $H^{(1)}_{\text{BDI}}, \ldots, H^{(8)}_{\text{BDI}}$.

Class AIII ($\mathcal{U}(1) \times \mathbb{Z}_2^T$-symmetry)

If we consider the even members of $H^{(n)}_{\text{BDI}}$, we can associate a $\mathcal{U}(1)$ symmetry in addition to time-reversal and commutes with it. Let us consider $H^{(2)}_{\text{BDI}}$

$$H^{(2)}_{\text{BDI}} = i \sum_{\alpha=1}^{2} \sum_{k} d_{\alpha,k} c_{\alpha,k+1}, \tag{3.84}$$

and the following $\mathcal{U}(1)$ operator which commutes with $\mathcal{T} = \mathcal{K}$,

$$D(\theta) = \prod_{k} e^{-\frac{\theta}{2}(c_1 c_2 + d_1 d_2)_k}. \tag{3.85}$$

To show invariance of (3.84) under $D(\theta)$, let us first look at the action on the Majorana operators,

$$D(\theta) \begin{pmatrix} c_1 \\ c_2 \end{pmatrix}_k D(\theta)^\dagger = \begin{pmatrix} \cos\theta & \sin\theta \\ -\sin\theta & \cos\theta \end{pmatrix} \begin{pmatrix} c_1 \\ c_2 \end{pmatrix}_k, \tag{3.86}$$

$$D(\theta) \begin{pmatrix} d_1 \\ d_2 \end{pmatrix}_k D(\theta)^\dagger = \begin{pmatrix} \cos\theta & \sin\theta \\ -\sin\theta & \cos\theta \end{pmatrix} \begin{pmatrix} d_1 \\ d_2 \end{pmatrix}_k. \tag{3.87}$$

Now, we write the Hamiltonian (3.84) in a suggestive form which makes invariance under $D(\theta)$ manifest,

$$H^{(2)}_{\rm BDI} = i\sum_k \begin{pmatrix} d_1 & d_2 \end{pmatrix}_k \begin{pmatrix} c_1 \\ c_2 \end{pmatrix}_{k+1}, \tag{3.88}$$

$$\begin{aligned} D(\theta)H^{(2)}_{\rm BDI}D(\theta)^\dagger &= i\sum_k \begin{pmatrix} d_1 & d_2 \end{pmatrix}_k \begin{pmatrix} \cos\theta & -\sin\theta \\ \sin\theta & \cos\theta \end{pmatrix} \begin{pmatrix} \cos\theta & \sin\theta \\ -\sin\theta & \cos\theta \end{pmatrix} \begin{pmatrix} c_1 \\ c_2 \end{pmatrix}_{k+1} \\ &= H^{(2)}_{\rm BDI}. \end{aligned} \tag{3.89}$$

Hence, the symmetry group is $\mathcal{G} = \mathcal{U}(1) \times \mathbb{Z}_2^T$. Note that $D(\pi) = \hat{P}_f$ and hence we have used calligraphic script to denote the $\mathcal{U}(1)$ symmetry. This free model belongs to class AIII and SRE phases of this class has a $\mathbb{Z}$ classification. The representatives of each phase $n \in \mathbb{Z}$ can be obtained by considering the even members, $H^{(2n)}_{\rm BDI}$. In the presence of interactions respecting $\mathcal{U}(1) \times \mathbb{Z}_2^T$, the classification reduces to $\mathbb{Z}_4$ whose representatives are simply $H^{(2)}_{\rm BDI}$, $H^{(4)}_{\rm BDI}$, $H^{(6)}_{\rm BDI}$, $H^{(8)}_{\rm BDI}$.

To make things clearer and for future convenience, we perform an on-site basis change using the unitary operator, $M \equiv \prod_k e^{\frac{\pi}{4}(c_2 d_1)_k}$ as shown in Fig.3.17. Let us see the action on $H^{(2)}_{\rm BDI}$:

$$H_{\rm AIII} \equiv MH^{(2)}_{\rm BDI}M^\dagger = i\sum_k \left(c_{2,k}c_{1,k+1} - d_{2,k}d_{1,k+1}\right), \tag{3.90}$$

$$\mathcal{S} \equiv M\mathcal{T}M^\dagger = MM^T\mathcal{K} = \prod_k (c_2 d_1)_k \mathcal{K}, \tag{3.91}$$

$$V(\theta) \equiv MD(\theta)M^\dagger = \prod_k e^{\frac{\theta}{2}(c_1 d_1 - c_2 d_2)_k}. \tag{3.92}$$

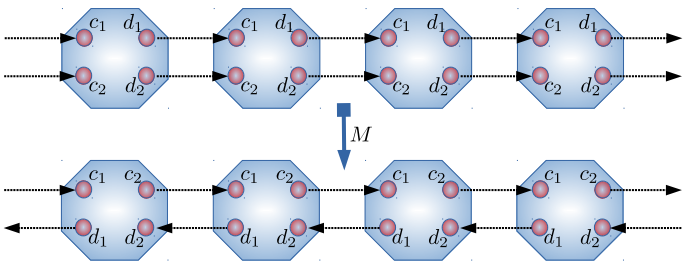

Figure 3.17: Non-trivial AIII chain before and after change of basis.

Let us rewrite the new Hamiltonian $H_{\rm AIII}$ in terms of the following fermion

creation and annihilation operators,

$$\psi_{1,k} \equiv \frac{1}{2}\left(c_1 - id_1\right)_k, \quad \psi_{1,k}^\dagger = \frac{1}{2}\left(c_1 + id_1\right)_k, \tag{3.93}$$

$$\psi_{2,k} \equiv \frac{1}{2}\left(c_2 + id_2\right)_k, \quad \psi_{2,k}^\dagger = \frac{1}{2}\left(c_2 - id_2\right)_k, \tag{3.94}$$

$$H_{\text{AIII}} = 2i\sum_k \left(\psi_{2,i}^\dagger \psi_{1,i+1} + \psi_{2,i}\psi_{1,i+1}^\dagger\right). \tag{3.95}$$

First, note that the $\mathcal{U}(1)$ represented by $V(\theta)$ is now manifest in this form of the Hamiltonian. If we interpret fermions labeled 1 and 2 to be residing on even and odd sites of a chain, H_{AIII} can be viewed as the bipartite hopping model [86, 124, 125] $\sum_{m,n} t_{mn}\psi_m^\dagger \psi_n$ with $t_{mn} = t_{nm}^*$ and has the following chiral symmetry:

$$\mathcal{S}\psi_m\mathcal{S}^{-1} = (-1)^m \psi_m^\dagger, \tag{3.96}$$

$$\mathcal{S}i\mathcal{S}^{-1} = -i. \tag{3.97}$$

For clarity, let us write down the Hamiltonian representatives and the symmetry operators of the four SRE phases written in the new form, labeled $n = 1, 2, 3, 4$.

$$H_{\text{AIII}}^{(n)} = i\sum_{\alpha=1}^{n}\sum_k \left(c_{\alpha,2,k}c_{\alpha,1,k+1} - d_{\alpha,2,k}d_{\alpha,1,k+1}\right), \tag{3.98}$$

$$\mathcal{S} = \prod_k \prod_{\alpha=1}^{n} \left(c_{\alpha,2}d_{\alpha,1}\right)_k \mathcal{K}, \tag{3.99}$$

$$V(\theta) = \prod_k e^{\frac{\theta}{2}\sum_{\alpha=1}^{n}\left(c_{\alpha,1}d_{\alpha,1} - c_{\alpha,2}d_{\alpha,2}\right)_k}. \tag{3.100}$$

Class CII ($\frac{(\mathcal{U}(1)\rtimes\mathcal{Z}_4^C)}{\mathcal{Z}_2^f} \times \mathbb{Z}_2^T$-symmetry)

Let consider two layers of H_{AIII} (3.90) and label them as $\uparrow$ and $\downarrow$ as shown in Fig.3.18,

$$H_{\text{AIII}}^{(2)} \equiv H_{\text{CII}} = i\sum_k \sum_{\sigma=\uparrow,\downarrow} \left(c_{\sigma,2,k}c_{\sigma,1,k+1} - d_{\sigma,2,k}d_{\sigma,1,k+1}\right). \tag{3.101}$$

Note that this contains four fermion species per unit cell labeled by $a = 1, 2$ and $\sigma = \uparrow, \downarrow$. We can now define a unitary charge conjugation symmetry that

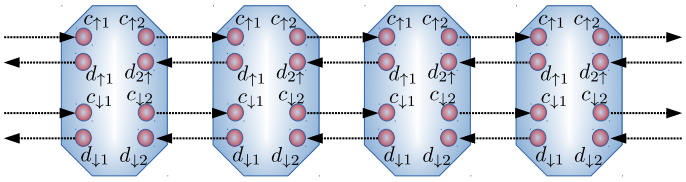

Figure 3.18: Non-trivial CII chain.

commutes with H_{CII} as follows,

$$\mathcal{C} = \prod_k e^{\frac{\pi}{4}\sum_{a=1}^{2}\left(c_{\downarrow,a}c_{\uparrow,a} - d_{\downarrow,a}d_{\uparrow,a}\right)_k}. \tag{3.102}$$

The action of $\mathcal{C}$ is best viewed on the creation and annihilation operators defined previously:

$$\psi_{\sigma,1,k} = \frac{1}{2}\left(c_{\sigma,1} - id_{\sigma,1}\right)_k, \quad \psi^\dagger_{\sigma,1,k} = \frac{1}{2}\left(c_{\sigma,1} + id_{\sigma,1}\right)_k, \tag{3.103}$$

$$\psi_{\sigma,2,k} = \frac{1}{2}\left(c_{\sigma,2} + id_{\sigma,2}\right)_k, \quad \psi^\dagger_{\sigma,2,k} = \frac{1}{2}\left(c_{\sigma,2} - id_{\sigma,2}\right)_k, \tag{3.104}$$

$$\mathcal{C}\psi_{a,\alpha,k}\mathcal{C}^{-1} = i\sigma^y_{\alpha,\beta}\psi^\dagger_{a,\beta,k}. \tag{3.105}$$

Note that $\mathcal{C}^2 = \hat{P}_f$ and the group generated by it is $\mathcal{Z}_4^C$. Furthermore, $\mathcal{C}$ commutes with the chiral symmetry $\mathcal{S}$ but not with the $\mathcal{U}(1)$ symmetries making the symmetry group $\mathcal{G} = \frac{(\mathcal{U}(1)\rtimes\mathcal{Z}_4^C)}{\mathcal{Z}_2^f} \times \mathbb{Z}_2^T$

$$\mathcal{S} = \prod_k \prod_{\sigma=\uparrow,\downarrow}^{n} \left(c_{\sigma,2}d_{\sigma,1}\right)_k \mathcal{K}, \quad \mathcal{C}\mathcal{S}\mathcal{C}^{-1} = \mathcal{S}, \tag{3.106}$$

$$V(\theta) = \prod_k e^{\frac{\theta}{2}\sum_{\sigma=\uparrow,\downarrow}^{n}\left(c_{\sigma,1}d_{\sigma,1} - c_{\sigma,2}d_{\sigma,2}\right)_k}, \quad \mathcal{C}V(\theta)\mathcal{C}^{-1} = V(-\theta). \tag{3.107}$$

With this symmetry, the free fermion Hamiltonian (3.101) belongs to class CII. SRE phases of this class has a $\mathbb{Z}$ classification in the non-interacting limit and H_{CII} is the generating representative of the non-trivial phases via stacking in the manner described in the previous subsections. In the presence of symmetry respecting interactions however, the classification breaks down to $\mathbb{Z}_2$ and H_{CII} is a representative of the non-trivial phase. Finally, for completion, let us also state the Hamiltonian that corresponds to the trivial phase for this symmetry group,

$$H^0_{\text{CII}} = i\sum_k \sum_{\sigma=\uparrow,\downarrow} \left(c_{\sigma,1,k}c_{\sigma,2,k} - d_{\sigma,1,k}d_{\sigma,2,k}\right). \tag{3.108}$$

3.4.2 Unwinding four-layer fermionic SPT phases: Class CII, AIII and BDI

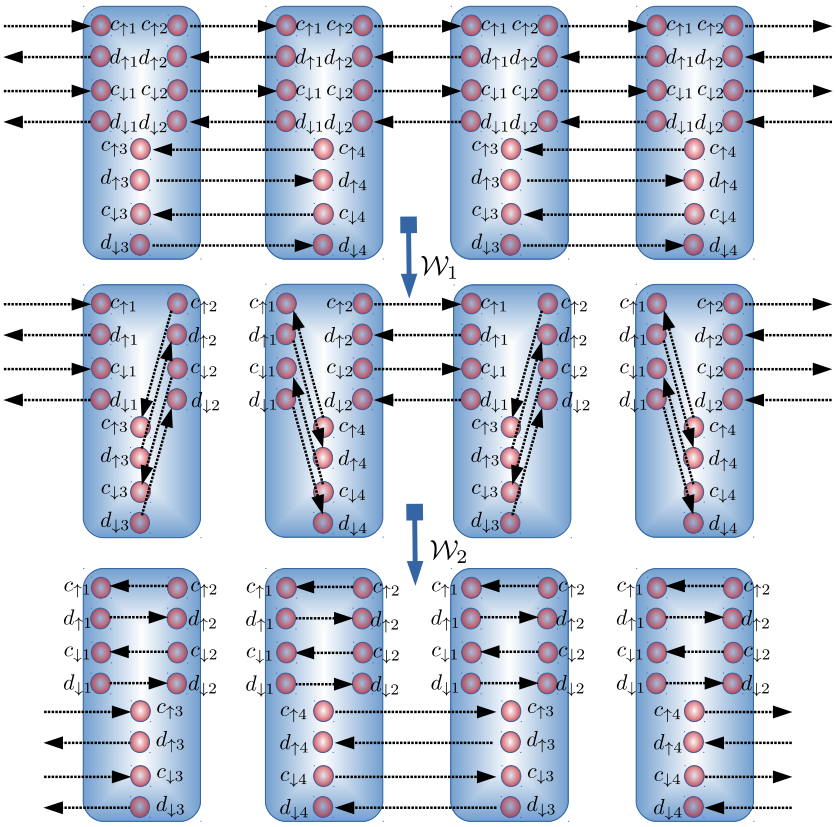

Figure 3.19: Trivialization of the non-trivial CII chain.

In this section we consider the fermion SPT phases that are constructed using 4 layers of Kitaev chains. Even though these are fermionic SPT phases, it has been understood that the non-trivial SPT nature for these phases can be understood as bosonic SPT phases belonging to Haldane phase [53, 126]. We trivialize these using an extension that was used before for the bosonic SPT phases that is we extend the anti-unitary $\mathbb{Z}_2^T$ part of the symmetry to $\mathbb{Z}_4^T$ and leave the other symmetry generators of unchanged.

$$1 \longrightarrow \mathbb{Z}_2 \xrightarrow{i} \mathbb{Z}_4^T \xrightarrow{s} \mathbb{Z}_2^T \longrightarrow 1. \tag{3.109}$$

Note that the symmetry groups described in the previous section for various

symmetry classes have the following embedding

$$\text{CII}\ \left(\frac{(\mathcal{U}(1)\rtimes\mathcal{Z}_4^C)}{\mathcal{Z}_2^f}\times\mathbb{Z}_2^T\right)\xrightarrow[\mathcal{Z}_4^C]{\text{Disregard}}\text{AIII}\ (\mathcal{U}(1)\times\mathbb{Z}_2^T)\xrightarrow[\mathcal{U}(1)]{\text{Disregard}}\text{BDI}\ (\mathbb{Z}_2^T\times\mathcal{Z}_2^f).$$

As a result by disregarding successive symmetries as mentioned above, trivializing H_{CII} results in trivializing the SPT phase of $H^{(2)}_{\text{AIII}}$ (n=2 in $\mathbb{Z}_4$ classification) and $H^{(4)}_{\text{BDI}}$ (n=4 in the $\mathbb{Z}_8$ classification). Let us now go into the details of how this is achieved. As we did for the bosonic case, we add additional degrees of freedom corresponding to two extra fermions per unit site. We will label the Majorana operators that correspond to these as $c_{3,\sigma,k}, d_{3,\sigma,k}$ for odd sites k and $c_{4,\sigma,k}, d_{4,\sigma,k}$ for even sites k. We will see that this makes the local Hilbert space transform as a faithful representation of the extended symmetry $\tilde{\mathcal{G}}=\left(\frac{(\mathcal{U}(1)\rtimes\mathcal{Z}_4^C)}{\mathcal{Z}_2^f}\times\mathbb{Z}_4^T\right)$. Furthermore, we add terms to the Hamiltonian H_{CII} corresponding to a trivial dimerized state for the new degrees of freedom. The new Hamiltonian and symmetry operators are

$$\begin{aligned}
\tilde{H}_{\text{CII}} &= i\sum_{\sigma=\uparrow,\downarrow}\left[\sum_k\left(c_{\sigma,2,k}c_{\sigma,1,k+1}-d_{\sigma,2,k}d_{\sigma,1,k+1}\right)-\sum_{\text{odd }k}\left(c_{\sigma,3,k}c_{\sigma,4,k+1}-d_{\sigma,3,k}d_{\sigma,4,k+1}\right)\right],\\
\tilde{\mathcal{S}} &= \prod_{\text{odd }k}\prod_{\sigma=\uparrow,\downarrow} i\left(c_{2,\sigma}d_{1,\sigma}d_{3,\sigma}\right)_k\quad\prod_{\text{even }k}\prod_{\sigma=\uparrow,\downarrow} i\left(c_{2,\sigma}d_{1,\sigma}c_{4,\sigma}\right)_k\quad\mathcal{K},\\
V(\theta) &= \prod_{\text{odd }k} e^{\frac{\theta}{2}\sum_{\sigma=\uparrow,\downarrow}\left(c_{\sigma,1}d_{\sigma,1}-c_{\sigma,2}d_{\sigma,2}+c_{\sigma,3}d_{\sigma,3}\right)_k}\quad\prod_{\text{even }k} e^{\frac{\theta}{2}\sum_{\sigma=\uparrow,\downarrow}\left(c_{\sigma,1}d_{\sigma,1}-c_{\sigma,2}d_{\sigma,2}-c_{\sigma,4}d_{\sigma,4}\right)_k},\\
\mathcal{C} &= \prod_{\text{odd }k} e^{\frac{\pi}{4}\sum_{a=1,2,3}\left(c_{\downarrow,a}c_{\uparrow,a}-d_{\downarrow,a}d_{\uparrow,a}\right)_k}\quad\prod_{\text{even }k} e^{\frac{\pi}{4}\sum_{a=1,2,4}\left(c_{\downarrow,a}c_{\uparrow,a}-d_{\downarrow,a}d_{\uparrow,a}\right)_k}.
\end{aligned}$$

It can be seen that $\tilde{S}^2$ is *locally* -1 on both even and odd sites and hence is an extension of the original symmetry. This system can be trivialized using a 2-layer FDUC $\mathcal{W}=\mathcal{W}_2\mathcal{W}_1$ as shown in Fig.3.19 where

$$\begin{aligned}
\mathcal{W}_1 &= \prod_{\text{odd }k}\exp\left[-\frac{\pi}{4}\sum_{\sigma=\uparrow,\downarrow}\left(c_{\sigma,3,k}c_{\sigma,1,k+1}+d_{\sigma,3,k}d_{\sigma,1,k+1}\right)\right], \qquad (3.110)\\
\mathcal{W}_2 &= \prod_{\text{odd }k}\exp\left[-\frac{\pi}{4}\sum_{\sigma=\uparrow,\downarrow}\left(c_{\sigma,3}c_{\sigma,1}+d_{\sigma,3}d_{\sigma,1}\right)_k\right]\prod_{\text{even }k}\exp\left[\frac{\pi}{4}\sum_{\sigma=\uparrow,\downarrow}\left(c_{\sigma,4}c_{\sigma,2}+d_{\sigma,4}d_{\sigma,2}\right)_k\right].
\end{aligned}$$

With a bit of straight forward algebra, it can be checked that $\mathcal{W}_1$ and $\mathcal{W}_2$ commute with the symmetry generators and the application of this FDUC

does indeed leave us with a trivial Hamiltonian.

$$\mathcal{W}\tilde{H}_{\mathrm{CII}}\mathcal{W}^{-1} = i\sum_{\sigma=\uparrow,\downarrow}\left[\sum_{k}\left(c_{\sigma,1,k}c_{\sigma,2,k} - d_{\sigma,1,k}d_{\sigma,2,k}\right) - \sum_{\text{even } k}\left(c_{\sigma,4,k}c_{\sigma,3,k+1} - d_{\sigma,4,k}d_{\sigma,3,k+1}\right)\right]. \tag{3.111}$$

We conclude this section by summarizing the result of symmetry extension presented above on the classification of fermionic SPT phases in 1+1D.

Cartan class	Symmetry group G	Extended group $\tilde{G}$	Reduced classification
BDI	$\mathbb{Z}_2^T \times \mathcal{Z}_2^f$	$\mathbb{Z}_4^T \times \mathcal{Z}_2^f$	$\mathbb{Z}_8 \to \mathbb{Z}_4$
AIII	$\mathcal{U}(1) \times \mathbb{Z}_2^T$	$\mathcal{U}(1) \times \mathbb{Z}_4^T$	$\mathbb{Z}_4 \to \mathbb{Z}_2$
CII	$\frac{(\mathcal{U}(1)\rtimes \mathcal{Z}_4^C)}{\mathcal{Z}_2^f} \times \mathbb{Z}_2^T$	$\frac{(\mathcal{U}(1)\rtimes \mathcal{Z}_4^C)}{\mathcal{Z}_2^f} \times \mathbb{Z}_4^T$	$\mathbb{Z}_2 \to 1$

Table 3.1: Summary of fermionic SPT phases and the change classification by symmetry extension.

3.5 Summary and outlook

In this chapter, using several examples, we have demonstrated how SPT phases can be unwound by symmetry extension. While the situation for bosonic SPT phases classified by group cohomology is clear, we have only been able to demonstrate this for fermionic SPT phases which can be interpreted as bosonic ones. Whether such an unwinding by symmetry extension is possible for inherently fermionic SPT phases is interesting to explore. Furthermore, for bosonic SPT phases, as shown in Ref. [92], the extended groups have a physical interepretation in terms of the data that can describe a symmetric long-range-entangled boundary theory for the SPT phase. It would also be interesting to see if a similar thing is also possible for fermionic SPT phases. Finally, working out concrete examples in higher dimensions might be instructive where the possibilities are more numerous and complex. We leave these questions for future investigation.

Part II

Computational phases of matter

Chapter 4

SPT phases for MBQC

The contents of this chapter are published in Ref. [36] completed in collaboration with Tzu-Chieh Wei. Follow up work, briefly mentioned in the last section is published in Refs.[34, 35] in collaboration with David Stephen, Robert Raussendorf, Dongsheng Wang and Tzu-Chieh Wei as well as in Ref. [127] in collaboration with Yanzhu Chen and Tzu-Chieh Wei.

4.1 Introduction

Symmetry-protected topological (SPT) phases have topological order that is not characterized by a local order parameter and their existence requires symmetry to be preserved [51–55]. Ground states of topologically non-trivial SPT phases cannot be continuously connected to trivial product states without either closing the gap or breaking the protected symmetry. In one dimension, a particularly useful way to describe ground states is the matrix-product-state (MPS) representation [67, 69, 128] and this has led to many interesting results including a complete classification of SPT phases [52]. In addition to classifying SPT phases, an intriguing connection of SPT phases to quantum computation was identified in Ref. [32] that SPT ground states of $\mathbb{Z}_2 \times \mathbb{Z}_2$ symmetry can serve as resource states for realizing certain gate operations in quantum computation by local measurement.

Measurement-based quantum computation (MBQC) [112, 113, 129] is a quantum computational scheme that makes use of only local measurements on a suitably entangled resource state. It was originally invented with a specific resource state, i.e., the cluster state [112] but was subsequently shown to be supported by a variety of systems [130–133], in particular, the Affleck-Kennedy-Lieb-Tasaki (AKLT) states [45, 134] on various one- and two-dimensional systems [135–140]. In Ref. [32] it was observed that both the 1D cluster and

AKLT states, which are capable of supporting arbitrary single-qubit gates, belong to a 1D SPT phase protected by $\mathbb{Z}_2 \times \mathbb{Z}_2$ on-site symmetry. Moreover other ground states of this phase also support a protected identity gate operation and can act as perfect wires for transmission of quantum information. The results in Ref. [32] hinge on features of specific Abelian groups, *i.e.*, groups whose projective representation possesses a maximally non-commutative factor system. This brings forth several interesting questions:

1. Can we extend the results of Ref [32] to get the ground-state form of SPT phases protected by an arbitrary group (both Abelian and non-Abelian)?

2. Are there SPT phases protected by other groups which protect the perfect operation of the identity gate?

3. Are there SPT phases where other non-trivial operations are also allowed? Is it possible to find an entire SPT phase whose ground states support universal one-qubit gates?

Here we develop a formalism that addresses (1) and allows us to treat an arbitrary finite group G, either Abelian or non-Abelian, so that we can examine the associated SPT ground states and protected gate operations. The results of Ref. [32] on the spin-1 system with $\mathbb{Z}_2 \times \mathbb{Z}_2$ are reproduced in this formulation. To address (2), we find that in addition to $\mathbb{Z}_2 \times \mathbb{Z}_2$, 1D topologically non-trivial SPT phases associated with the symmetry groups A_4 (the alternating group of degree 4) and S_4 (the symmetric group of degree 4), see Sec 4.4, acting on a three-dimensional on-site irreducible representation (i.e., physical spin-1 entities) also protect the identity gate operation. The latter group was also studied in Ref. [37].

We only make partial progress in answering (3) in this chapter. We consider an example Hamiltonian with A_4 and parity invariance and study its ground states in various parameter regimes. This Hamiltonian can be regarded as perturbing the AKLT Hamiltonian. We find an extended region in the parameter space where the ground state is exactly the AKLT state and hence can be used as a resource state capable of universal single-qubit gate operations. Whether or not it is generic that the imposition of an appropriate set of symmetries can allow the entire region of an SPT phase to support protected universal single-qubit gates remains an open question. There has however been progress in reducing certain SPT ground states into resource states that support universal single-qubit operations by a 'buffering' technique [37], which in some sense gives an affirmative answer to (3).

The rest of the chapter is organized as follows. In Sec 4.2, we review the matrix-product state formalism and its connection to quantum computation,

and their utility in SPT phases. In Sec 4.3, we present the key results of our formalism that can determine, in terms of MPS, the structure of SPT ground states constrained by symmetry. The method we used was inspired by Refs. [141–144] where they consider imposing global symmetries such as $SU(2)$ and $U(1)$ for application in numerical simulations. The formalism we develop here might also find its application in numerical simulations with discrete symmetries imposed [71]. In Sec. 4.4, we use our formalism to examine SPT phases and their non-trivial ground states protected by symmetries such as $\mathbb{Z}_2 \times \mathbb{Z}_2$, D_4, A_4 and S_4. In Sec. 4.5, we study a specific Hamiltonian that is A_4 symmetric by perturbing the AKLT Hamiltonian and study its ground states. We find an extended region where the ground states are identical to the AKLT state, which allows universal single qubit operations. We conclude in Sec. 4.6.

4.2 Review of relevant definitions and results

4.2.1 Definition of a gapped phase of matter

In Ref. [51], it was argued that in order to talk about phases of matter, we need to specify the class of Hamiltonians we are considering. Two gapped Hamiltonians from a given class are in the same phase if we can 'connect' them smoothly without closing the spectral gap. Otherwise, there is a boundary in the space of Hamiltonians where the gap closes separating different phases of matter [51, 52]. In 1D, if we consider the class of all gapped local Hamiltonians, it has been shown [51] that they all belong to the same phase and we can connect any two such Hamiltonians without closing the gap by adding suitable local operators. Thus, there is no *intrinsic* topological order in 1D and all Hamiltonians can be connected to those in the trivial phase with product ground states. In other words, any ground state can be connected to a product state. On the other hand, if we restrict ourselves to a class of Hamiltonians that respect some global symmetry, there are generally phase boundaries which arise. We cannot connect Hamiltonians in different phases through symmetry respecting operators without closing the gap. Different phases are characterized by a combination of *symmetry fractionalization* and *symmetry breaking* [52]. When symmetry is not broken, the unique ground states of these *Symmetry Protected Topological* (SPT) phases respect the symmetry of the Hamiltonian and allow us to write down their form using tools from the representation theory of groups. Much of this is possible by using the matrix-product-state representation of gapped ground states of 1D spin chains which we shall briefly review below.

4.2.2 Matrix product states

We begin by giving a brief review of the *Matrix Product State* representation of many-body wavefunctions in 1D [67] which was introduced in Ch.2. Consider a one-dimensional chain of N spins. If the Hilbert space of each spin is d-dimensional, the Hilbert space of the spin chain itself is d^N-dimensional. This means that the number of coefficients needed to describe the wavefunction of the spin chain grows exponentially with the length of the chain. However, if the spin chain is in the ground-state configuration of a gapped Hamiltonian, it can be efficiently written as an MPS wavefunction [68–70]. To do this, we need to associate for every spin site (labeled by $m = 1 \dots N$), a $D_m \times D_{m+1}$-dimensional matrix $A_m^{i_m}$ for each basis state $|i_m\rangle = |1\rangle \dots |d\rangle$. $D = max_m(D_m)$ is the maximum 'virtual' or 'bond' dimension and approaches a constant value that is independent of the size of the chain for gapped spin chains [69]. With these matrices (which we shall refer to as MPS matrices), we can write the wavefunction with periodic boundary conditions as:

$$|\psi\rangle = \sum_{i_1 \dots i_N} Tr[A_1^{i_1} A_2^{i_2} \dots A_N^{i_N}] |i_1\rangle \dots |i_N\rangle. \tag{4.1}$$

We can also write down the wavefunction for a finite chain as

$$|\psi\rangle = \sum_{i_1 \dots i_N} \langle L| A_1^{i_1} A_2^{i_2} \dots A_N^{i_N} |R\rangle |i_1\rangle \dots |i_N\rangle, \tag{4.2}$$

where, the vectors $|L\rangle$ and $|R\rangle$ live in the virtual space and encode the boundary conditions for the finite chain. If we consider the class of local gapped Hamiltonians without any symmetry constraint, Eqs. (4.1,4.2) would represent the general form of ground states. This means we need about Nd matrices to specify the ground state.

4.2.3 Matrix product states and measurement-based quantum computation

To demonstrate the motivation for this work, we first see how we can use MPS wavefunctions for MBQC in the virtual space. Consider encoding quantum information that needs to be processed in one of the virtual boundary vectors of Eq. (4.2), say $|R\rangle$ [131, 132, 145, 146]. If we perform a projective measurement of the N-th spin in some basis $\{|\phi_N^i\rangle\}$ with the outcome being a projection of the spin onto state $|\phi_N'\rangle \in \{|\phi_N^i\rangle\}$, we can write the wavefunction

of the remaining $N-1$ spins as $|\psi'\rangle = \langle\phi'_N|\psi\rangle$ *i.e*

$$|\psi'\rangle = \sum_{i_1 \ldots i_{N-1}} \langle L|A_1^{i_1} A_2^{i_2} \ldots A_{N-1}^{i_{N-1}}|R'\rangle|i_1\rangle \ldots |i_{N-1}\rangle, \tag{4.3}$$

where $|R'\rangle = A'_N|R\rangle$ can be regarded as resulting from $|R\rangle$ undergoing a linear transformation $A'_N = \sum_{i_N} \langle\phi'_N|i_N\rangle A_N^{i_N}$.

Thus, if we know all the MPS matrices $A_m^{i_m}$ and if these matrices span the space of relevant operations on the virtual vector, we can hope to induce any transformation on the vector by measurement in an appropriate choice of basis. Usually, there is also an overall residual operator which we can account for by adapting subsequent bases of measurement.

Let us demonstrate this using two translationally invariant canonical resource states. First, the cluster state [113, 134] is a $d = 2$ spin chain whose wavefunction can be written in terms of $D = 2$ MPS matrices:

$$A^0 = \begin{pmatrix} 1 & 0 \\ 1 & 0 \end{pmatrix}, \; A^1 = \begin{pmatrix} 0 & 1 \\ 0 & -1 \end{pmatrix} \tag{4.4}$$

Measuring in the $|\pm\rangle = \frac{1}{\sqrt{2}}(|0\rangle \pm |1\rangle)$ basis results in the operation $|R\rangle \mapsto H(\sigma_z)^s|R\rangle$ where s labels the measurement outcome and is 0/1 if the outcome is $|\pm\rangle$ and H is the Hadamard gate $H \equiv \frac{1}{\sqrt{2}}\begin{pmatrix} 1 & 1 \\ 1 & -1 \end{pmatrix}$. The measurement thus induces the Hadamard operation up to residual operators $(\sigma_x)^s$ as $H(\sigma_z)^s = (-1)^s(\sigma_x)^s H$.

We can induce a different operation, say $R_z(\theta) = e^{-i\theta\sigma_z/2}$ by measuring in the basis $|\phi, \pm\rangle = \frac{1}{\sqrt{2}}(|0\rangle \pm e^{i\phi}|1\rangle)$. This results in the operation $|R\rangle \mapsto H(\sigma_z)^s e^{-i\phi\sigma_z/2}|R\rangle$ where s is the measurement outcome which is 0/1 if the outcome is $|\phi, \pm\rangle$. This is a single-qubit rotation by ϕ about the Z axis up to the operator $H(\sigma_z)^s$.

Similarly, we can also perform rotations about the other orthogonal axes and using sequential rotations about different axes by appropriate angles (using, for example, the Euler angle parametrization for rotations), we can perform any arbitrary single-qubit rotation.

The second prominent resource state is the AKLT state [45, 134, 135] which is a spin-1 ($d = 3$) system whose wavefunction can be described by $D = 2$ MPS matrices:

$$A^i = \sigma_i \;\; (i = x, y, z), \tag{4.5}$$

where the basis of the spins $\{|x\rangle, |y\rangle, |z\rangle\}$ is chosen as

$$|x\rangle \equiv \frac{1}{\sqrt{2}}(|-1\rangle - |1\rangle), |y\rangle \equiv \frac{i}{\sqrt{2}}(|-1\rangle + |1\rangle), |z\rangle \equiv |0\rangle,$$

with $|\pm 1\rangle$ and $|0\rangle$ being eigenstates of the spin-1 S_z operator. If we measure the spin in $\{|x\rangle, |y\rangle, |z\rangle\}$ basis, we can induce the operation $|R\rangle \mapsto \sigma_s|R\rangle$ which is the identity operation up to the residual operator σ_s. We can also induce $R_z(\theta) = e^{-i\theta\sigma_z/2}$ by measuring in the basis $\{|\theta, x\rangle = \cos(\frac{\theta}{2})|x\rangle - \sin(\frac{\theta}{2})|y\rangle, |\theta, y\rangle = \sin(\frac{\theta}{2})|x\rangle + \cos(\frac{\theta}{2})|y\rangle, |z\rangle\}$. If the measurement outcome is $|z\rangle$ then we have the identity operation with residual operator σ_z. However, if the outcome is $|\theta, x\rangle$ or $|\theta, y\rangle$ then the operation is $|R\rangle \mapsto \sigma_i e^{(-i\theta\sigma_z/2)}|R\rangle$ where $i = x/y$ if the outcome is $|\theta, i\rangle$. Thus, if we keep measuring till we get either $|\theta, x\rangle$ or $|\theta, y\rangle$ as the outcome, we can induce the required operation up to Pauli residual operators. The extension to rotations about other axes and ultimately to a full set of single-qubit rotations is straightforward. An important difference between the AKLT and cluster states is that for the latter, the length of the spin chain needed for computation is fixed while for the former, it is not.

It was noted that both the 1D AKLT and cluster states belong to a non-trivial topological phase protected by $\mathbb{Z}_2 \times \mathbb{Z}_2$ symmetry [46, 54] and there have been investigations to see if the ability to support quantum computation can be a property of the phase [32, 33, 116, 147, 148]. In particular, the authors of [32, 33] deduce that any non-trivial MPS ground state in the non-trivial $\mathbb{Z}_2 \times \mathbb{Z}_2$ invariant spin-1 Hamiltonians (Haldane phase) must have the form $A^i = B_i \otimes \sigma_i$ $(i = x, y, z)$. Thus, there always exists a 'protected' two-dimensional virtual subspace in the ground states of the Haldane phase on which the Pauli matrices act and in which quantum information can in principle be encoded and processed. While the ground states of the Haldane phase in general do not support non-trivial gate operations, they do allow a protected identity gate operation by measurements in the $\{|x\rangle, |y\rangle, |z\rangle\}$ basis that only induces Pauli operation on the boundary vectors.

4.3 Main result: Tensor decomposed ground-state form in the presence of a global symmetry

4.3.1 SPT phases with an on-site internal symmetry

Let us now consider symmetric phases of Hamiltonians that are invariant under the action of a certain symmetry group G on each spin according to some representation $u(g)$. i.e. $[H, \hat{U}(g)] = 0$ where $\hat{U}(g) = u_1(g) \otimes \cdots \otimes u_N(g)$. We consider ground states that do not break the symmetry of the Hamiltonian and are hence left invariant under the transformation $\hat{U}(g)$ up to a complex phase

$$\hat{U}(g)|\psi\rangle = \chi(g)^N|\psi\rangle. \tag{4.6}$$

Eq. (4.6) can be imposed as a condition on the MPS matrix level (Suppressing the site labels for brevity) as [51–54]

$$u(g)_{ij}A^j = \chi(g)V^{-1}(g)A^iV(g). \tag{4.7}$$

Note that here and henceforth, when no confusion will arise, we use the Einstein summation convention wherein repeated indices are summed over. Because u is a group representation, group properties impose χ to be a 1D representation and V to be a *projective representation* of G. A projective representation respects group multiplication up to an overall complex phase.

$$V(g_1)V(g_2) = \omega(g_1, g_2)V(g_1g_2). \tag{4.8}$$

The complex phases $\omega(g_1, g_2)$ are constrained by associativity of group action and fall into classes labelled by the elements of the second cohomology group of G $H^2(G, U(1))$ (See Appendix B.1 for some comments on projective representations). In other words, the different elements of $H^2(G, U(1))$ label different classes of projective representations. It was also shown in [51–55] that the different elements of $H^2(G, U(1))$ represent different SPT phases of matter. In particular, the identity element labels the set of *linear representations* of G (which respect group multiplication exactly) and the corresponding phase of matter is trivial, containing product ground states. We now use the symmetry constraint of Eq. (2.10) to deduce the form of the MPS matrices for a given phase labelled by $\omega \in H^2(G, U(1))$ using a technique similar to the one presented in [141].

With only on-site symmetry, the different 1D representations χ all correspond to the same SPT phase [51, 52]. Hence, we just consider the case when

$\chi(g) = 1$ *i.e.* the trivial 1D irreducible representation (irrep) of G. With this, we can rewrite Eq. (2.10) in a more illuminating form:

$$u(g)_{ii'} V(g)_{\alpha\alpha'} V^{-1}(g)_{\beta'\beta} A^{i'}_{\alpha'\beta'} = A^{i}_{\alpha\beta}. \tag{4.9}$$

Eq. (4.9) shows that the matrices A^i are invariant 3 index tensors. We now organize the vector space of each index as a reduced representation constructed out of copies of linear or projective irreps of G.

$$\mathbb{V} \cong \bigoplus_a n_a \mathbb{V}_a \cong \bigoplus_a \mathbb{D}_a \otimes \mathbb{V}_a. \tag{4.10}$$

If $\mathbb{V}$ is the vector space of any index, a runs over the irreps, n_a is the degeneracy (number of copies) of the irrep a and $\mathbb{D}_a$ is the corresponding degeneracy vector space of a. Any basis element in the vector space $\mathbb{V}$ can be labelled by three numbers as $|a_i, m_i, d_i\rangle$ where a_i labels the irreducible representation and is analogous to the angular momentum label in $SU(2)$, m_i labels the state in a_i and is analogous to the azimuthal quantum number m_i and d_i labels which copy of the irreducible representation a_i is being considered. Symmetry transformations are block-diagonal and act on the m_i labels of each sector a_i but leave the d_i labels alone. So if $U(g)$ is a symmetry that acts on the vector space Eq. (4.10) and if $U^a(g)$ is the representation of the a-th irrep then

$$U(g) \cong \bigoplus_a \mathbb{1}^a \otimes U^a(g). \tag{4.11}$$

Note that for a given physical system, we assume that the vector space of the physical index is known in terms of which irreps and how many copies are contained. However, for a given $\omega \in H^2(G, U(1))$ which labels the phase we are trying to study the ground-state form of, we have to allow an arbitrary number of copies of each projective irrep from the class ω to appear in the virtual space indices. Using this organization, Eq. (4.9) and an application of Schur's lemma after decomposing the fusion of the irreps a_i and a_α determined by the Clebsch-Gordan (CG) series $i \otimes \alpha = \oplus_\gamma n_{i\alpha}^\gamma \gamma$ (see Appendix 4.3.2 for more details), we can write down the MPS matrices for the SPT phase labelled by ω using a generalized Wigner-Eckart theorem as follows

$$A[\omega]^{a_i m_i d_i}_{(a_\alpha m_\alpha d_\alpha)(a_\beta m_\beta d_\beta)} = \sum_{n=1}^{n_{i\alpha}^\beta} B^{a_i d_i}_{(a_\alpha d_\alpha)(a_\beta d_\beta; n)} C[\omega]^{a_\beta m_\beta; n}_{a_i m_i, a_\alpha m_\alpha}, \tag{4.12}$$

where $C[\omega]^{a_\beta m_\beta; n}_{a_i m_i, a_\alpha m_\alpha}$ denotes the CG coefficients associated with the change of

basis of the direct product of linear irrep i and the irrep α of projective class ω, to the n-th copy of irrep β of the same projective class ω (See Appendix 4.3.2 for more details)

$$|a_\beta, m_\beta; n\rangle = \sum_{a_i, m_i, a_\alpha, m_\alpha} C[\omega]^{a_\beta m_\beta; n}_{a_i m_i, a_\alpha m_\alpha} |a_i, m_i\rangle |a_\alpha, m_\alpha\rangle. \tag{4.13}$$

The entries $B^{a_i d_i}_{(a_\alpha d_\alpha)(a_\beta d_\beta; n)}$ of the MPS matrices are not determined by on-site symmetry considerations alone and depend on the parameters of the Hamiltonian amongst other things. Finally, putting back the site dependence, $\mathfrak{m} = 1 \cdots N$ in the MPS matrices, we have

$$A[\omega]^{a_i m_i d_i}_{(a_\alpha m_\alpha d_\alpha)(a_\beta m_\beta d_\beta); \mathfrak{m}} = \sum_{n=1}^{n^\beta_{i\alpha}} B^{a_i d_i}_{(a_\alpha d_\alpha)(a_\beta d_\beta; n); \mathfrak{m}} C[\omega]^{a_\beta m_\beta; n}_{a_i m_i, a_\alpha m_\alpha}, \tag{4.14}$$

We see that to construct the ground-state form of an SPT phase labelled by ω, we need the CG coefficients for the direct product of the linear representation of the physical spins and the projective irreps of class ω: $|i\rangle$ and $|\alpha\rangle$. To make sense this, we use the result that every finite group G has associated to it at least one other finite group $\tilde{G}$, called a Schur cover, with the property that every projective representation of G can be lifted to a linear representation of $\tilde{G}$ [149]. So we can reinterpret the CG coefficients of a linear and projective representation of G simply as the CG coefficients of two linear representations of $\tilde{G}$. For example, half odd integer j representations are projective representations of $SO(3)$ while integer j are linear representations. However, if we consider the group $SU(2)$ which is the cover of $SO(3)$, both half odd integer and integer j are linear representations and we know that we can find CG coefficients for decompositions of the kind $1 \otimes \frac{1}{2} = \frac{1}{2} \oplus \frac{3}{2}$.

To summarize, in order to find the ground-state forms of different SPT phases of a spin chain that transforms under a certain representation $u(g)$ of G, we need to follow the following steps:

1. Obtain the second cohomology group of G, $H^2(G, U(1))$ whose elements ω will label the different SPT phases.
2. Obtain the covering group $\tilde{G}$
3. Identify the irreps 'i' of the physical spin among the irreps of $\tilde{G}$.
4. Identify the irreps 'α' that correspond to the projective class ω.
5. Obtain CG coefficients corresponding to the fusion of the irreps of the physical spin with each irrep of the projective class ω. (Ref. [150] and

Appendix B.4 gives a technique to calculate the CG coefficients for certain types of decompositions of finite group irreps)

6. Use the CG coefficients in Eq. (4.14) allowing α and β to run over all the irreps of class ω and i to run over the irreps of the physical spin. Each block of the MPS matrices split into a part that is calculated purely from the group G for each phase ω and a part that is undetermined.

4.3.2 Obtaining the tensor decomposition of Eq. (4.12)

For what follows, it is useful to employ a basis independent representation of the tensor A,

$$\hat{A} = \sum_{i\alpha\beta} A^i_{\alpha\beta} |i\alpha\rangle\langle\beta| \tag{4.15}$$

We organize the vector space of each index and label it by three quantum numbers–the irrep a_j (analogous to the spin label j), the irrep multiplicity m_j (analogous to the azimuthal quantum number m_j) and the irrep degeneracy (the number of copies of the irrep, d_j), i.e., $|i\rangle = |a_i, m_i, d_i\rangle$, $|\alpha\rangle = |a_\alpha, m_\alpha, d_\alpha\rangle$ and so on.

$$\hat{A} = A^{a_i m_i d_i}_{(a_\alpha m_\alpha d_\alpha)(a_\beta m_\beta d_\beta)} |a_i, m_i, d_i; a_\alpha, m_\alpha, d_\alpha\rangle\langle a_\beta, m_\beta, d_\beta|.$$

The invariance condition is

$$\hat{U}(g)\hat{A} = \hat{A}, \tag{4.16}$$

where $\hat{U}(g)$ effects a symmetry transformation on the basis bras and kets of each irrep as

$$\hat{U}(g)\hat{A} \equiv A^{a_i m_i d_i}_{(a_\alpha m_\alpha d_\alpha)(a_\beta m_\beta d_\beta)} U(g)^i_{m_i m_i'} V(g)^\alpha_{m_\alpha m_\alpha'} V(g)^{-1\beta}_{m_\beta' m_\beta} \\ |a_i, m_i', d_i; a_\alpha, m_\alpha', d_\alpha\rangle\langle a_\beta, m_\beta', d_\beta|. \tag{4.17}$$

Note that symmetry transformations act on the m indices for each irrep but leave the d indices unchanged. Eqs. (4.16) and (4.17) together give us back the tensor invariance condition

$$U(g)^i_{m_i m_i'} V(g)^\alpha_{m_\alpha m_\alpha'} V(g)^{-1\beta}_{m_\beta' m_\beta} A^{a_i m_i' d_i}_{(a_\alpha m_\alpha' d_\alpha)(a_\beta m_\beta' d_\beta)} = A^{a_i m_i d_i}_{(a_\alpha m_\alpha d_\alpha)(a_\beta m_\beta d_\beta)}. \tag{4.18}$$

This condition is valid for each set of irreps labelled by $(a_i, d_i, a_\alpha, d_\alpha, a_\beta, d_\beta)$. Now consider the Clebsch-Gordan (CG) series $i \otimes \alpha = \oplus_\beta n^\beta_{i\alpha}\beta$. On the basis

level we have,

$$|a_\beta, m_\beta; n\rangle = \sum_{a_i,m_i,a_\alpha,m_\alpha} C^{a_\beta m_\beta;n}_{a_i m_i, a_\alpha m_\alpha} |a_i, m_i\rangle |a_\alpha, m_\alpha\rangle. \tag{4.19}$$

$C[\omega]^{a_\beta m_\beta;n}_{a_i m_i a_\alpha m_\alpha}$ denotes the CG coefficients associated with the change of basis of the direct product of irreps i and α to the n-th copy of irrep β. With this, we rewrite Eq. (4.15) as

$$\hat{A} = A^{a_i m_i d_i}_{(a_\alpha m_\alpha d_\alpha)(a_\beta m_\beta d_\beta)} (C^{-1})^{a_\gamma m_\gamma;n}_{a_i m_i, a_\alpha m_\alpha} |a_\gamma, m_\gamma; n, d_i, d_\alpha\rangle\langle a_\beta, m_\beta, d_\beta| \tag{4.20}$$

The ket $|a_\gamma, m_\gamma; n, d_i, d_\alpha\rangle$ denotes a basis in the n-th copy of a_γ irrep obtained from fusing the d_i-th copy of irrep a_i and d_α-th copy of irrep a_α. If we impose invariance Eq. (4.16) in this new form, we get

$$\begin{aligned} V(g)^{\gamma;n}_{m_\gamma m'_\gamma} (C^{-1})^{a_\gamma m'_\gamma;n}_{a_i m_i, a_\alpha m_\alpha} A^{a_i m_i d_i}_{(a_\alpha m_\alpha d_\alpha)(a_\beta m'_\beta d_\beta)} V(g)^{-1\beta}_{m'_\beta m_\beta} \\ = (C^{-1})^{a_\gamma m_\gamma;n}_{a_i m_i, a_\alpha m_\alpha} A^{a_i m_i d_i}_{(a_\alpha m_\alpha d_\alpha)(a_\beta m_\beta d_\beta)}, \end{aligned} \tag{4.21}$$

which is equivalent to

$$\begin{aligned} V(g)^{\gamma;n}_{m_\gamma m'_\gamma} \left[(C^{-1})^{a_\gamma m'_\gamma;n}_{a_i m_i, a_\alpha m_\alpha} A^{a_i m_i d_i}_{(a_\alpha m_\alpha d_\alpha)(a_\beta m_\beta d_\beta)} \right] = \\ \left[(C^{-1})^{a_\gamma m_\gamma;n}_{a_i m_i, a_\alpha m_\alpha} A^{a_i m_i d_i}_{(a_\alpha m_\alpha d_\alpha)(a_\beta m'_\beta d_\beta)} \right] V(g)^{\beta}_{m'_\beta m_\beta} \end{aligned} \tag{4.22}$$

Using Schur's lemmas, we can now determine that

$$\begin{aligned} \gamma \neq \beta \quad &: \quad (C^{-1})^{a_\gamma m_\gamma;n}_{(a_i m_i)(a_\alpha m_\alpha)} A^{a_i m_i d_i}_{(a_\alpha m_\alpha d_\alpha)(a_\beta m_\beta d_\beta)} = 0, \\ \gamma = \beta \quad &: \quad (C^{-1})^{a_\gamma m_\gamma;n}_{(a_i m_i)(a_\alpha m_\alpha)} A^{a_i m_i d_i}_{(a_\alpha m_\alpha d_\alpha)(a_\beta m_\beta d_\beta)} \propto \delta_{m_\gamma m_\beta}. \end{aligned}$$

This gives us

$$\left[(C^{-1})^{a_\beta m_\beta;n}_{a_i m_i, a_\alpha m_\alpha} A^{a_i m_i d_i}_{(a_\alpha m_\alpha d_\alpha)(a_\beta n_\beta d_\beta)} \right] = \delta_{m_\beta n_\beta} \; B^{a_i d_i}_{(a_\alpha d_\alpha)(a_\beta d_\beta;n)} \tag{4.23}$$

This is again a condition valid for each set of irreps labelled by $(a_i, d_i, a_\alpha, d_\alpha, a_\beta, d_\beta)$. Finally, moving C to the right hand side, we get

$$A^{a_i m_i d_i}_{(a_\alpha m_\alpha d_\alpha)(a_\beta m_\beta d_\beta)} = \sum_{n=1}^{n^\beta_{i\alpha}} B^{a_i d_i}_{(a_\alpha d_\alpha)(a_\beta d_\beta;n)} C^{a_\beta m_\beta;n}_{a_i m_i, a_\alpha m_\alpha} \tag{4.24}$$

If we restrict V to contain only irreps of a class ω, we get Eq. (4.12).

4.3.3 SPT phases with on-site symmetry and lattice translation invariance

Gapped Hamiltonians with only lattice translation invariance all belong to the same phase [51, 52]. Ground-states of such Hamiltonians and can be described by MPS matrices $A_m^{i_m}$ that are site independent *i.e.* A^{i_m} [67]. This means that unlike the case for an arbitrary gapped phase where we needed Nd matrices to describe a ground state, we now only need d matrices. Eq. (4.1) is simplified to

$$|\psi\rangle = \sum_{i_1 \ldots i_N} Tr[A^{i_1} A^{i_2} \ldots A^{i_N}] |i_1\rangle \ldots |i_N\rangle. \tag{4.25}$$

If we consider gapped Hamiltonians invariant under translation and an on-site symmetry transformation $u(g)$, the conditions of Eqs. (4.6, 2.10) again hold. However, unlike the case for just on-site symmetry, the different 1D irreps, $\chi(g)$ that appear in Eq. (2.10) now label distinct phases of matter [51, 52]. Different SPT phases are now labelled by $\{\omega, \chi\}$ where, $\omega \in H^2(G, U(1))$ labels the different projective classes and χ labels the different 1D irreps of the group G. We now see how we can constrain the ground-state form of these SPT phases extending the results of Sec 4.3.1

Let us rewrite Eq. (2.10) by absorbing $\chi(g)$ on the right hand side into $u(g)$ on the left and call $\tilde{u}(g) = \chi^*(g)u(g)$

$$\tilde{u}(g)_{ij} A^j = V^{-1}(g) A^i V(g), \tag{4.26}$$

Since re-phasing a representation with a 1D irrep is still a representation, we can find the new irrep content of $\tilde{u}(g)$. With this, we can repeat the procedure of Sec 4.3.1 and obtain the MPS matrices for ground states of a given spin system in any phase labelled by $\{\omega, \chi\}$ as

$$A[\omega,\chi]^{a_i m_i d_i}_{(a_\alpha m_\alpha d_\alpha)(a_\beta m_\beta d_\beta)} = \sum_{n=1}^{n^\beta_{i\alpha}} B^{a_i d_i}_{(a_\alpha d_\alpha)(a_\beta d_\beta; n)} C[\omega,\chi]^{a_\beta m_\beta; n}_{a_{i'} m_{i'}, a_\alpha m_\alpha}. \tag{4.27}$$

Where $i \otimes \chi \cong i'$ is some linear irrep of G that can easily be identified by calculating the characters of i' and $C[\omega,\chi]^{a_\beta m_\beta; n}_{a_{i'} m_{i'} a_\alpha m_\alpha}$ denote the CG coefficients associated with the change of basis of the direct product of linear irrep i' and the irrep α of projective class ω, to the n-th copy of irrep β of the same projective class ω.

To summarize, in order to find the ground-state forms of different SPT phases for a spin chain that transforms under a certain representation $u(g)$ of

G and that is translationally invariant, we need to follow the steps below:

1. Obtain $H^2(G, U(1))$ and the covering group $\tilde{G}$.
2. Identify the irreps 'i' of the physical spin among the irreps of $\tilde{G}$.
3. Identify the different 1D irreps of G, χ among the 1D irreps of $\tilde{G}$.
4. Identify the irreps 'i'' corresponding to re-phasing the physical spin irreps 'i' with χ.
5. Identify which irreps 'α' correspond to the projective class ω.
6. Obtain CG coefficients corresponding to the fusion of the re-phased irreps of the physical spin with each irrep of the projective class ω.
7. Use the CG coefficients in Eq. (4.27) allowing α and β to run over all the irreps of class ω and i' to run over the re-phased irreps of the physical spin.

We can also consider the ground-state forms constrained by other space-time symmetries like inversion and time-reversal and combinations with on-site symmetry which have also been classified. While there are constraints imposed on the entries of the MPS matrices, we do not immediately see a useful structure like we do with on-site symmetries with or without translation invariance mentioned above. However, for the sake of completeness, we have presented the results in the Appendices. B.2,B.3.

4.4 Examples of ground-state forms for various on-site symmetries

In this section, we use the results of the decomposition scheme discussed in the previous section to write down several ground-state forms of SPT phases protected by various on-site symmetries.

We will focus on some subgroups of $SO(3)$ that have a particular non-trivial second cohomology group $H^2(G, U(1)) = \mathbb{Z}_2$ and hence one class of non-trivial projective representations. (But our formalism can be applied to groups of other second cohomology group as well.) We will also focus on constructing ground states that are topologically non-trivial *i.e.* states that cannot be connected to the product state and whose virtual space representation corresponds to non-trivial projective representation. This is because these non-trivial states are sufficiently entangled and may offer advantages for information processing. We shall use the following conventions:

1. Groups are defined by a *presentation* $\langle S|R\rangle$ *i.e.* by listing the set S of generators and the set R of relations between them.

2. Representations are written by listing those of the generating set S. Any element in the group can always be written as the product of powers of the subset of S.

3. $\tilde{G}$ denotes the Schur cover of G that contains the linear and projective irreps of G.

4. We list the irreps of $\tilde{G}$ and label different classes of irreps by elements of $H^2(G, U(1))$. These correspond to the linear and projective irreps of G. Many of the irreps of the examples considered have been found collected in Ref [151].

5. χ_i denotes different 1D irreps of G (and $\tilde{G}$).

6. MPS matrices are constructed up to a similarity transformation for a particular basis of the physical spin that will be mentioned.

7. Pauli matrices are denoted as $\sigma_i = \{\sigma_x, \sigma_y, \sigma_z\}$ or $\sigma_i = \{\sigma_1, \sigma_2, \sigma_3\}$.

4.4.1 Haldane phase ($\mathbb{Z}_2 \times \mathbb{Z}_2$)

Consider a chain of three level spins (d=3) that is invariant under a three-dimensional representation of $\mathbb{Z}_2 \times \mathbb{Z}_2$ written as a restricted set of spin-1 $SO(3)$ rotations,

$$u(g) = \{\mathbb{1}, R_x(\pi), R_y(\pi), R_z(\pi)\}. \tag{4.28}$$

$\mathbb{Z}_2 \times \mathbb{Z}_2$, also known as the Klein four-group, is the group of symmetries of a rhombus or a rectangle (which are not squares) generated by π flips about perpendicular axes in the plane of the object. Some information about the group are follows:

- $G = \mathbb{Z}_2 \times \mathbb{Z}_2 : \langle a, x | a^2 = x^2 = (ax)^2 = e\rangle$
- $H^2(G, U(1)) = \mathbb{Z}_2 = \{e, a\}$
- $\tilde{G} = D_8 : \langle a, x | a^4 = x^2 = (ax)^2 = e\rangle$
- Class e irreps of $\tilde{G}$:
  $1_{(p,q)} : a \mapsto (-1)^p,\ x \mapsto (-1)^q,\ \ (p, q) \in \{0, 1\}$
- Class a irreps of $\tilde{G}$:
  $\tilde{2} : a \mapsto i\sigma_z,\ x \mapsto \sigma_x$

The three-dimensional representation can be shown to be $u(g) \cong 1_{(0,1)} \oplus 1_{(1,0)} \oplus 1_{(1,1)}$. Which means, with an appropriate choice of basis, each basis state of the 3 level spin transforms as one of the non-trivial 1D irreps. We can check that $\{|x\rangle \equiv \frac{1}{\sqrt{2}}(|-1\rangle - |1\rangle),\ |y\rangle \equiv \frac{i}{\sqrt{2}}(|-1\rangle + |1\rangle),\ |z\rangle \equiv |0\rangle\}$ is such an appropriate basis where $u(g)$ is block diagonal. Calculating the CG coefficients, we get the following MPS matrices:

$$A^i = B_i \otimes \sigma_i, \tag{4.29}$$

where B_i are undetermined and σ_i are the Pauli matrices. We thus have reproduced the result of Ref. [32] using our general framework.

4.4.2 D_4 invariant SPT phase

D_n, the dihedral group is the symmetry group of a planar n sided polygon and has projective representations when n is even. Some information about the group are as follows. We only look at the case of even n.

1. G $= D_n$: $\langle a, x | a^n = x^2 = (ax)^2 = e \rangle$
2. $H^2(G, U(1)) = \mathbb{Z}_2 = \{e, a\}$
3. $\tilde{G} = Q_n$: $\langle a, x | a^{2n} = x^4 = e, a^n = x^2, xax^{-1} = a^{-1} \rangle$.
4. Class e irreps of $\tilde{G}$:
   (a) $1_{(p,q)} : a \mapsto (-1)^p,\ x \mapsto (-1)^q,\ (p,q) \in \{0,1\}$
   (b) $2_{(k)} : a \mapsto \begin{pmatrix} e^{-ik\pi/n} & 0 \\ 0 & e^{ik\pi/n}, \end{pmatrix}$, $x \mapsto \sigma_y, \quad k = 2, 4, \ldots n-2$
5. Class a irreps of $\tilde{G}$:
   (a) $\tilde{2}_{(k)} : a \mapsto \begin{pmatrix} e^{-ik\pi/n} & 0 \\ 0 & e^{ik\pi/n} \end{pmatrix}$, $x \mapsto -i\sigma_y\ , \quad k = 1, 3, \ldots n-1$

Let us now consider the group D_4. This is the group of symmetries of a square generated by $\frac{\pi}{2}$ rotations about the symmetry axis perpendicular to the plane and reflections about symmetry axes in the plane of the square. We consider the following irreps (using a different choice of basis than the one mentioned above).

1. Linear irrep $2_{(2)} : a \mapsto -i\sigma_y,\ x \mapsto \sigma_z$
2. Projective irreps: $\tilde{2}_{(1/3)} : a \mapsto \frac{\pm 1}{\sqrt{2}}(\mathbb{1} - i\sigma_y),\ x \mapsto i\sigma_z$

If we consider a $d = 2$ physical spin transforming under the 2D irrep $2_{(2)}$ the non-trivial MPS matrices associated with the two basis states $|i\rangle = |0\rangle, |1\rangle$ are obtained by calculating the CG coefficients:

$$A^0 = B^0 \otimes \sigma_z \tag{4.30}$$

$$A^1 = B^1 \otimes \sigma_x \tag{4.31}$$

$$B^i = \begin{pmatrix} B_{11} & (-1)^i\, B_{13} \\ (-1)^i\, B_{31} & B_{33} \end{pmatrix} \tag{4.32}$$

Similar to Eq. (4.29) the MPS matrices are factorized into to two parts, and the indenity gate is protected by the symmetry [1].

4.4.3 A_4 invariant SPT phase

A_4, the alternating group of degree four, is the group of chiral or rotational symmetries of a regular tetrahedron generated by rotations (no reflections) about various symmetry axes. It is also the group of even permutations on four elements, i.e. a subgroup of S_4 to be discussed next. Some information about the group are as follows.

1. G $= A_4 = \langle a, x | a^3 = x^2 = (ax)^3 = e \rangle$
2. $H^2(G, U(1)) = \mathbb{Z}_2 = \{e, a\}$
3. $\tilde{G} = \tilde{T} : \langle a, x | a^3 = x^2 = v, v^2 = (ax)^3 = e \rangle$.
4. Class e irreps of $\tilde{G}$:
   (a) $1_{(p)} : a \mapsto e^{2\pi i p/3},\ x \mapsto 1,\ p = 0, 1, 2$
   (b) $3 : a \mapsto \begin{pmatrix} 0 & 1 & 0 \\ 0 & 0 & 1 \\ 1 & 0 & 0 \end{pmatrix},\ x \mapsto \begin{pmatrix} 1 & 0 & 0 \\ 0 & -1 & 0 \\ 0 & 0 & -1 \end{pmatrix}$
5. Class a irreps of $\tilde{G}$:
   (a) $\tilde{2}_{(p)} : a \mapsto \frac{e^{2\pi i p/3}}{2}[\mathbb{1} + i(\sigma_x + \sigma_y + \sigma_z)]$,
   $x \mapsto i\sigma_x,\ p = 0, 1, 2$

[1] In the paper this result was published [36], we state that the MPS matrices do not factorize and cannot be used for protected identity gate operation. It was later realized that this was just because of a bad choice of basis and the right choice does indeed lead to decomposition as stated in this chapter

If we consider the physical spin transforming under the only 3D linear irrep, the non-trivial MPS matrices associated with the three basis states $|i\rangle = |1\rangle, |2\rangle, |3\rangle$ are obtained by calculating the CG coefficients:

$$\begin{aligned} A^i &= B_i \otimes \sigma_i && (4.33)\\ B_i &= V^{i-1} B V^{*i-1} && (4.34)\\ V &= \begin{pmatrix} \mathbb{1} & 0 & 0 \\ 0 & \omega\,\mathbb{1} & 0 \\ 0 & 0 & \omega^*\,\mathbb{1} \end{pmatrix},\ \omega = e^{2\pi i/3} \\ B &= \begin{pmatrix} B_{00} & B_{01} & B_{02} \\ B_{10} & B_{11} & B_{12} \\ B_{20} & B_{21} & B_{22} \end{pmatrix}. \end{aligned}$$

Similar to Eq. (4.29) the MPS matrices are factorized into to two parts, and the indenity gate is protected by the symmetry. We remark that imposing inversion or time-reversal symmetry does not further simplify the B's structure.

4.4.4 S_4 invariant SPT phase

S_4, the symmetric group of degree four, is the group of achiral or full symmetries of a tetrahedron generated by rotations and reflections about various symmetry axes. It is also the group of all permutations of four elements. Some information about the group are as follows.

1. $\mathrm{G} = S_4 = \langle a, b, c | a^2 = b^3 = c^4 = abc = e \rangle$
2. $H^2(G, U(1)) = \mathbb{Z}_2 = \{e, a\}$
3. $\tilde{G} = O' : \langle a, b, c | a^2 = b^3 = c^4 = abc = v, v^2 = e \rangle$
4. Class e irreps of $\tilde{G}$: $(a = tk,\ b = s,\ c = s^2kt)$
   (a) $1_{(p)} : t \mapsto (-1)^p,\ k \mapsto 1,\ s \mapsto 1,\ p = \{0, 1\}$
   (b) $s : t \mapsto \sigma_x,\ k \mapsto \mathbb{1},\ s \mapsto \begin{pmatrix} e^{2\pi i/3} & 0 \\ 0 & e^{-2\pi i/3} \end{pmatrix}$
   (c) $3_{(p)}$: $k \mapsto \begin{pmatrix} 1 & 0 & 0 \\ 0 & -1 & 0 \\ 0 & 0 & -1 \end{pmatrix}$, $s \mapsto \begin{pmatrix} 0 & 1 & 0 \\ 0 & 0 & 1 \\ 1 & 0 & 0 \end{pmatrix}$,
   $t \mapsto (-1)^p \begin{pmatrix} 1 & 0 & 0 \\ 0 & 0 & 1 \\ 0 & 1 & 0 \end{pmatrix}$, $p = 0, 1$

5. Class a irreps of $\tilde{G}$:

   (a) $\tilde{2}_{(p)} : t \mapsto (-1)^p \frac{i}{\sqrt{2}}(\sigma_z - \sigma_y),\ k \mapsto i\sigma_x,$
   $s \mapsto \frac{1}{2}[\mathbb{1} + i(\sigma_x + \sigma_y + \sigma_z)]\ ,\ p = 0, 1$

   (b) $\tilde{4} = 2 \otimes \tilde{2}_{(0)}$

If we consider the physical spin transforming under one of the 3D linear irreps, $3_{(1)}$ the non-trivial MPS matrices associated with the three basis states are obtained by calculating the CG coefficients:

$$\begin{aligned} A^i &= B_i \otimes \sigma_i \\ B_i &= \begin{pmatrix} B_{2_0 2_0} & 0 & B_{2_0 4} \otimes u_{i-1}^\dagger \\ 0 & B_{2_1 2_1} & B_{2_1 4} \otimes v_{i-1}^\dagger \\ B_{42_0} \otimes u_{i-1} & B_{42_1} \otimes v_{i-1} & B_{44} \otimes \mathbb{1}_2 + \tilde{B}_{44} \otimes f_{i-1} \end{pmatrix} \\ u_i &= \begin{pmatrix} \omega^{*i} \\ \omega^i \end{pmatrix},\ v_i = \begin{pmatrix} \omega^{*i} \\ -\omega^i \end{pmatrix} \\ f_i &= \begin{pmatrix} 0 & \omega^i \\ \omega^{*i} & 0 \end{pmatrix},\ \omega = e^{2\pi i/3} \end{aligned} \tag{4.35}$$

We observe that if we restrict the B_i matrix to only the bottom right block and set the two matrices to scalars, $B_{44} = \cos(\frac{\theta}{2})$ and $\tilde{B}_{44} = e^{i\phi}\sin(\frac{\theta}{2})$, then it reduces to the one used for the buffering scheme in Ref. [37] up to a change of basis.

4.4.5 Summary of new SPT phases with identity gate protection

We see that all the examples in the previous section allow the perfect operation of the identity gate according to the scheme reviewed in Sec. 4.2.3 as the MPS matrices for non-trivial ground states all have the form

$$A^i = B_i \otimes \sigma_i. \tag{4.36}$$

This is because the groups considered $D_4,\ A_4,\ S_4$ all have a $\mathbb{Z}_2 \times \mathbb{Z}_2$ subgroup which gives the protected subspace. The additional symmetry only constrains the junk matrices, B_i to have more structure. Note that following the convention of Ref. [32], we call B_i the junk part and σ_i the protected part. We also note that our convention of placing the protected and junk parts is in reverse order as compared to the convention used in Refs. [32, 33, 37]. This is for notational consistency in this chapter.

Consider encoding qubit information $|\psi\rangle$ in the protected part of the right boundary virtual space with the junk part arbitrarily set to some state $|J\rangle$ in any of these ground states.

$$|R\rangle = |J\rangle \otimes |\psi\rangle \tag{4.37}$$

If we perform a measurement on the rightmost *i.e* N-th spin in the basis $|x\rangle, |y\rangle, |z\rangle$ in which the MPS matrices have the form of Eq. (4.36) with an outcome $|k_N\rangle$, we induce a transformation of the boundary vector by (4.2.3)

$$|R\rangle \mapsto A^{k_N}|R\rangle \tag{4.38}$$

$$\implies |J\rangle \otimes |\psi\rangle \mapsto B_{k_N}|J\rangle \otimes \sigma_{k_N}|\psi\rangle \tag{4.39}$$

The qubit information $|\psi\rangle$ is unchanged upto an inconsequential Pauli operator σ_{k_N} which can be corrected for by a change of readout basis. In fact, we can measure several spins (say m from the right) and we still have the perfect operation of the identity gate upto a residual operator $\sigma_{k_{N-m}} \dots \sigma_{k_N}$. This means all these ground states allow a protected subspace with perfect identity gate operation, which allows for perfect transmission of quantum information encoded in the projected subspace.

However, note that if we measure in a different basis formed by a linear combination of $|x\rangle, |y\rangle, |z\rangle$, it is easy to check that the boundary vector $|R\rangle = |J\rangle \otimes |\psi\rangle$ no longer remains decomposed into protected and junk parts and, in general, there will be mixing between the two vector spaces. As an illustration, if a measurement outcome of $\frac{1}{\sqrt{2}}(|x\rangle + |y\rangle)$ is obtained, the induced transformation on $|R\rangle$ is (up to an overall factor)

$$|J\rangle \otimes |\psi\rangle \mapsto B_x|J\rangle \otimes \sigma_x|\psi\rangle + B_y|J\rangle \otimes \sigma_y|\psi\rangle. \tag{4.40}$$

Thus, in general only the identity gate is protected in the ground states of these phases. However, if it were possible that B_i is independent of physical index i, then arbitrary single-qubit gates would be possible, as mixing will not occur. It is worth noting that when B_i is independent of the index i, the corresponding wavefunction is identically the AKLT state. We had hoped that imposing additional symmetry like parity and/or time reversal invariance might give further constraints on the matrices B_i's and thereby allow non-trivial gate operations. But we checked (using results of Appendix. B.3) that imposing these additional symmetries on the $\mathbb{Z}_2 \times \mathbb{Z}_2$, D_4, A_4 and S_4 SPT ground states listed above does not induce ground states that could provide universal qubit operations.

4.5 An A_4 symmetric Hamiltonian

Here we ask a slightly less general question: can one find a particular Hamiltonian with symmetry such that there is an extended region (not necessarily at all points of a phase) in the phase diagram that the ground states can provide universal qubit operations in the framework of MBQC? Below we first construct a specific Hamiltonian that possesses A_4 and parity symmetry, which can be regarded as perturbing the spin-1 AKLT Hamiltonian. Then we present a numerical investigation and show that indeed there exists a finite parameter region where the ground states are exactly (here and henceforth, exact is defined up to machine precision) the AKLT state, and can therefore serve as a resource state for implementing universal single-qubit gates. After the numerical investigation, we present analytic understanding why such an extended region of AKLT ground states can exist.

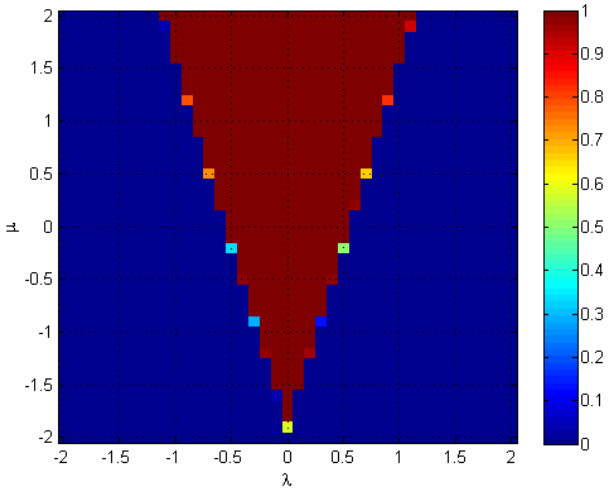

Figure 4.1: Fidelity of ground states with the AKLT state. It is seen that there is an extended region such that the ground state is exactly the AKLT state.

The A_4 and inversion symmetric Hamiltonian we will study is the following:

$$H = H_{AKLT} + \lambda H_c + \mu H_q, \tag{4.41}$$

$$H_{AKLT} = \sum_i \left[\boldsymbol{S}_i \cdot \boldsymbol{S}_{i+1} + \frac{1}{3} (\boldsymbol{S}_i \cdot \boldsymbol{S}_{i+1})^2 \right], \tag{4.42}$$

where $\boldsymbol{S}_i \cdot \boldsymbol{S}_{i+1} \equiv S_i^x S_{i+1}^x + S_i^y S_{i+1}^y + S_i^z S_{i+1}^z$.

$$H_q = \sum_i \left[(\boldsymbol{S}_i^2 \cdot \boldsymbol{S}_{i+1}^2) - \frac{1}{3}(\boldsymbol{S}_i \cdot \boldsymbol{S}_{i+1})^2 \right], \quad (4.43)$$
$$\text{where} \qquad \boldsymbol{S}_i^2 \cdot \boldsymbol{S}_{i+1}^2 \equiv (S_i^x S_{i+1}^x)^2 + (S_i^y S_{i+1}^y)^2 + (S_i^z S_{i+1}^z)^2,$$

and

$$\begin{aligned} H_c = \sum_i [& (S^x S^y)_i S_{i+1}^z + (S^z S^x)_i S_{i+1}^y + (S^y S^z)_i S_{i+1}^x \\ & + (S^y S^x)_i S_{i+1}^z + (S^x S^z)_i S_{i+1}^y + (S^z S^y)_i S_{i+1}^x \\ & + S_i^x (S^y S^z)_{i+1} + S_i^z (S^x S^y)_{i+1} + S_i^y (S^z S^x)_{i+1} \\ & + S_i^x (S^z S^y)_{i+1} + S_i^z (S^y S^x)_{i+1} + S_i^y (S^x S^z)_{i+1}]. \end{aligned} \quad (4.44)$$

This Hamiltonian is constructed using invariant operators built out of A_4 invariant polynomials using the technique detailed in Appendix. A.1. However, the form of H_c and H_q are different from that used in Appendix. A.1 and Chapter. 2. Also, the $\{\lambda, \mu\} = \{0, 0\}$ Hamiltonian of Eq. 2.3 corresponds to the AKLT Hamiltonian which can be thought of as a particular combination of A_4 invariant operators but which has a larger symmetry group, $SO(3)$ and is known to have the AKLT state as the unique ground state.

4.5.1 Checking AKLT as the ground state

The AKLT state $|\psi_{\text{AKLT}}\rangle$ has the MPS representation $A^x = \sigma_x$, $A^y = \sigma_y$, and $A^z = \sigma_z$ in the basis of $\{|x\rangle, |y\rangle, |z\rangle\}$ defined earlier. We know that at $\lambda = \mu = 0$ the ground state of the Hamiltonian (4.41) is uniquely the AKLT state. We would like to know whether there is an extended region of (λ, μ) around $(0, 0)$ such that the ground state is also the AKLT state. We do this numerically by first solving the ground state $|\psi_G\rangle$ of the Hamiltonian (4.41) using the infinite time-evolving bond decimation (iTEBD) algorithm invented by Vidal [60] and then calculating the fidelity between these two states $f = |\langle\psi_G|\psi_{\text{AKLT}}\rangle|^2$. As shown in Fig. 4.1 we indeed see that there is an extended region in this Hamiltonian such that the ground state is exactly the AKLT state and thus a useful resource state for universal single-qubit MBQC.

4.5.2 Analytic understanding

We now analyze why such an extended region of AKLT is possible and calculate analytically the boundary of the AKLT region in the λ-μ plane,

shown in Fig. 4.1. First we recall that the interaction between sites i and $i+1$ of H_{AKLT} is a projection to the joint $S=2$ subspace. More precisely,

$$(H_{AKLT})_{i,i+1} = 2\sum_{m=-2}^{2} P_{|S=2,m\rangle} - \frac{2}{3}\mathbb{1}, \tag{4.45}$$

where we have defined the projector $P_{|\psi\rangle} \equiv |\psi\rangle\langle\psi|$ associated with the state $|\psi\rangle$, $|S=2,m\rangle$ denotes the eigenbasis of the joint spin-2 states for neighboring sites i and $i+1$, and $\mathbb{1}$ is the identity operator in the spin-2 subspace.

For the quartic Hamiltonian, it is seen by straightforward calculation that

$$(H_q)_{i,i+1} = P_{(|S=2,2\rangle+|S=2,-2\rangle)/\sqrt{2}} + P_{|S=2,0\rangle} + \frac{2}{3}\mathbb{1}. \tag{4.46}$$

For the cubic Hamiltonian, it is seen that

$$(H_c)_{i,i+1} = 2\sqrt{3}\Big(P_{|\phi^+\rangle} - P_{|\phi^-\rangle}\Big), \tag{4.47}$$

where

$$\begin{aligned} |\phi^{\pm}\rangle \;\equiv\; & (|S=2,m=2\rangle + |S=2,m=-2\rangle \\ & \pm i\sqrt{2}|S=2,m=0\rangle)/2. \end{aligned} \tag{4.48}$$

Since the AKLT state is annihilated by any spin-2 projectors, it will remain the ground state if the following operator is positive,

$$\begin{aligned} h(\lambda,\mu) \;\equiv\; & 2P_{|S=2,m=2\rangle} + 2P_{|S=2,m=-2\rangle} + 2P_{|S=2,m=0\rangle} \\ & +2\sqrt{3}\lambda\Big(P_{|\phi^+\rangle} - P_{|\phi^-\rangle}\Big) + \mu\, P_{|S=2,m=0\rangle} \\ & +\mu\, P_{(|S=2,m=2\rangle+|S=2,m=-2\rangle)/\sqrt{2}}, \end{aligned} \tag{4.49}$$

which, in the basis of $|S=2,m=\{\pm 2,0\}\rangle$ is the following 3×3 matrix,

$$h(\lambda,\mu) = \begin{pmatrix} 2+\mu/2 & \mu/2 & -i\sqrt{6}\lambda \\ \mu/2 & 2+\mu/2 & -i\sqrt{6}\lambda \\ i\sqrt{6}\lambda & i\sqrt{6}\lambda & 2+\mu \end{pmatrix}. \tag{4.50}$$

By direct diagonalization, we find that the matrix $h(\lambda,\mu)$ is non-negative when $\mu \pm 2\sqrt{3}\lambda + 2 > 0$ which indeed gives the region of the AKLT in Fig. 4.1.

4.6 Summary and Outlook

We have presented a straightforward and general formalism for investigating the structure of a wavefunction as constrained (or protected) by a discrete symmetry group. The wavefunction is organized into two parts: (1) a CG part, whose form is inferred from the symmetry group and (2) a part whose form is not constrained by the symmetry. From the viewpoint of measurement-based quantum computation, one can then use this formalism to discuss whether the ground state of an SPT phase protected by a given symmetry group allows protected gate operations. This happens when, for example, the MPS matrices A^i decompose into the form $A^i = B_i \otimes \sigma_i$ *i.e.* the virtual vector space decomposes into junk and protected parts. Generically speaking, the identity gate is not necessarily protected in an arbitrary SPT phase. With the new formalism, we recovered the results of the $\mathbb{Z}_2 \times \mathbb{Z}_2$ case previously obtained in Ref. [32] and obtain the MPS forms for several other groups– D_4, A_4 and S_4. We also constructed a Hamiltonian with A_4 and inversion symmetry and found that in an extended region of a two-parameter space, the ground state is exactly the AKLT state. Using the formulation developed here, further exploration of 1D SPT phases and gate protection can be made with arbitrary finite groups. The MPS forms can also allow the study of the properties of 1D SPT phases which would be of interest to the condensed matter community.

Our hope was to find a computational phase in an SPT phase that can generically support arbitrary single-qubit gates. However, in the scheme of MBQC mentioned here on pure states corresponding to SPT ground states, it might be the case that the only gate that can be naturally protected generically in an entire SPT phase is the identity gate which is useful in terms of transmitting quantum information over long distances. One way around this is the buffering technique invented in Ref. [37] is one way to bring forth universal gates, as demonstrated for the S_4 symmetry.

In a follow-up work, published in Refs [34, 35], an alternative protocol based on mixed states for MBQC was introduced as compared to the one introduced in Refs [131, 132] which was also used in this chapter. Using the mixed-state protocol, we can use the ground states corresponding to several SPT phases (including the ones mentioned in this chapter) which have a protected identity gate operation in the pure-state protocol, for universal single qubit MBQC! Thus, indeed providing support that SPT phases can be potentially computational phases.

The real challenge is to find a computational phase that is not only useful for single qubit MBQC, but for universal MBQC. It is known that one-dimensional systems cannot host universal quantum computation and we need to go to atleast two dimensions. There has been increasing evidence to show

that certain two dimensional SPT phases [127, 153, 154] can potentially be universal computational phases. A concrete proof, example and protocol is still lacking and is left for future work. In particular, a class of SPT phases with a so-called decorated domain wall construction considered in [127] have an appealing structure where we can hope for a general proof.

Part III

Out-of-equilibrium phases of matter

Chapter 5

Eigenstate phases with finite on-site non-abelian symmetry

The contents of this chapter are published in Ref.[155] completed in collaboration with Sriram Ganeshan, Lukasz Fidkowski and Tzu-Chieh Wei.

5.1 Introduction

Statistical mechanics and thermodynamics are bridges that connect microscopic laws such as Newtonian and quantum mechanics to macroscopic phenomena that we measure in the laboratory. The validity of statistical physics relies on the existence of thermal equilibrium. For an isolated quantum system, the notion of thermalization is understood in the form of the *Eigenstate Thermalization hypothesis* (ETH) [17, 156]. ETH posits that for a quantum system, an eigenstate embodies an ensemble and thermalization can be diagnosed by monitoring if subsystems are thermal with respect to the rest of the system. Furthermore, if the system thermalizes, all eigenstates are thermal. Integrable systems violate ETH due to the existence of an extensive number of conserved quantities that prevent the system from acting as a bath for itself. However, quantum integrable models are highly fine tuned and one recovers thermalization by any infinitesimal deviation from the integrable point.

Recently, many-body localization (MBL) has emerged as a *generic* class of interacting and disordered isolated systems which violate ETH. Basko et al. [15] showed that all many-body eigenstates remain localized to all orders in perturbation for an effective interacting disordered model. Several numerical works subsequently verified that all many-body eigenstates are localized in one dimensional disordered lattice models with short-range interactions [16, 24, 157–160]. Furthermore, there has been a mathematical proof by

Imbrie [161] for the existence of MBL in a particular disordered spin model with short range interactions. The absence of thermalization has been further quantified as a consequence of emergent integrability due to the presence of a complete set of local integrals of motion (LIOMs). The key distinction from fine tuned integrable models is that the LIOMs or 'lbits' (for localized bits) in the MBL phase are robust against perturbations. One can use these lbits to construct a phenomenological lbit Hamiltonian that captures the entanglement dynamics [162–165].

Having established the existence of MBL and its violation of ETH in certain models, natural questions that arise are "what is the most robust version of MBL?" and "does it lead to a refined notion of ETH?" To this end, it is worthwhile to consider instabilities to the MBL phase that lead to delocalization and thereby the restoration of thermalization. Recent works have considered instabilities to the MBL phase due to a small bath [166, 167], external drive [168], Griffiths effects and dimensionality [169, 170], topologically protected chiral edge [171] and a single particle mobility edge [172, 173]. Contrary to the common wisdom that these instabilities would lead to the complete restoration of thermalization, preliminary numerical results have indicated that the lack of thermalization tends to survive in some form in all these cases. However, the fate of these exotic phases in the thermodynamic limit is still an open question.

Potter and Vasseur [174] have recently added another instability to this list. It was argued that the l-bit Hamiltonian 'enriched' with non-abelian symmetry that is not spontaneously broken is unstable to perturbations. This instability arises from the extensive degeneracy in the spectrum of the l-bit Hamiltonian associated with the higher-dimensional irreducible representations (irreps) of the non-abelian group. Any perturbation of such a spectrum results in resonant delocalization making MBL unstable, driving the system to thermalization or a quantum critical glass (QCG)-like phase [175, 176]. On the other hand, if the non-abelian symmetry was spontaneously broken to an abelian subgroup, the system could localize and be driven to the so-called many-body localized spin-glass (MBL-SG) phase which is characterized by MBL as well as long range order arising from spontaneous symmetry breaking [24, 25, 177].

Thus symmetry provides a platform to search for exotic violations of ETH beyond MBL in strongly interacting systems. To this end, in this chapter, we develop a procedure to construct general Hamiltonians with global symmetries and analyze the thermalization and localization indicators for individual eigenstates. As a particular example, we construct a two-parameter Hamiltonian with on-site S_3 symmetry. Using numerical exact diagonalization of our model Hamiltonian, we calculate cut-averaged entanglement entropy (CAEE) distributions and level statistics which are indicators of localization and a spin-glass

diagnostic which detects symmetry breaking. Within the accuracy of our numerical analysis, we are able to distinctly observe both a thermal phase and an MBL-SG phase with spontaneous symmetry breaking of S_3 to $\mathbb{Z}_3$ symmetry.

We also employ the same diagnostics to quantify an intermediate region between the aforementioned two phases where the full S_3 symmetry is intact. However, we cannot ascertain the fate of this region in thermodynamic limit, due to the possibility of quantum critical cone like finite-size effects [178]. The chapter is organized as follows. In Sec. 5.2 we construct a general S_3 symmetric Hamiltonian using group theory methods. We numerically diagonalize our model and compute indicators of localization and symmetry breaking in 5.3. We end the chapter with discussion of results and conclusion. We provide a review of the conjecture by Potter and Vasseur [174] on the incompatibility of MBL with non-abelian symmetries and other details of our analysis in the Appendices.

5.2 Model S_3 invariant Hamiltonian

In this section, we analyze a specific spin-1 Hamiltonian that is invariant under the smallest non-abelian group, S_3. In terms of the spin angular momentum basis $|S = 1, S_z = +1, 0, -1\rangle$, the spin operators are

$$\begin{aligned} S^x &= \frac{1}{\sqrt{2}} \begin{pmatrix} 0 & 1 & 0 \\ 1 & 0 & 1 \\ 0 & 1 & 0 \end{pmatrix}, \; S^z = \begin{pmatrix} 1 & 0 & 0 \\ 0 & 0 & 0 \\ 0 & 0 & -1 \end{pmatrix}, \\ S^y &= \frac{1}{\sqrt{2}} \begin{pmatrix} 0 & -i & 0 \\ i & 0 & -i \\ 0 & i & 0 \end{pmatrix}, \; S^{\pm} = \frac{1}{\sqrt{2}}(S^x \pm iS^y). \end{aligned} \tag{5.1}$$

The symmetry group S_3 contains six elements: $S_3 = \{1, a, a^2, x, xa, xa^2\}$, and the two generators, a and x, satisfy the properties $a^3 = x^2 = 1$ and $xax = a^{-1}$. Note that in this chapter, we refer to the identity element of the group simply as 1. In the spin basis, they are chosen to have the following representations,

$$V(a) = \begin{pmatrix} \omega & 0 & 0 \\ 0 & 1 & 0 \\ 0 & 0 & \omega^* \end{pmatrix}, \; V(x) = \begin{pmatrix} 0 & 0 & 1 \\ 0 & -1 & 0 \\ 1 & 0 & 0 \end{pmatrix}, \tag{5.2}$$

where $\omega = e^{2\pi i/3}$. It can be verified that the spin operators transform under the generators as follows,

$$V(a)\, S^{\pm}\, V(a)^{\dagger} = \omega^{\pm 1} S^{\pm},\ V(a)\, S^{z}\, V(a)^{\dagger} = S^{z} \tag{5.3}$$

$$V(x)\, S^{\pm}\, V(x)^{\dagger} = -S^{\mp},\ V(x)\, S^{z}\, V(x)^{\dagger} = -S^{z}. \tag{5.4}$$

Using the symmetry arguments detailed in Appendix C.2, we construct the following Hamiltonian:

$$\begin{aligned}
H(\lambda,\kappa) &= \lambda H_d(\kappa) + H_t, \qquad (5.5)\\
H_d(\kappa) &= \sum_{i=1}^{L} (1-\kappa)\ h_i\ (S_i^z)^2 + \kappa\ J_i\ S_i^z S_{i+1}^z,\\
H_t &= \Delta_t \left[H_a + H_b + H_c\right],\\
H_a &= a \sum_{i=1}^{L} (S_i^+)^2 (S_{i+1}^-)^2 + (S_i^-)^2 (S_{i+1}^+)^2 + h.c,\\
H_b &= b \sum_{i=1}^{L} (S_i^+ S_i^z)(S_{i+1}^- S_{i+1}^z) + (S_i^- S_i^z)(S_{i+1}^+ S_{i+1}^z) + h.c,\\
H_c &= c \sum_{i=1}^{L} (S_i^+)^2 (S_{i+1}^+ S_{i+1}^z) + (S_i^-)^2 (S_{i+1}^- S_{i+1}^z) + h.c.
\end{aligned}$$

The above Hamiltonian consists of two parts: 1) The disordered part H_d with a one body (disordered h_i term) and a two-body l-bit term (disordered J_i term). The two-body term is designed to drive spontaneous symmetry breaking of non-abelian S_3 symmetry down to an abelian $\mathbb{Z}_3$ symmetry. The relative strengths of these two terms are controlled by the $\kappa \in [0,1]$ parameter, where $\kappa = 1$ is expected to be the SSB limit. 2) The second term H_t, the thermalizing term, contains a representative subset of the most general two-body symmetric operators. The intention is to keep H_t sufficiently generic while retaining invariance under symmetry action (see Appendix C.2 for details of how this Hamiltonian is constructed and can be generalized to arbitrary symmetry groups). The λ parameter controls disorder strength.

Using the transformation of the spin operators listed above, it is straightforward to verify that the Hamiltonian has the desired symmetry, that is, $\forall g \in S_3$

$$U(g) H(\lambda,\kappa) U(g)^{\dagger} = H(\lambda,\kappa), \quad U(g) = \bigotimes_{i=1}^{L} V(g)_i. \tag{5.6}$$

For numerical analysis, the parameters in the Hamiltonian are selected as follows, (a) $h_i = w_h\ g_h(i)$, $J_i = w_J\ g_J(i)$ and $g_{h/J}(i)$ are random numbers drawn from a normal distribution with mean 0 and standard deviation 1; (b) $(w_h, w_J, \Delta_t, a, b, c)$ are free real parameters. We arbitrarily fix these to the values $(1.0, 0.6, 0.17, 0.74, 0.67, 0.85)$ respectively for our numerical study without loss of generality.

5.3 Numerical Results

We perform exact diagonalization of the Hamiltonian in Eq. 5.5. The local Hilbert space for the S_3 symmetric Hamiltonian is three dimensional, in contrast to the spin $\frac{1}{2}$ case and this constraints our maximum system size accessible to be $L = 10$ sites. We study the properties of the eigenstates pertaining to localization and thermalization of this Hamiltonian for various values of $\lambda \in (0, \infty)$ and $\kappa \in [0, 1]$. For clarity of presentation of certain analysis, we use the rescaled variable $\frac{\lambda}{1+\lambda} \in (0, 1)$ instead of λ (wherever mentioned). We employ periodic boundary conditions for all our analysis. To characterize the phases, we study below several relevant diagnostics that quantify the nature of localization and thermalization of the eigenstates. First, we consider the full entanglement distributions evaluated using the cut averaged entanglement entropy.

5.3.1 Cut averaged entanglement entropy distributions

Since MBL is a characteristic of a single eigenstate, it is useful to quantify this phase without averaging across different eigenstates. Recent work by Yu, Luitz and Clark [179] has proposed cut averaged entanglement entropy (CAEE) to quantify the MBL phase at the level of a single eigenstate. CAEE for a subsystem size, d, is obtained by taking the average of the entanglement entropy computed for all subsystems of a specific size d (contiguous spins contained in a segment of length d) located on the spin chain with periodic boundary conditions. The CAEE scaling, $S(d)$ is then evaluated by repeating this procedure for different subsystem sizes, d. The key advantage of the CAEE is that strong sub-additivity condition constrains the shape of the entanglement scaling as a function of subsystem size, *i.e.* , $S(d)$ is guaranteed to be a smooth convex function of the subsystem size, d without any average over disorder or eigenstates [179]. This allows us to quantify the entanglement scaling of each eigenstate using the slope of the CAEE (SCAEE), $S'(d^*)$, at some fixed subsystem size, d^* as in Ref [179]. We can then construct the

full distribution of the slopes across the disorder snapshots and eigenstates. Fig. 5.1 shows sample CAEE, along with a spline fit for 200 randomly chosen eigenstates for 4 different $\{\lambda, \kappa\}$ from a few disorder realizations of a 10-site Hamiltonian [5.5]. It can be seen that the eigenstates for small λ are mostly

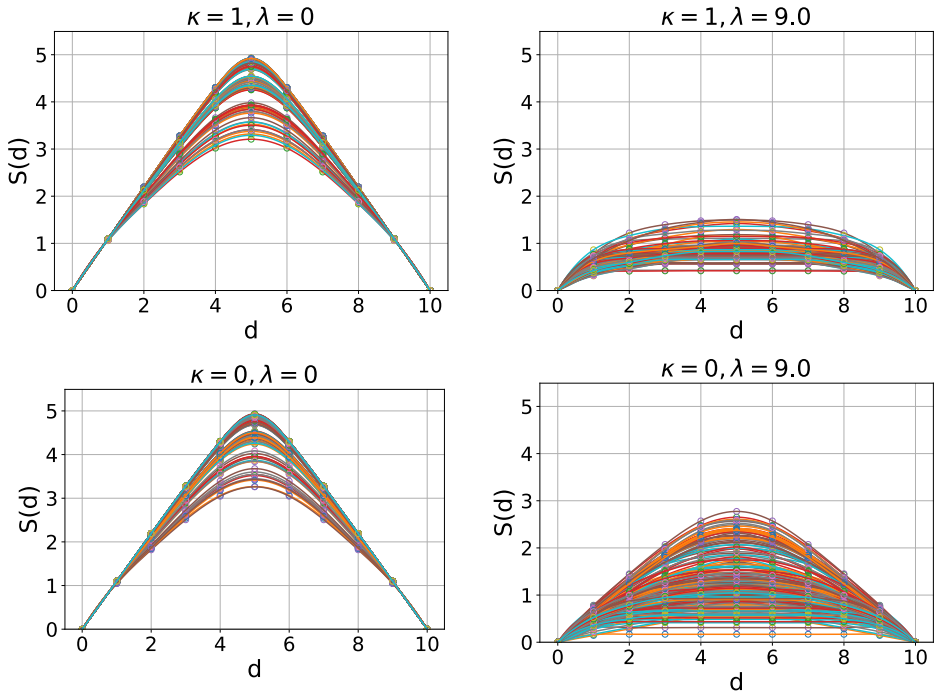

Figure 5.1: CAEE and spline fit for 200 eigenstates randomly sampled from the spectra of 19 disorder realizations of the 10 site Hamiltonian (5.5).

volume law, while for large λ, there exists mixture of area-law and volume-law states. In order to identify the nature of the eigenstate transitions for various parameter regimes, we monitor the full distribution of the slope of the CAEE (SCAEE) evaluated at subsystem size $L/4$ ($S'(L/4)$) for different values of λ and κ and disorder realizations. Operationally, we compute SCAEE as follows: for each eigenstate, we obtain the CAEE scaling, $S(d)$ for $d = 0 \ldots L$, fit the data to a curve using a spline fit and then evaluate the slope, $S'(d)$ for this fit curve at $d = L/4$.

There is however a potential issue because of the non-abelian nature of the S_3 symmetry of the Hamiltonian. Generally, at finite-sizes, the eigenstates of a Hamiltonian invariant under the action of a symmetry group G transform as irreps of the same group. For our case, S_3 has 3 irreps- two 1D irreps ($\mathbf{1}$, $\mathbf{1}'$) and one 2D irrep ($\mathbf{2}$). Eigenstates that transform as the $\mathbf{2}$ are two-fold degenerate. We may get different entanglement scaling depending on

which precise orthonormal states in this 2D vector space is produced as the eigenstates [1]. To avoid this issue, we diagonalize the Hamiltonian in the 1D irrep sector. In addition to ensuring that we only sample non-degenerate eigenstates which transform as 1D irreps, this also helps us in reaching higher system sizes (See Appendix [C.3] for more details).

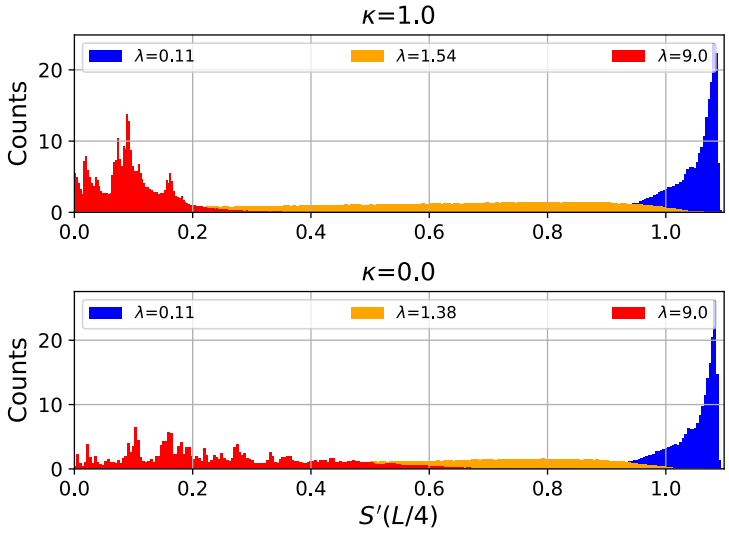

Figure 5.2: Slope histograms for 9 sites and 879 disorder samples for representative $\{\lambda, \kappa\}$. 243 Eigenstates that transform as 1D irreps chosen sampled for each disorder realization. The plot is normalized to have unit area.

Fig. 5.2 shows the distribution of $S'(L/4)$ for different λ and κ. The values of λ are chosen so as to show what the distribution looks like when the system has strong, weak and intermediate disorder strength. For all values of the SSB parameter κ, for weak disorder λ, we see that the $S'(L/4)$ distribution becomes increasingly narrow with system size with a peak located close to $1.1 \approx log(3)$ which is the maximum value possible for $S'(d)$ for any state of spin-1 chain. This is also evident from the large number of eigenstates with volume-law entanglement entropy scaling $S(d) \propto d$ in Fig. 5.1. These properties are consistent with an ergodic/ thermal phase. For high disorder however, we see that the distribution for $\kappa = 0$ in Fig. 5.2 is different from $\kappa = 1$. For the former, there is a relatively extended thermal tail which is suppressed for the latter. To gain a better understanding we present the first two moments (mean and variance) of this slope distribution which are indicators of a potential MBL transition.

[1] We thank Bela Bauer for pointing this out.

$\kappa = 1$ *with* $S_3 \to \mathbb{Z}_3$ *symmetry breaking:* The entanglement distribution for the $\kappa = 1$ limit Fig. 5.2 and its moments, displayed in the upper panels of Figs. 5.3,5.4 are consistent with the existence of an MBL phase for the large disorder limit and transitions to a fully thermal phase for weak disorder. One way to estimate the transition point is by locating where the mean, $\overline{S'(L/4)}$ curves for different system sizes cross on the λ axis in Fig. 5.3. This is roughly at $\lambda/(1+\lambda) \approx 0.72$. Another is by locating the peak of the variance, $\sigma^2(S'(L/4))$ curve on the λ axis which is believed to be close to the point of phase transition in the thermodynamic limit [26, 178]. The drift of this point towards the disorder side *i.e.* larger λ with increase in system size is considered to be typical for exact diagonalization (ED) studies of MBL [178]. Since our model has a non-abelian symmetry, the existence of a full MBL phase must accompany SSB to an abelian subgroup. We confirm SSB (S_3 to $\mathbb{Z}_3$ in this case) by computing a spin-glass diagnostic in 5.3.2.

$\kappa = 0$ *with full* S_3 *symmetry:* The entanglement distribution for the $\kappa = 0$ limit, shown in Fig. 5.2, and its moments, displayed in the lower panels of Figs. 5.3 and 5.4 shows an enhanced variance and mean at the $\kappa = 0$ for the large disorder limit. The enhanced mean value is an indication of the presence of sub-thermal volume law states and area law states. However, the crossing of the $\overline{S'(L/4)}$ curves persists (roughly at $\lambda/(1+\lambda) \approx 0.70$) as does the peak in the $\sigma^2(S'(L/4))$ plot. How this peak value changes as we approach the thermodynamic limit is an open question and we hope that better tools of numerical analysis like matrix product state methods can shed some light on this issue. We leave this for future work.

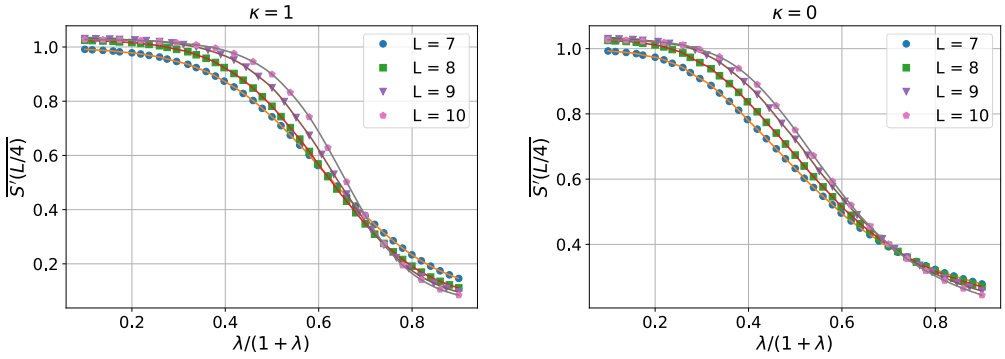

Figure 5.3: Mean of $S'(L/4)$ distribution (with spline fit) as a function of $\lambda/(1+\lambda)$ for $\kappa = 0$ and $\kappa = 1$. 243 eigenstates per disorder realization that transform as 1D irreps sampled for 800 (7,8 sites), 879 (9 sites) and 654 (10 sites) disorder realizations respectively.

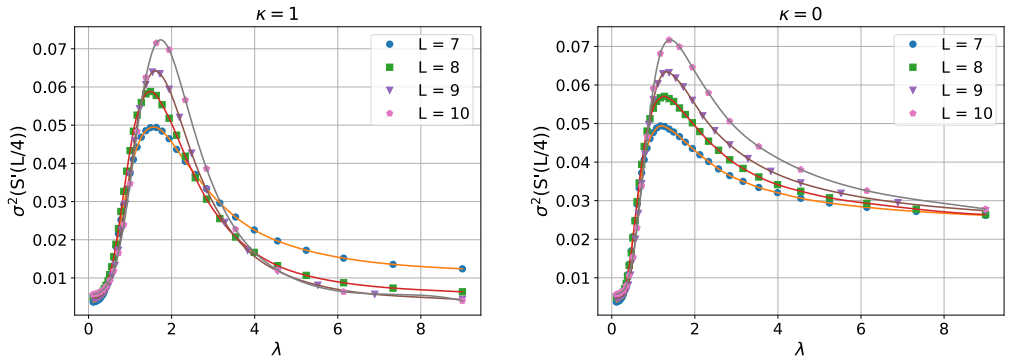

Figure 5.4: Variance of $S'(L/4)$ distribution (with spline fit) as a function of λ for $\kappa = 0$ and $\kappa = 1$. 243 eigenstates per disorder realization that transform as 1D irreps sampled for 800 (7,8 sites), 879 (9 sites) and 654 (10 sites) disorder realizations respectively.

5.3.2 Spontaneous symmetry breaking in excited states

As indicated by the entanglement distributions, the full MBL phase appears only in the $\kappa = 1$ limit. This is the limit where the disordered 'l-bit' term is dominated by $\sum_i J_i \; S_i^z S_{i+1}^z$ which triggers the spontaneous symmetry breaking (SSB). To confirm that SSB has indeed taken place for the many-body excited states, we use a spin-glass diagnostic which we describe below. In the study of classical spin glasses [180, 181], one is interested in order parameters sensitive to the spin-glass phase characterized by long-range order in the presence of disorder. One such important quantity of study is the spin-glass susceptibility [182]

$$\chi = \frac{1}{N} \sum_{i,j=1}^{N} \left[\langle s_i s_j \rangle^2 \right], \tag{5.7}$$

where, s_i are classical Ising variables, $\langle * \rangle$ indicates statistical averaging and $[*]$ indicates disorder averaging. In Ref [24], the authors defined a similar quantum mechanical diagnostic to detect spin-glass (SG) order arising from SSB of $\mathbb{Z}_2 \rightarrow$ *trivial group* in a $\mathbb{Z}_2$ invariant Ising- like disordered spin chain:

$$\chi^{SG} = \frac{1}{L} \sum_{i,j=1}^{L} |\langle \epsilon | \sigma_i^z \sigma_j^z | \epsilon \rangle|^2, \tag{5.8}$$

where, $|\epsilon\rangle$ is an energy eigenstate and σ^z is the Pauli-Z operator. In their model, it was shown that the average $\overline{\chi^{SG}}$ scales with system size as $\overline{\chi^{SG}} \sim L$ in the MBL-SG phase and approaches a constant value set by normalization

for the paramagnetic phase. Similar to eq. 5.8, for our model, we define the following spin-glass diagnostic that looks for signatures of spin glass order arising from SSB of $S_3 \to \mathbb{Z}_3$

$$\chi^{SG}_{\mathbb{Z}_3} = \frac{1}{L-1} \sum_{i \neq j=1}^{L} |\langle \epsilon | S^z_i S^z_j | \epsilon \rangle|^2. \tag{5.9}$$

Note that we choose to exclude the $i = j$ term in the summation unlike Eq [5.8]. We look at the statistics of $\chi^{SG}_{\mathbb{Z}_3}$ across randomly sampled eigenstates and disorder realizations. We find signatures for transition to an MBL-SG phase as we vary λ similar to what was found in Ref [24]. Fig. 5.5 shows $\overline{\chi^{SG}_{\mathbb{Z}_3}}$ versus λ for $\kappa = 0, 1$. For $\kappa = 1$, we indeed observe that the SG diagnostic increases

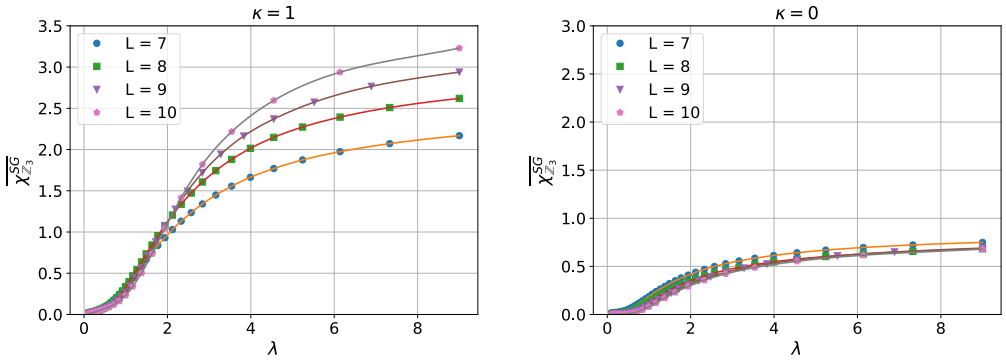

Figure 5.5: $\overline{\chi^{SG}_{\mathbb{Z}_3}}$ versus λ (with spline fit) for $\kappa = 0$ and $\kappa = 1$. 243 eigenstates per disorder realization that transform as 1D irreps sampled for 800 (7,8 sites), 879 (9 sites) and 715 (10 sites) disorder realizations respectively.

with system size for large disorder. For $\kappa = 0$, we see that the SG diagnostic at best saturates to a constant value independent of system size and at worst reduces with system size but certainly does not increase with it indicating the lack of SSB. To rule out SSB to other subgroups in the $\kappa = 0$ regime, we have to use other SG diagnostics that can detect spontaneous breaking of S_3 down to one of the other subgroups like $\mathbb{Z}_2$ and trivial group. In Appendix C.4, we construct appropriate SG diagnostics and present numerical evidence that the full S_3 is indeed intact for $\kappa = 0$.

5.3.3 Level statistics

Level statistics is a basis independent diagnostic that indicates localization and thermalization based on the statistics of the adjacent gap ratio ($\delta_n =$

$E_{n+1} - E_n$) defined as,

$$r_n = \min(\delta_n, \delta_{n+1}) / \max(\delta_n, \delta_{n+1}). \tag{5.10}$$

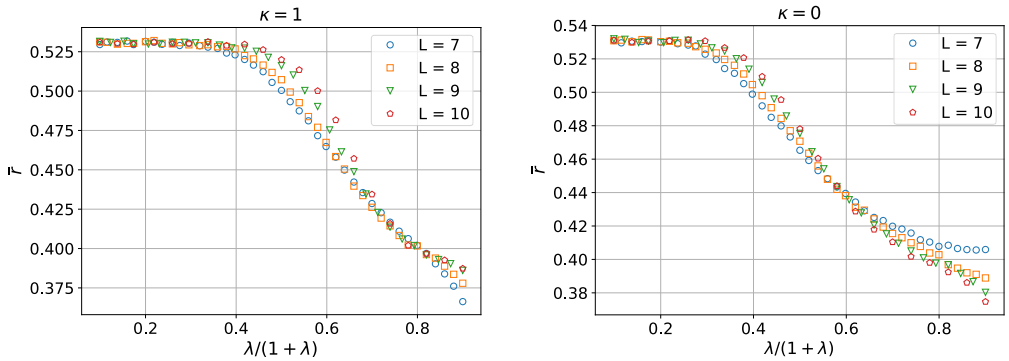

Figure 5.6: $\bar{r}$ versus $\lambda/(1+\lambda)$ for $\kappa = 0$ and $\kappa = 1$. 243 eigenstates per disorder realization that transform as 1D irreps sampled for 800 (7,8 sites), 879 (9 sites) and 715 (10 sites) disorder realizations respectively.

In the presence of symmetry, no interaction term in the Hamiltonian can mix eigenstates that transform as different irreducible representations of the symmetry group. Thus, it is meaningful to compute $r_n(\Gamma)$, the level statistics ratio for the eigenstates that transform as each irrep Γ of the group separately. In this chapter, in Fig. 5.6, we present $\bar{r} = \frac{\bar{r}(\mathbf{1})+\bar{r}(\mathbf{1}')}{2}$ as a function of λ where $\bar{r}(\Gamma)$ is obtained by averaging $r_n(\Gamma)$ computed for randomly sampled eigenstates which transform as the Γ irrep (see Appendix C.3 for details on how we detect the irrep of each eigenstate), across disorder realizations. On the side with low disorder, for both $\kappa = 0$ and $\kappa = 1$, we observe $\bar{r} \approx 0.53$. This is typical for a fully thermal phase indicating a Wigner-Dyson (WD) distribution. For a fully localized phase, typically, $\bar{r} \approx 0.39$, corresponding to Poisson distribution. However, the application of this diagnostic to the degenerate spectrum of our S_3 invariant Hamiltonian can be tricky. In particular, closer to the l-bit point of large λ, the extensively degenerate spectrum may mimic level clustering and result in $\bar{r} < 0.39$ which we do indeed observe. Hence, this diagnostic is only reliable at the thermal side, where we obtain the WD value of $\bar{r} \approx 0.53$. For the strong disorder, the level statistics approaches Poisson value but a clear reading is plagued by the degeneracies for both $\kappa = 0, 1$.

5.3.4 Finite size scaling

In order to determine the location and nature of the putative transitions, we perform finite size scaling collapse for MBL and SG diagnosics using the following scaling ansatz used in Ref [24].

$$g(\lambda, L) = L^a f((\lambda - \lambda_c)L^{\frac{1}{\nu}}) \tag{5.11}$$

Fig. 5.7 shows the scaling collapse of the diagnostics $\overline{S'(L/4)}$, $\sigma^2(S'(L/4))$ and $\overline{\chi^{SG}_{\mathbb{Z}_3}}$ for 8, 9 and 10 site data. For $\kappa = 1$, we obtain a good collapse for both the MBL and SG diagnostics at $\lambda_c \approx 2.65$ and $\nu \approx 2.5$. For $\kappa = 0$, we do not get a scaling collapse for the SG diagnostic $\chi^{SG}_{\mathbb{Z}_3}$ for non-zero λ_c and positive ν which is consistent with the absence of SSB. On the other hand, we get a reasonable collapse for $\overline{S'(L/4)}$ and $\sigma^2(S'(L/4))$ at $\lambda_c \approx 2.35$ and $\nu \approx 2.5$.

Note that the value of the finite size exponent ν used in Fig. 5.7 is consistent with the Harris [183]/CCFS [184, 185]/CLO [186] criterion of $\nu \geq 2$ for one dimensional spin chains with quenched disorder. However, we emphasize that the our estimate is very rough and even for values of ν that violates the criterion (eg: $\nu \approx 1.5$), we still get a decent collapse. This violation is a common feature of ED studies of small system sizes [24, 187]. Indeed, recent work by Khemani and Huse [188] suggests that this might be an indication of the system not exhibiting true thermodynamic behavior and is expected to undergo a crossover after which we obtain ν consistent with the Harris/CCFS/CLO bounds. Within the accuracy of our numerical investigation however, we can neither confirm nor rule out the possibility of our system being en-route to such a crossover.

5.4 Discussion

Based on the above analysis, we are in a position to put together an approximate phase diagram for the model Hamiltonian H. Fig. 5.8 shows a color map of $\overline{S'(L/4)}$, $\overline{\chi^{SG}_{\mathbb{Z}_3}}$ and $\overline{r}$ plotted in the κ, λ space. Fig. 5.9 shows a schematic plot that indicates a thermal phase for the weak disorder limit and a MBL+SSB phase for strong disorder limit. In addition to these two phases, there is a hint of a third regime for strong disorder and no SSB, where there seems to be a coexistence of localized and delocalized states in the many-body spectrum. We now discuss each of this regimes separately.

Thermal phase. For the thermal phase, the distribution of slopes has a mean that saturates at the maximal entropy per unit site. This indicates a substantial presence of volume law scaling eigenstates. The distribution of $\chi^{SG}_{\mathbb{Z}_3}$ has mean that does not increase with system size and implies absence of

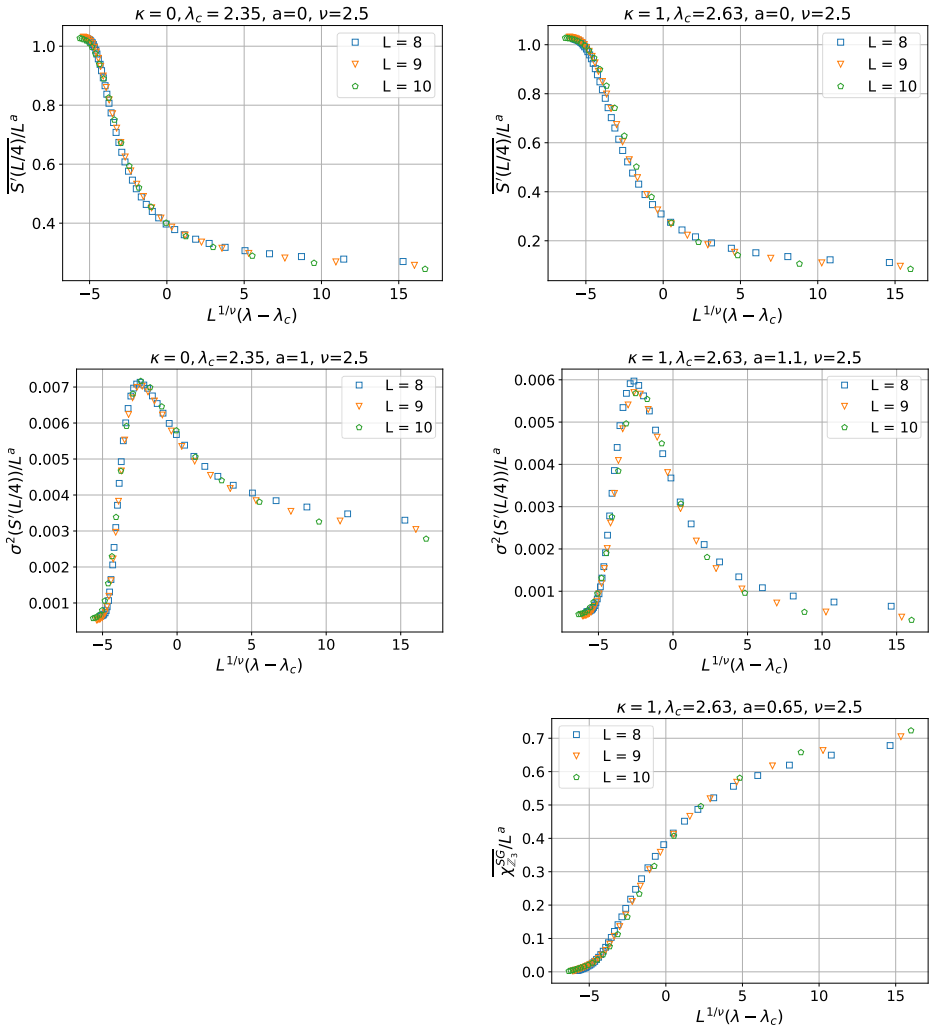

Figure 5.7: Scaling collapse of MBL and SG diagnostics for 8, 9 and 10 sites.

SSB. The level statistics clearly show Wigner-Dyson distribution highlighting the thermal nature of this regime.

MBL+SSB phase. For the MBL+ SSB phase, the distribution of slopes has mean close to 0. This indicates the presence of area-law scaling eigenstates. The distribution of $\chi^{SG}_{\mathbb{Z}_3}$ parameter (designed to detect $S_3 \to \mathbb{Z}_3$ symmetry breaking) increases with system size. This indicates a substantial presence of eigenstates with SSB. The above results are consistent with a spin-glass phase with a residual abelian symmetry group that supports a full MBL states with strong signatures of SSB at all eigenstates. The level statistics data is more noisy due to the level clustering as a result of degeneracies in this regime but

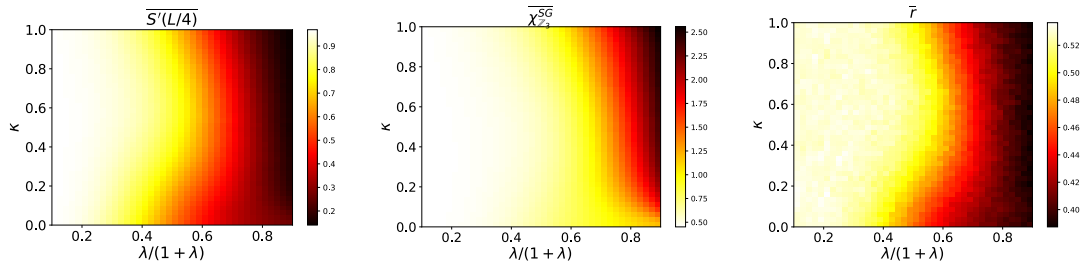

Figure 5.8: Color map of $\overline{S'(L/4)}$, $\overline{\chi^{SG}_{\mathbb{Z}_3}}$ and $\overline{r}$ for $\lambda/(1+\lambda) \in [0.1, 0.9]$ and $\kappa \in [0, 1]$. 200 eigenstates of the 7 site Hamiltonian [5.5] that transform as 1D irreps sampled randomly for 238 disorder realizations.

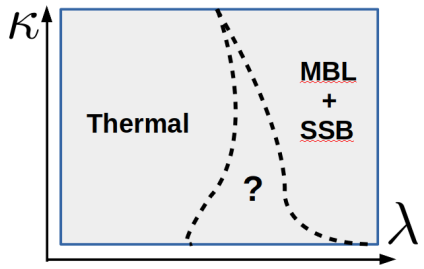

Figure 5.9: The three regions labeled in a schematic plot.

hovers around the Poisson value.

Intermediate phase. This case is shown as dashed region in the schematic Fig 5.9. The full S_3 symmetry is intact in this regime and is incompatible with the full MBL phase. At the l-bit point ($\lambda \to \infty$), the many-body spectrum has extensive number of states with extensive degeneracy. Any infinitesimal thermal perturbation is expected to split this extensive degeneracy down to the minimal values set by the size of the irreps of the group (2 and 1 in our case). This is expected to result in resonant delocalization of an extensive number of states. Thus the most plausible scenario is a fully thermal phase. Our numerical results, however, are not fully consistent with a thermal phase, but do not have the strong signatures of MBL-SG or MBL phases, either. A possibility for this regime is a marginal MBL phase that may be separating another MBL+SSB phase that is not explored within our parameter space. This can be uncovered introducing disorder to some of the relevant two-body thermal terms which are non-disordered in our current analysis. We leave this investigation for future work.

Finite-size effects such as the critical-cone region [178] are important in this putative intermediate phase. Indeed, such finite-size effects play an important role at large λ, and one has to be careful about the order of the thermodynamic

and large λ limits. At finite-size L, large λ corresponds to adding a small perturbation of H_t on top of the lbit Hamiltonian, and for $1/\lambda$ much smaller than the lbit many-body level spacing $\sim 3^{-L}$ one can apply first-order perturbation theory. One effect is to split the exponentially degenerate lbit states, resulting presumably in volume law eigenstates. However, there are also states in the lbit spectrum which are not highly degenerate, corresponding to sectors where most of the sites sit in the one dimensional irrep, and only a few sit in the two dimensional irrep. These are area law states, and could remain area law upon the addition of such a small perturbation. Thus some vestiges of localization are expected to remain at large λ for a finite-size L. More numerical work at larger sizes will have to be done to distinguish these effects from a truly thermodynamic intermediate phase.

5.5 Summary and outlook

In this chapter, we construct and study a spin-1 Hamiltonian invariant under an on-site S_3 symmetry using various disorder and symmetry diagnostics. We study the eigenstate phases that can arise via ergodicity and symmetry breaking. Within the accuracy of our numerical analysis, we can identify three regions in the two-parameter Hamiltonian space two of which are consistent with thermal, MBL- spin-glass phases and a third whose identity is not established with certainty in the present study. We state our observations about various characteristics of this region and speculate with regard to its identity.

There are other interesting questions that are left for future study. In this work, we are limited to small system sizes by the tools of numerical analysis employed *i.e.* exact diagonalization. There is much to be gained in designing and employing other numerical techniques to study larger system sizes. In this regard, it would be useful to explore the extension of tensor network techniques, which have been shown to be effective in the case of full-MBL, where eigenstates are expected to have area-law properties, to other settings, in particular to further study the disordered region with unbroken S_3 symmetry. Another extension of is to repeat our study in a Floquet setting where exotic possibilities have been conjectured in the presence of global symmetries [27–31]. Here, the arguments for instability of disordered Floquet systems with non-abelian symmetries to thermalization would be stronger because of energy pumping. However, as we saw in the equilibrium case, such a system might have interesting features worth exploring. Furthermore, we could consider relaxing the setting of indefinitely stable phases, like MBL, to the so-called 'pre-thermal' setting [189, 190] where the system is stable for large times and study the role of non-abelian symmetries.

Appendix A

Appendix to Chapter 2

A.1 Constructing the symmetric Hamiltonian

We provide details of the construction of the Hamiltonian in Sec 2.2. We remind the reader that the group of on-site symmetries we consider is A_4, the alternating group of degree four and the group of even permutations on four elements. The order of this group is 12 and can be enumerated with two generators,

$$\langle a, x | a^3 = x^2 = (ax)^3 = e \rangle. \tag{A.1}$$

The on-site representation, $u(g)$ we consider that the spins transform under is the faithful 3D irrep of A_4 with generators

$$a = \begin{pmatrix} 0 & 1 & 0 \\ 0 & 0 & 1 \\ 1 & 0 & 0 \end{pmatrix}, \; x = \begin{pmatrix} 1 & 0 & 0 \\ 0 & -1 & 0 \\ 0 & 0 & -1 \end{pmatrix} \tag{A.2}$$

We use group invariant polynomials as building blocks to construct Hermitian operators invariant under group action. A group G invariant n-variable polynomial $f(x_1, x_2, \ldots x_n)$ is unchanged when the n-tuplet of variables $(x_1, x_2 \ldots x_n)$ is transformed under an n-dimensional representation of the group $U(g)$.

$$f(x_1', x_2' \ldots x_n') \;\; = \;\; f(x_1, x_2 \ldots x_n), \tag{A.3}$$

where $x_i' = U(g)_{ij} x_j$. If we have n Hermitian operators $X_{i=1\ldots n}$ that are n-dimensional and transform covariantly like the n variables of the polynomial $x_{i=1\ldots n}$, *i.e.* $U(g) X_i U^\dagger(g) = U(g)_{ij} X_j$, then we can elevate the group invariant polynomials to group invariant operators as $f(x_1, x_2, \ldots x_n) \to f(X_i, X_2 \ldots X_n)$ carefully taking into account that unlike the numbers x_i, the operators X_i do

not commute.

Since we need three-dimensional operators of A_4, we consider the set of independent three variable polynomials invariant under the action of the 3D irrep of A_4 [152]:

$$f_1(x,y,z) = x^2+y^2+z^2, \tag{A.4}$$
$$f_2(x,y,z) = x^4+y^4+z^4, \tag{A.5}$$
$$f_3(x,y,z) = xyz. \tag{A.6}$$

We know that the spin operators S^i satisfying $[S^i, S^j] = i\epsilon_{ijk}S^k$ transform covariantly under any $SO(3)$ rotation, in particular for the finite set of rotations that corresponds to the subgroup $A_4 \subset SO(3)$. Thus, to find invariant operators for the three-dimensional representation, we need to take the spin operators in the appropriate three-dimensional basis in terms of the Spin-1 states $|J=1, m_z\rangle \cong |m_z\rangle = \{|\pm 1\rangle, |0\rangle\}$ so as to get the irrep defined above.

$$|x\rangle = \frac{1}{\sqrt{2}}(|-1\rangle - |1\rangle),\ |y\rangle = \frac{i}{\sqrt{2}}(|-1\rangle + |1\rangle),\ |z\rangle = |0\rangle,$$

and elevate the polynomials f_1, f_2, f_3 to operators as

$$\begin{aligned} F_1 &= S^x_a S^x_b + S^y_a S^y_b + S^z_a S^z_b, \\ F_2 &= (S^x_a S^x_b)^2 + (S^y_a S^y_b)^2 + (S^z_a S^z_b)^2, \\ F_3 &= S^x_a S^y_b S^z_c + S^z_a S^x_b S^y_c + S^y_a S^z_b S^x_c + S^y_a S^x_b S^z_c + S^x_a S^z_b S^y_c + S^z_a S^y_b S^x_c, \end{aligned}$$

where the indices a, b, c label any other quantum numbers collectively like lattice sites and can be chosen as per convenience, say to make the operators local as we will do next. As a model Hamiltonian, we could use any function of the invariant operators F_1, F_2 and F_3 and ensure that everything is symmetric under the exchange of lattice labels to impose inversion symmetry.

We start with the Hamiltonian for the Spin-1 Heisenberg antiferromagnet which is constructed using F_1 with $\{a, b\}$ chosen to make the interactions nearest neighbor:

$$H_{Heis} = \sum_i \boldsymbol{S}_i \cdot \boldsymbol{S}_{i+1} \text{ where } \boldsymbol{S}_i \cdot \boldsymbol{S}_{i+1} \equiv S^x_i S^x_{i+1} + S^y_i S^y_{i+1} + S^z_i S^z_{i+1}.$$

We add the two other combinations to the Heisenberg Hamiltonian so as to break the $SO(3)$ symmetry to A_4 by using F_2 and F_3 as follows:

$$H_q = \sum_i \boldsymbol{S}^2_i \cdot \boldsymbol{S}^2_{i+1} \text{ where, } \boldsymbol{S}^2_i \cdot \boldsymbol{S}^2_{i+1} \equiv (S^x_i S^x_{i+1})^2 + (S^y_i S^y_{i+1})^2 + (S^z_i S^z_{i+1})^2,$$

and

$$H_c = \sum_i [(S^x S^y)_i S^z_{i+1} + (S^z S^x)_i S^y_{i+1} + (S^y S^z)_i S^x_{i+1} + (S^y S^x)_i S^z_{i+1} + (S^x S^z)_i S^y_{i+1} + (S^z S^y)_i S^x_{i+1} + S^x_i (S^y S^z)_{i+1} + S^z_i (S^x S^y)_{i+1} + S^y_i (S^z S^x)_{i+1} + S^x_i (S^z S^y)_{i+1} + S^z_i (S^y S^x)_{i+1} + S^y_i (S^x S^z)_{i+1}]. \quad \text{(A.7)}$$

The operators are symmetrized so that the Hamiltonian is invariant under inversion as well as lattice translation. With these pieces, we arrive at the total Hamiltonian which is invariant under $A_4 \times G_{\mathcal{P}}$:

$$H = H_{Heis} + \lambda H_c + \mu H_q. \quad \text{(A.8)}$$

A.2 Review of classification of SPT phases protected by Time reversal symmetry

A.2.1 Without on-site symmetry or parity

The time reversal symmetry group $G_{\mathcal{T}}$ is generated by the anti-unitary action $\mathcal{T}$ which is a combination of an on-site unitary operator v and complex conjugation, θ

$$\mathcal{T} = v_1 \otimes v_2 \cdots \otimes v_N \; \theta \quad \text{(A.9)}$$

where, if the basis at each site $|i\rangle$ is real, the action of θ is simply

$$\theta : c_{i_1 \ldots i_N} \rightarrow c^*_{i_1 \ldots i_N} \quad \text{(A.10)}$$

$$\theta : Tr[A^{i_1}_1 \ldots A^{i_N}_N] \rightarrow Tr[(A^{i_1}_1)^* \ldots (A^{i_N}_N)^*] \quad \text{(A.11)}$$

$\mathcal{T}^2 = \pm 1$ in general. However, it was shown in Refs. [51, 52] that only the case of $\mathcal{T}^2 = 1$ corresponds to gapped phases and we will consider only this case. $G_{\mathcal{T}} = \{e, \mathcal{T}\}$. The action on the MPS matrices is

$$\mathcal{T} : A^i_M \rightarrow v_{ij} (A^j_M)^* \quad \text{(A.12)}$$

If $G_{\mathcal{T}}$ is a symmetry of the Hamiltonian which is not broken by the ground state $|\psi\rangle$, we have, under the action of $\mathcal{T}$,

$$\mathcal{T}|\psi\rangle = |\psi\rangle. \quad \text{(A.13)}$$

Note that the possibility of $\alpha(T)$ analogous to $\alpha(P)$ of Sec. (2.3.5) can be eliminated by re-phasing the spin basis (See Refs. [36, 52]). The condition Eq. (2.26) can also be imposed on the level of the MPS matrices that describe $|\psi\rangle$:

$$v_{ij}(A_M^j)^* = M^{-1}A_M^i M, \tag{A.14}$$

Here, M has the property $M^T = \beta(T)M = \pm M$. $\beta(T) = \pm 1$ *labels the two SPT phases protected by* $G_{\mathcal{T}}$. [52]

A.2.2 With parity

If the actions of parity and time reversal commute, the 8 SPT phases protected by $G_{\mathcal{P}} \times G_{\mathcal{T}}$ are labeled by $\{\alpha(P), \beta(P), \beta(T)\}$ as defined before in Secs (2.3.5,A.2.1). [52].

A.2.3 With on-site symmetry

If the action of the on-site symmetry transformation $U(g)$ commutes with $\mathcal{T}$, we have a similar result to Eq. (2.29).

$$U(g)\mathcal{T}|\psi\rangle = \mathcal{T}U(g)|\psi\rangle, \tag{A.15}$$

this imposes constraints on the matrix M defined as [52].

$$M^{-1}V(g)M = \gamma_T(g)V^*(g). \tag{A.16}$$

The different SPT phases protected by $G \times \mathcal{T}$ are labeled by $\{\omega, \beta(T), \gamma_T(g)\}$ where, $\omega \in H^2(G_{int}, U(1))$ which satisfy $\omega^2 = e$, $\gamma_T \in \mathcal{G}/\mathcal{G}^2$ using the same arguments as Sec (2.3.5). If translation invariance is also a symmetry, the set of 1D representations $\chi(g)$ in Eq (2.10) which satisfy $\chi(g)^2 = 1$ also label different phases in addition to the ones already mentioned before. [52]

A.2.4 With on-site and parity

The different SPT phases protected by $G \times \mathcal{T} \times G_{\mathcal{P}}$ are labeled by

$$\{\omega, \chi(g), \alpha(P), \beta(P), \beta(T), \gamma(g), \gamma_T(g)\},$$

where, $\omega \in H^2(G_{int}, U(1))$ which satisfy $\omega^2 = e$, $\gamma(g)$ and $\gamma_T(g) \in \mathcal{G}/\mathcal{G}^2$, $\chi(g)^2 = 1$ and $\mathcal{G}$ is the set of 1D representations of G_{int}. [52]

Appendix B

Appendix to Chapter 4

B.1 Some remarks on projective representations

A projective representation respects group multiplication up to a complex phase i.e.,

$$V(g_1)V(g_2) = \omega(g_1, g_2)V(g_1 g_2), \tag{B.1}$$

Group associativity places constrains the phase ω:

$$\begin{aligned} V(g_1)(V(g_2)V(g_3)) &= (V(g_1)V(g_2))V(g_3) && \text{(B.2)} \\ \implies \omega(g_1, g_2 g_3)\omega(g_2, g_3) &= \omega(g_1, g_2)\omega(g_1 g_2, g_3). && \text{(B.3)} \end{aligned}$$

The possible ω's fall into different classes and each class has its own set of irreducible representations. These classes are labelled by the elements of the second cohomology group of G, $H^2(G, U(1))$. The identity element of this group labels the familiar set of linear irreducible representations.

We also note that there exists a gauge freedom that preserves the equivalence class of ω: If we re-phase ω as

$$\omega(g_1, g_2) \mapsto \tilde{\omega}(g_1, g_2) = \omega(g_1, g_2)\frac{\beta(g_1)\beta(g_2)}{\beta(g_1 g_2)}, \tag{B.4}$$

it still satisfies the condition (B.2) and $\tilde{\omega} \sim \omega$. This means that while the re-phasing transforms each element of the projective representation as $V(g) \mapsto \tilde{V}(g) = \beta(g)V(g)$, the new $\tilde{V}$ belongs to the same class of projective representations as V *i.e.* $\tilde{V}(g_1).\tilde{V}(g_2) = \tilde{\omega}(g_1, g_2)\tilde{V}(g_1.g_2)$.

B.2 SPT phases with spatial-inversion and time-reversal invariance

The action of spatial-inversion or parity, $\hat{P}$ can be effected by a combination of an on-site action by some unitary operator w and a reflection, $\hat{R}$ that exchanges lattice sites n and $-n$.

$$\hat{P} = w_1 \otimes w_2 \cdots \otimes w_N \ \hat{R}. \tag{B.5}$$

Since we cannot talk about inversion in disordered systems, we assume the system also has lattice translation invariance. If parity is a symmetry of a wavefunction $|\psi\rangle$, we have

$$\hat{P}|\psi\rangle = \alpha(P)^N |\psi\rangle. \tag{B.6}$$

The condition Eq. (B.6) can also be imposed on the level of the MPS matrices that describe $|\psi\rangle$:

$$w_{ij}(A^j)^T = \alpha(P) N^{-1} A^i N, \tag{B.7}$$

where, $\alpha(P) = \pm 1$ labels parity even or odd and the action of parity on the virtual space N has the property $N^T = \beta(P)N = \pm N$. $\{\alpha(P), \beta(P)\}$ label the 4 distinct phases protected by parity [52].

The anti-unitary action of time-reversal $\hat{T}$ on the other hand is effected by a combination of an on-site unitary action acting on the internal spin degrees of freedom, v and a complex conjugation $\hat{K}$: $\hat{T} = v_1 \otimes v_2 \cdots \otimes v_n \ \hat{K}$. If this is a symmetry of a wavefunction $|\psi\rangle$, we have

$$\hat{T}|\psi\rangle = |\psi\rangle. \tag{B.8}$$

We no longer need to allow an overall phase $\alpha(T)^N$ because of the anti-unitary nature of $\hat{T}$ that allows it to be absorbed into redefining each basis $|i\rangle \to \sqrt{\alpha(T)}|i\rangle$.

Proof.

$$\begin{aligned}
\hat{T}|\psi\rangle &= \alpha(T)^N |\psi\rangle, && \text{(B.9)}\\
\sqrt{\alpha^*(T)^N}\hat{T}|\psi\rangle &= \sqrt{\alpha(T)^N}|\psi\rangle, && \text{(B.10)}\\
\hat{T}\sqrt{\alpha(T)^N}|\psi\rangle &= \sqrt{\alpha(T)^N}|\psi\rangle, && \text{(B.11)}\\
\hat{T}|\psi'\rangle &= |\psi'\rangle. && \text{(B.12)}
\end{aligned}$$

□

The condition of Eq. (B.6) can also be imposed on the level of the MPS matrices that describes $|\psi\rangle$

$$v_{ij}(A^j)^* = M^{-1}A^iM, \tag{B.13}$$

where, $MM^* = \beta(T)\mathbb{1} = \pm\mathbb{1}$ and $\beta(T)$ labels the two distinct phases of time-reversal invariant Hamiltonians.

Finally if we consider systems invariant under both parity and time-reversal, there are 8 distinct phases labelled by $\{\alpha(P), \beta(P), \beta(T)\}$ as defined before. However, since the action of parity and time-reversal should commute, this imposes constraints on the matrices M and N as

$$MN^\dagger MN^\dagger \propto\ e^{i\theta}\mathbb{1} \tag{B.14}$$

We direct the reader to Ref. [52] for details on several results used in this section.

B.3 SPT Phases with combination of on-site symmetry, spatial-inversion and time-reversal invariance

We now look at ground states of SPT phases of gapped Hamiltonians with on-site symmetry combined with parity, time-reversal invariance or both. We find that the 'B' matrices of decomposition of Sec. 4.3.1 have further constraints in the way described in Sec. B.2.

On-site symmetry + parity

Let us consider SPT phases protected by an on-site symmetry G under a representation $u(g)$ combined with parity. If the actions of the two symmetry transformations commute on the physical level,

$$\hat{U}\hat{P}|\psi\rangle = \hat{P}\hat{U}|\psi\rangle, \tag{B.15}$$

this imposes constraints on the matrix N defined in Sec. B.2 as [52].

$$N^{-1}V(g)N = \gamma(g)V^*(g). \tag{B.16}$$

Where, $\gamma(g)$ is a one-dimensional irrep of G that arises from the commutation of on-site and parity transformations [52] and $V(g)$ is the reduced (block-diagonal) representation of G acting on the virtual space as discussed

in Sec 4.3.1 that contains all the irreps, $V_1 \cdots V_r$ of a certain projective class ω.

$$V(g) = \begin{pmatrix} \mathbb{1}_1 \otimes V_1(g) & 0 & \dots & 0 \\ 0 & \mathbb{1}_2 \otimes V_2(g) & \dots & \vdots \\ \vdots & & \ddots & \vdots \\ 0 & \dots & 0 & \mathbb{1}_r \otimes V_r(g) \end{pmatrix}. \tag{B.17}$$

$\mathbb{1}_i$ is the trivial action on the degeneracy space of 'B' matrices as defined earlier. Different phases of matter are now labeled by $\{\omega, \chi(g), \alpha(P), \beta(P), \gamma(g)\}$ [52]:

1. The different projective classes $\omega \in H^2(G, U(1))$ which satisfy $\omega^2 = 1$.
2. The different one-dimensional irreps χ of G since the system is translationally invariant.
3. $\alpha(P)$, the parity of the spin chain
4. $\beta(P)$ which denotes whether the virtual space parity representation is symmetric or anti-symmetric.
5. $\gamma(g) \in \mathcal{G}/\mathcal{G}_2$ where $\mathcal{G}$ labels the group of 1D irreps of G and $\mathcal{G}_2$ labels the group of the square of 1D irreps of G. This arises due to the commutation of parity and on-site symmetry transformations in the virtual space.

Given a set of labels, $\{\omega, \chi(g), \alpha(P), \beta(P), \gamma(g)\}$, we constrain the MPS ground-state wavefunction We observe that the right hand side of Eq. (B.16) can be written as

$$\gamma(g)V^*(g) = L_\gamma V(g) L_\gamma^{-1}, \tag{B.18}$$

where, L_γ involves permutation of irrep blocks and possibly a change of basis on the irreps of $V(g)$ and can be obtained by considering the effect of re-phasing each of the complex conjugated irrep blocks $V_\alpha^*(g)$ with $\gamma(g)$.

Proof. To see this, we first note that when $\omega^2 = 1$ *i.e.* $\omega = \omega^*$, $V_\alpha^*(g)$ is a representation that belongs to the same class of projective irreps ω as $V_\alpha(g)$ as seen by complex conjugating Eq. (4.8). $\gamma(g)V_\alpha^*(g)$ also belongs to the same class because $\gamma(g)$ belongs to the class labelled by the trivial element $e \in H^2(G, U(1))$ and hence $\gamma(g)V_\alpha^*(g)$ belongs to the class $e * \omega = \omega$. To show that $\gamma(g)V_\alpha^*(g)$ is also an irrep, we start with the characters χ_α of the irrep V_α which satisfy the irrep condition of the group of order $|G|$ [152]

$$\frac{1}{|G|} \sum_{g \in G} \chi(g)\chi^*(g) = 1 \tag{B.19}$$

The characters of $\gamma(g)V^*_\alpha(g)$, $\bar{\chi}_\alpha = \gamma\chi^*_\alpha$ can also easily be shown to satisfy the same condition

$$\frac{1}{|G|}\sum_{g\in G}\bar{\chi}(g)\bar{\chi}^*(g) = \frac{1}{|G|}\sum_{g\in G}\gamma(g)\chi^*(g)\gamma^*(g)\chi(g) = 1 \tag{B.20}$$

Thus $\gamma(g)V^*_\alpha(g) \sim V_{p(\alpha)}(g)$ is some other irrep in the class $\omega \in H^2(G, U(1))$. We can check that $V_{p(\alpha)}$ again form the complete set of irreps as we run over α. This means that the reduced representation $\gamma(g)V^*(g)$ can be obtained from Eq. (B.17) by permuting the irrep blocks and with a change of basis and can be done using a matrix L_γ.

$$\gamma(g)V^*(g) = L_\gamma V(g) L_\gamma^{-1} \tag{B.21}$$

□

Using this, Eq. (B.16) can be rewritten as

$$(NL_\gamma)^{-1}V(g)(NL_\gamma) = V(g). \tag{B.22}$$

Eq. (B.22) imposes constraints on the matrix NL_γ block-wise using Schur's lemma for each irrep block of $V(g)$,

$$NL_\gamma = \begin{pmatrix} N_1 \otimes \mathbb{1}'_1 & 0 & \dots & 0 \\ 0 & N_2 \otimes \mathbb{1}'_2 & \dots & \vdots \\ \vdots & & \ddots & \vdots \\ 0 & \dots & 0 & N_r \otimes \mathbb{1}'_r \end{pmatrix}, \tag{B.23}$$

where $\mathbb{1}'_\alpha$ is the identity matrix in the irrep V_α. Moving L_γ to the other side of the equation gives the form of N. This form can be used in the condition Eq. (B.7) which effectively results in conditions of the 'B' matrices of A^i of Eq. (4.27) determined from labels $\{\omega, \chi\}$. So far, we have used the labels $\{\omega, \chi(g), \gamma(g)\}$ to constrain the MPS matrices. The labels $\alpha(P)$ and $\beta(P)$ determine the form of the blocks N_α and are imposed on the 'B' matrices when we use Eq. (B.7) and the results of Sec. B.2.

On-site symmetry + time reversal

We can repeat the same exercise for time-reversal invariance combined with on-site symmetry G. If the actions of the two symmetry transformations commute

$$\hat{U}\hat{T}|\psi\rangle = \hat{T}\hat{U}|\psi\rangle, \tag{B.24}$$

We find that the condition on the matrix M that results is identical to Eq. (B.16) [52].

$$M^{-1}V(g)M = \gamma'(g)V^*(g) \tag{B.25}$$

With additional translation invariance, different SPT phases are labelled by $\{\omega, \chi(g), \beta(T), \gamma'(g)\}$ [52] *i.e.*

1. The different projective classes $\omega \in H^2(G, U(1))$ which satisfy $\omega^2 = 1$.
2. The different one-dimensional irreps χ of G which satisfy $\chi^2 = 1$ if the system is translationally invariant. If not, different χ all label the same phase.
3. $\beta(T)$ defined by $MM^* = \beta(T)\mathbb{1}$
4. $\gamma'(g) \in \mathcal{G}/\mathcal{G}_2$ where $\mathcal{G}$ labels the group of 1D irreps of G and $\mathcal{G}_2$ labels the group of the square of 1D irreps of G. This arises due to the commutation of time-reversal and on-site symmetry transformations in the virtual space.

In the same way as for parity, we can find $L_{\gamma'}$ and the condition on M

$$ML_{\gamma'} = \begin{pmatrix} M_1 \otimes \mathbb{1}'_1 & 0 & \dots & 0 \\ 0 & M_2 \otimes \mathbb{1}'_2 & \dots & \vdots \\ \vdots & & \ddots & \vdots \\ 0 & \dots & 0 & M_r \otimes \mathbb{1}'_r \end{pmatrix} \tag{B.26}$$

Moving $L_{\gamma'}$ to the right hand side, we get the form of M and can use this in Eq. (B.13) to constrain the 'B' matrices of A^i in Eq. (4.27) employing labels $\{\omega, \chi(g), \gamma'(g)\}$ thus far. The label $\beta(T)$ determines the form of the blocks M_α and is imposed on the 'B' matrices when we use Eq. (B.13) and the results of Sec. B.2.

On-site symmetry + parity + time reversal

Finally, we consider the combined action of on-site symmetry, spatial-inversion and time-reversal invariance. The distinct SPT phases are labelled by $\{\omega, \chi(g), \alpha(P), \beta(P), \beta(T), \gamma(g), \gamma'(g)\}$ where all labels are defined as before with additional conditions $\omega^2 = 1$ and $\chi^2 = 1$ [52]. To write down the MPS form for the ground state of a phase labelled by these labels, we repeat the same procedure as we did before and obtain the forms of L_γ and $L_{\gamma'}$. Using this, we constrain the block form of M, N using Eqs. (B.23,B.26). The blocks

of M and N encode the information about $\{\alpha(P), \beta(P), \beta(T)\}$ and are used to constrain the 'B' matrix blocks of A^i in Eq. (4.27) using Eqs. (B.7,B.13).

We summarize this section with steps used to constrain ground states of SPT phases of Hamiltonians invariant under combinations of on-site symmetry with parity and/or time reversal:

1. The different SPT phases are labelled by a subset of the following labels $\{\omega, \chi(g), \alpha(P), \beta(P), \beta(T), \gamma(g), \gamma'(g)\}$ with $\omega^2 = 1$ and $\chi^2 = 1$.

2. Impose the labels from on-site symmetry *i.e.* $\{\omega, \chi(g)\}$ using the steps of Sec 4.3.3).

3. Impose the label γ (γ') from parity (time-reversal) symmetry by constructing L_γ ($L_{\gamma'}$) and thus constraining the matrices N (M) to a block form using Eqs. (B.23,B.26)).

4. Impose labels $\{\alpha(P), \beta(P), \beta(T)\}$ by restricting the form of the blocks of N, M appropriately and then using Eqs. (B.7,B.13).

We remark that while we can use $L_\gamma, L_{\gamma'}$ to determine the block form of M and N, constraining the individual blocks themselves is not straightforward and we do not investigate a way to do it in this chapter.

B.4 Obtaining the Clebsch-Gordan coefficients

We now review a method to obtain the CG matrices corresponding to finite group irrep decompositions of a certain kind. We follow the technique developed in Ref. [150]. Essentially what is needed are the two theorems presented below.

Theorem 1. *Consider a finite group G and a certain irrep $D(r)$, $r \in G$. If $D'(r)$ is an equivalent irrep i.e. $D'(g) = UD(g)U^\dagger$ then $\sum_{r\in G} D'(r)AD^\dagger(r) = \lambda U$ where A is an arbitrary matrix which is of the same size as D and λ is a constant which is a function of the elements of A*

To prove Theorem 1, we need the following two lemmas.

Lemma 1. *$M = \sum_{r\in G} D(r)BD(r)^\dagger \propto \mathbb{1}$ where B is an arbitrary matrix of the same size as D.*

Proof.

$$\begin{aligned} D(g)M &= D(g)\sum_{r\in G} D(r)BD(r)^\dagger = \sum_{r\in G} D(g)D(r)BD(r)^\dagger \\ &= \sum_{r\in G} D(gr)BD(r)^\dagger = \sum_{gr\in G} D(gr)BD(gr)^\dagger D(g) = MD(g), \\ \implies & [M, D(g)] = 0 \ \forall g \in G. \end{aligned} \tag{B.27}$$

From Schur's second lemma, we get $M \propto \mathbb{1}$ □

Lemma 2. *If $D^\alpha(g)$ and $D^\beta(g)$ are two inequivalent irreps, $M' = \sum_{r\in G} D^\alpha(r)BD^\beta(r)^\dagger = 0$*

Proof. Using the same arguments as before, we get $D^\alpha(g)M' = M'D^\beta(g)$. From Schur's first lemma we get $M' = 0$ □

To prove theorem 1, let us start with

$$\sum_{r\in G} D(r)BD(r)^\dagger = \lambda\mathbb{1}. \tag{B.28}$$

Then take $B = U^\dagger A$, we have

$$\begin{aligned} &\sum_{r\in G} D(r)U^\dagger AD(r)^\dagger = \lambda\mathbb{1} \\ &\therefore \sum_{r\in G} UD(r)U^\dagger AD(r)^\dagger = \lambda U \implies \sum_{r\in G} D'(r)AD(r)^\dagger = \lambda U. \end{aligned} \tag{B.29}$$

Theorem 2. *Let $D^\alpha(g)$ and $D^\beta(g)$ be two irreps of G. Let $D'(g) = D^\alpha(g) \otimes D^\beta(g)$ be the direct product representation of irreps whose CG decomposition is multiplicity free i.e. $\alpha \otimes \beta = \oplus_\gamma n^\gamma_{\alpha\beta}\gamma$ has all $n^\gamma_{\alpha\beta} \leq 1$. Let $D(g)$ be the completely reduced representation which is block diagonal containing all irreps in the decomposition of $\alpha \otimes \beta$ labelled $\gamma = 1 \dots m$.*

$$D(g) = \begin{pmatrix} D_1(g) & 0 & \dots & 0 \\ 0 & D_2(g) & \dots & \vdots \\ \vdots & & \ddots & \vdots \\ 0 & \dots & 0 & D_m(g) \end{pmatrix}. \tag{B.30}$$

If U consists of the CG matrices such that $D'(r) = UD(r)U^\dagger$, organized ac-

cording to the irrep sizes,

$$U = \begin{pmatrix} U_{11} & U_{12} & \dots & U_{1m} \\ U_{21} & U_{22} & \dots & U_{2m} \\ \vdots & \ddots & & \vdots \\ \vdots & & \ddots & \vdots \\ U_{m1} & U_{m2} & \dots & U_{mm} \end{pmatrix}, \tag{B.31}$$

then

$$\sum_{r\in G} D'(r) A D(r)^\dagger = \begin{pmatrix} \lambda_1 U_{11} & \lambda_2 U_{12} & \dots & \lambda_m U_{1m} \\ \lambda_1 U_{21} & \lambda_2 U_{22} & \dots & \lambda_m U_{2m} \\ \vdots & \ddots & & \vdots \\ \vdots & & \ddots & \vdots \\ \lambda_1 U_{m1} & \lambda_2 U_{m2} & \dots & \lambda_m U_{mm} \end{pmatrix}. \tag{B.32}$$

We need the following Lemma to prove Theorem 2.

Lemma 3.

$$\sum_{r\in G} D(r) B D(r)^\dagger = \begin{pmatrix} \lambda_1 \mathbb{1}_1 & 0 & \dots & 0 \\ 0 & \lambda_2 \mathbb{1}_2 & \dots & 0 \\ \vdots & \ddots & & \vdots \\ \vdots & & \ddots & \vdots \\ 0 & \dots & & \lambda_m \mathbb{1}_m \end{pmatrix}. \tag{B.33}$$

Proof.

$$\sum_{r\in G} D(r) B D(r)^\dagger = \sum_r \begin{pmatrix} D_1(r) B_{11} D_1(r)^\dagger & \dots & D_1(r) B_{1m} D_m(r)^\dagger \\ \vdots & \ddots & \vdots \\ D_m(r) B_{m1} D_1(r)^\dagger & \dots & D_m(r) B_{mm} D_m(r)^\dagger \end{pmatrix}. \tag{B.34}$$

Using the results of the last two Lemmas, we get

$$\sum_{r\in G} D(r) B D(r)^\dagger = \begin{pmatrix} \lambda_1 \mathbb{1}_1 & 0 & \dots & 0 \\ 0 & \lambda_2 \mathbb{1}_2 & \dots & 0 \\ \vdots & \ddots & & \vdots \\ \vdots & & \ddots & \vdots \\ 0 & \dots & & \lambda_m \mathbb{1}_m \end{pmatrix}. \tag{B.35}$$

□

To prove Theorem 2, we once again take $B = U^\dagger A$, and thus

$$\sum_{r\in G} UD(r)BD(r)^\dagger = \sum_{r\in G} D'(r)AD(r)^\dagger = \begin{pmatrix} \lambda_1 U_{11} & \lambda_2 U_{12} & \dots & \lambda_m U_{1m} \\ \lambda_1 U_{21} & \lambda_2 U_{22} & \dots & \lambda_m U_{2m} \\ \vdots & \ddots & & \vdots \\ \vdots & & \ddots & \vdots \\ \lambda_1 U_{m1} & \lambda_2 U_{m2} & \dots & \lambda_m U_{mm} \end{pmatrix}. \tag{B.36}$$

Thus, normalizing $\sum_{r\in G} D'(r)AD(r)^\dagger$ appropriately gives us all the required CG matrices up to multiplication by a complex number. This ambiguity gets absorbed into the 'B' matrices when we use the CG coefficients to write down MPS matrices.

We note that for the groups $\mathbb{Z}_2 \times \mathbb{Z}_2$, D_4 and A_4, when we take a direct product of the irreps of the physical spin with any projective irrep, we get a multiplicity-free CG decomposition for which we can use the technique mentioned above to obtain CG coefficients. However, for the case of S_4, the irrep of the physical spin $3_{(1)}$ has the following decomposition when we take the direct product with the projective irrep $\tilde{4}$: $3_{(1)} \otimes \tilde{4} = \tilde{2}_{(0)} \oplus \tilde{2}_{(1)} \oplus \tilde{4} \oplus \tilde{4}$. Clearly, $\tilde{4}$ has multiplicity 2 in the decomposition. In this case, if we apply the procedure above nonetheless, we get the following:

$$\sum_{r\in G} D'(r)AD(r)^\dagger = \left(\begin{pmatrix} \lambda_1 C^{\tilde{2}_{(0)}}_{3_{(1)}\tilde{4}} \end{pmatrix} \quad \begin{pmatrix} \lambda_2 C^{\tilde{2}_{(1)}}_{3_{(1)}\tilde{4}} \end{pmatrix} \quad \begin{pmatrix} \lambda_3 C^{\tilde{4};1}_{3_{(1)}\tilde{4}} \\ + \\ \lambda_4 C^{\tilde{4};2}_{3_{(1)}\tilde{4}} \end{pmatrix} \quad \begin{pmatrix} \mu_3 C^{\tilde{4};1}_{3_{(1)}\tilde{4}} \\ + \\ \mu_4 C^{\tilde{4};2}_{3_{(1)}\tilde{4}} \end{pmatrix} \right) \tag{B.37}$$

Where $D'(g) = D_{3_{(1)}} \otimes D_{\tilde{4}}$, $D(g) = D_{\tilde{2}_{(0)}} \oplus D_{\tilde{2}_{(1)}} \oplus D_{\tilde{4}} \oplus D_{\tilde{4}}$ and the $C^{\tilde{2}_{(1)}}_{3_{(1)}\tilde{4}}$ etc represent blocks of CG coefficients with the m labels suppressed.

We can see that $C^{\tilde{4};1}_{3_{(1)}\tilde{4}}$ and $C^{\tilde{4};2}_{3_{(1)}\tilde{4}}$ cannot in principle be separated which is why the method fails for decompositions with irrep multiplicities. However, in our case, it so happens that because of a convenient block structure we can separate the matrices by hand and obtain all CG coefficients.

Appendix C

Appendix to Chapter 5

C.1 Incompatibility of non-Abelian symmetries with full MBL

Here, we review the main hypothesis of Potter and Vasseur [174]. The authors consider the case of a fully MBL system (as opposed to the case of a partially local, partially thermal system with mobility edges), and study the compatibility of MBL in the presence of various global symmetries. The working definition of an MBL system they consider is the existence of a complete set of quasi-local conserved quantities with associated quasi-local projectors in terms of which the Hamiltonian, H can be defined as [162, 164, 191],

$$H = \sum_{i=1}^{L}\sum_{\alpha=1}^{D} E[i]_\alpha \hat{P}[i]_\alpha + \sum_{i\neq j=1}^{L}\sum_{\alpha,\beta=1}^{D} E[i,j]_{\alpha,\beta}\hat{P}[i]_\alpha\hat{P}[j]_\beta + \sum_{i\neq j\neq k=1}^{L}\sum_{\alpha,\beta,\gamma=1}^{D} E[i,j,k]_{\alpha,\beta,\gamma}\hat{P}[i]_\alpha\hat{P}[j]_\beta\hat{P}[k]_\gamma + \dots \quad \text{(C.1)}$$

Here, L is the number of spins, $\hat{P}[i]_\alpha$ is the projector onto the α^{th} quasi-local conserved quantity at the i^{th} location, D is the number of conserved quantities and the E's are constants that fix the energy eigenvalues. Furthermore, we can apply a finite depth quantum unitary circuit, W, that re-expresses the conserved quantities as local degrees of freedom. These local objects are called l-bits in terms of which the original spins (p-bits [1]) and Hamiltonian can be

[1]Note that we do not restrict ourselves to a local two-dimensional Hilbert space. This means, we should be talking about p-dits and l-dits instead of p-bits and l-bits. However, to keep with standard terminology, we will use the latter names.

defined. This is typically called the l-bit Hamiltonian, H_{lbit}.

Let us now consider the case when the Hamiltonian H has a global on-site symmetry *i.e* H commutes with the unitary representation of some group, G of the form $U(g) = \bigotimes_{i=1}^{L} V_i(g)$, where, $V_i(g)$ acts on each physical spin.

$$g : H \to U(g) H U^{\dagger}(g) = H \tag{C.2}$$

In this case, representation theory of the group G plays a role in constraining the allowed form of the l-bit Hamiltonian [C.1]. For spins (p-bits) to allow a well defined on-site group action, the local Hilbert space of each spin must correspond to some faithful representation of that group. This must also be true for a tensor product of the p-bits that constitute an l-bit. In other words, we can write the l-bit- projectors $\hat{P}[i]_{\alpha}$ using a fully reduced basis that can be labeled as $|\Gamma, m_{\Gamma}; d_{\Gamma}\rangle$

$$\hat{P}_{\Gamma, m_{\Gamma}; d_{\Gamma}} = |\Gamma, m_{\Gamma}; d_{\Gamma}\rangle\langle\Gamma, m_{\Gamma}; d_{\Gamma}| \tag{C.3}$$

We define the different labels below and compare them with the well known case of the representations of the rotation group $SO(3)$:

- $\Gamma = 1 \ldots N_R$ labels the irreducible representation (irrep) of the group and is equivalent to the total angular momentum quantum number, j. The number of values it can take is equal to the number of irreps of G, N_R.
- $m_{\Gamma} = 1 \ldots |\Gamma|$ is equivalent to the azimuthal quantum number m_j. The number of values it can take is equal to the dimension of the irrep, $|\Gamma|$.
- $d_{\Gamma} = 1 \ldots D_{\Gamma}$ labels which of the D_{Γ} copies of the Γ irrep is being considered.

In this basis, the action of the group is

$$g : |\Gamma, m_{\Gamma}; d_{\Gamma}\rangle \to \sum_{n_{\Gamma}=1}^{|\Gamma|} \Gamma(g)_{n_{\Gamma}, m_{\Gamma}} |\Gamma, n_{\Gamma}; d_{\Gamma}\rangle \tag{C.4}$$

Demanding the invariance of the Hamiltonian [C.1] under group action and invoking Schur's lemma [152] irrep-wise, we get the constrained form of the

Hamiltonian compatible with on-site symmetry as

$$H = \sum_{i=1}^{L} \sum_{\Gamma=1}^{N_R} \sum_{d_\Gamma^i=1}^{D_\Gamma^i} E[i]_{\Gamma,d_\Gamma^i} \hat{P}[i]_{\Gamma,d_\Gamma^i} + \sum_{i\neq j=1}^{L} \sum_{\Gamma,\Gamma'=1}^{N_R} \sum_{d_\Gamma^i=1}^{D_\Gamma^i} \sum_{d_{\Gamma'}^j=1}^{D_{\Gamma'}^j} E[i,j]_{\Gamma,d_\Gamma^i,\Gamma',d_{\Gamma'}^j} \hat{P}[i]_{\Gamma,d_\Gamma^i} \hat{P}[j]_{\Gamma',d_{\Gamma'}^j} + \dots \quad \text{(C.5)}$$

where,

$$\hat{P}_{\Gamma;d_\Gamma} \equiv \sum_{m_\Gamma=1}^{|\Gamma|} |\Gamma, m_\Gamma; d_\Gamma\rangle\langle\Gamma, m_\Gamma; d_\Gamma|. \quad \text{(C.6)}$$

We now consider the cases of Abelian and non-Abelian symmetries separately. If G is an Abelian group, all irreps are one dimensional ($|\Gamma| = 1$). This means that all projectors $P_{\Gamma;d_\Gamma}$ are rank-1 which preserves the form [C.1]. With sufficient disorder, resulting in sufficiently random $E's$, we can imagine that all degeneracies are lifted and we can obtain an MBL phase stable to perturbations. However, if G is non-Abelian, not all irreps are one dimensional. This means that we invariably have higher-rank local projectors giving us only a partial set of conserved quantities rather than complete which leads to degeneracies that are extensive in system size. This is clearly seen by examining the eigenvalues and eigenvectors of Eq [C.5].

$$H|\{\Gamma, m_\Gamma; d_\Gamma\}\rangle = \mathcal{E}(\{\Gamma; d_\Gamma\})|\{\Gamma; d_\Gamma\}\rangle, \quad \text{(C.7)}$$

$$\mathcal{E}(\{\Gamma; d_\Gamma\}) = \sum_{i=1}^{L} E[i]_{\Gamma_i,d_{\Gamma_i}^i} + \sum_{i\neq j=1}^{L} E[i,j]_{\Gamma_i,d_{\Gamma_i}^i,\Gamma_j',d_{\Gamma_j'}^j} + \dots \quad \text{(C.8)}$$

$$|\{\Gamma, m_\Gamma; d_\Gamma\}\rangle = \bigotimes_{i=1}^{L} |\Gamma_i, m_{\Gamma_i}; d_{\Gamma_i}^i\rangle. \quad \text{(C.9)}$$

Note that none of the eigenvalues, $\mathcal{E}$ have any labels corresponding to the inner multiplicity of the irreps m_Γ. This means that the eigenstate $|\{\Gamma, m_\Gamma; d_\Gamma\}\rangle$ has a degeneracy of $|\Gamma_1| \times |\Gamma_2| \times \dots |\Gamma_L|$ which is clearly extensive in system size when G is non-Abelian. The authors of Ref [174] state that under the influence of perturbations, such a degeneracy is susceptible to long range resonances which destabilizes MBL. Furthermore, they suggest a possible set of phases for the system to be in depending on the nature of the global symmetry group G. Here we list the possibilities for the case of finite groups such as $S_{n\geq 3}$ and $D_{n\geq 3}$, (i) Ergodic/ thermal phase, (ii) The so-called MBL

spin-glass (MBL-SG) [25] phase characterized by localization with symmetry spontaneously broken (SSB) to an Abelian subgroup, and (iii) The so-called quantum critical glass phase (QCG) [175–177] characterized by critical scaling of entanglement entropy. Within the accuracy of our numerical analysis, our findings are consistent with the conjecture of Potter and Vasseur.

C.2 Constructing symmetric Hamiltonians

In this appendix, we give details of how the Hamiltonian used in the main text, Eq [5.5] was constructed. We also detail a general technique to construct local symmetric operators with which we can build spin Hamiltonians invariant under any on-site symmetry in any dimension. The construction of the 1D S_3 invariant Hamiltonian of the main text is a specific application of this general technique.

C.2.1 Building the S_3 invariant Hamiltonian

Basis properties of S_3 and its representation used.

We first review some basic properties of the group S_3 and its representation used in this chapter. S_3, the symmetry group of three objects is the smallest non-Abelian group. It is of order 6 and can be generated using two elements and the following presentation

$$S_3 : \langle a, x | a^3 = x^2 = 1, xax = a^{-1} \rangle. \tag{C.10}$$

It has three irreducible representations, $\mathbf{1}, \mathbf{1}', \mathbf{2}$ which can be written as

1. $\chi^{\mathbf{1}}(a) = 1$, $\chi^{\mathbf{1}}(x) = 1$,
2. $\chi^{\mathbf{1}'}(a) = 1$, $\chi^{\mathbf{1}'}(x) = -1$,
3. $\Gamma^{\mathbf{2}}(a) = \begin{pmatrix} \omega & 0 \\ 0 & \omega^* \end{pmatrix}$, $\Gamma^{\mathbf{2}}(x) = \begin{pmatrix} 0 & 1 \\ 1 & 0 \end{pmatrix}$,

where $\omega = e^{2\pi i/3}$. The local Hilbert space we have chosen for each spin lives is the three-dimensional reducible representation $\mathbf{2} \oplus \mathbf{1}'$. We use the eigenspace of the spin-1 angular momentum operator S^z to label the irreps. The $\mathbf{2}$ irrep is encoded in the two-dimensional ± 1 eigenspace of S^z (which we will call $|\pm\rangle$) and the $\mathbf{1}'$ is encoded in the one-dimensional 0 eigenspace of S^z (which we will call $|0\rangle$). The matrix representation of a general group element in this basis

looks like

$$V(g) = \begin{pmatrix} \Gamma^{\mathbf{2}}(g)_{11} & 0 & \Gamma^{\mathbf{2}}(g)_{12} \\ 0 & \chi^{\mathbf{1}'}(g) & 0 \\ \Gamma^{\mathbf{2}}(g)_{21} & 0 & \Gamma^{\mathbf{2}}(g)_{22}. \end{pmatrix} \tag{C.11}$$

In particular, the generators have the following representation

$$V(a) = \begin{pmatrix} \omega & 0 & 0 \\ 0 & 1 & 0 \\ 0 & 0 & \omega^* \end{pmatrix}, \; V(x) = \begin{pmatrix} 0 & 0 & 1 \\ 0 & -1 & 0 \\ 1 & 0 & 0 \end{pmatrix}. \tag{C.12}$$

1-spin operator

We first construct a 1-spin invariant operator. We start with a general operator that acts on the space of a single spin

$$\hat{\lambda} = \begin{pmatrix} \lambda_{11} & \lambda_{12} & \lambda_{13} \\ \lambda_{21} & \lambda_{22} & \lambda_{23} \\ \lambda_{31} & \lambda_{32} & \lambda_{33} \end{pmatrix} \tag{C.13}$$

We now demand that $\hat{\lambda}$ is invariant under conjugation by $V(g)$, *i.e.*, the representation of symmetry on a single spin.

$$V(g)\hat{\lambda}V^{\dagger}(g) = \hat{\lambda} \tag{C.14}$$

Schur's lemma [152] constrains the matrix elements of $\hat{\lambda}$ in the following way:

1. $\hat{\lambda}$ cannot mix basis states corresponding to *different* irreps.
2. $\hat{\lambda}$ must be proportional to the identity operator when acting on basis states corresponding to the *internal* states of the *same* irrep.
3. If there are *multiple copies* of the same irrep, $\hat{\lambda}$ can mix the basis states corresponding the *same internal state* of different copies but should still be proportional to the identity operator as an action on the internal states.

The meaning of these constraints should become clearer with the applications that will follow. For a single spin operator, since we have only one copy of each irrep, constraint 3 does not apply. Applying constraints 1 and 2, we get

the form of $\hat{\lambda}$:

$$\begin{aligned}\hat{\lambda} &= \begin{pmatrix} \lambda_{\mathbf{2}} & 0 & 0 \\ 0 & \lambda_{\mathbf{1'}} & 0 \\ 0 & 0 & \lambda_{\mathbf{2}} \end{pmatrix} = \lambda_{\mathbf{1'}} |0\rangle\langle 0| + \lambda_{\mathbf{2}} \left(|+\rangle\langle +| + |-\rangle\langle -|\right) \\ &= (\lambda_{\mathbf{2}} - \lambda_{\mathbf{1'}})(S^z)^2 + \lambda_{\mathbf{1'}} \mathbb{1}_3 \end{aligned} \tag{C.15}$$

From this, we can read off the only non-trivial 1-spin symmetric operator, $(S^z)^2$ which is also Hermitian.

2-spin operator

In order to find a symmetric 2-spin operator, we follow the same logic as that of a 1-spin operator. First, we start with a general operator that acts on the 9 dimensional vector space of 2 spins,

$$\hat{J} = \begin{pmatrix} J_{11} & J_{12} & \dots & J_{19} \\ J_{21} & J_{22} & \dots & J_{29} \\ \vdots & & \ddots & \vdots \\ J_{91} & J_{92} & \dots & J_{99}. \end{pmatrix} \tag{C.16}$$

Next, we demand invariance under conjugation by $V(g) \otimes V(g)$, *i.e.*, the representation of symmetry on two spins.

$$V(g) \otimes V(g) \hat{J} V^\dagger(g) \otimes V^\dagger(g) = \hat{J} \tag{C.17}$$

We now have to impose the constraints coming from Schur's lemma. However, in order to do that, we need to find out the irrep content of $V(g) \otimes V(g)$. For this, we first list the Clebsch Gordan (CG) decomposition that gives us the outcomes of fusing different S_3 irreps. This is the generalization of angular momentum addition of $SU(2)$ irreps. Note that we exclude the trivial case of fusion with the trivial irrep $\mathbf{1}$,

$$\begin{aligned} \mathbf{1'} \otimes \mathbf{1'} &\cong \mathbf{1} \\ \mathbf{2} \otimes \mathbf{1'} &\cong \mathbf{2} \\ \mathbf{2} \otimes \mathbf{2} &\cong \mathbf{2} \oplus \mathbf{1'} \oplus \mathbf{1} \end{aligned}$$

The irrep content of $V(g) \otimes V(g)$ is obtained from the CG decomposition,

$$(\mathbf{2} \oplus \mathbf{1'}) \otimes (\mathbf{2} \oplus \mathbf{1'}) \cong \mathbf{1} \oplus \mathbf{1} \oplus \mathbf{1'} \oplus \mathbf{2} \oplus \mathbf{2} \oplus \mathbf{2}. \tag{C.18}$$

Since the are multiple copies of the same irrep ($\mathbf{1}$) in this decomposition, Schur's lemma implies that there are off-diagonal operators that acts on this multiplicity space which are invariant under symmetry transformations. Let us now list and label the different instances of each irrep appearing in the decomposition for convenience:

$$\begin{aligned}
\mathbf{1}' &\otimes \mathbf{1}' \to \mathbf{1}_A \\
\mathbf{2} &\otimes \mathbf{2} \to \mathbf{1}_B \\
\mathbf{2} &\otimes \mathbf{2} \to \mathbf{1}' \\
\mathbf{1}' &\otimes \mathbf{2} \to \mathbf{2}_A \\
\mathbf{2} &\otimes \mathbf{1}' \to \mathbf{2}_B \\
\mathbf{2} &\otimes \mathbf{2} \to \mathbf{2}_C
\end{aligned}$$

The subscripts label the copy of the irrep. We next need the basis of the representation of each irrep in $V(g) \otimes V(g)$. These can be written in terms of the original basis states (labeled by S^z eigenvalues) using CG coefficients which we calculate using the technique by Sakata [150] (also see [36]).

$$\begin{aligned}
|\mathbf{1}_A\rangle &= |0\rangle|0\rangle \\
|\mathbf{1}_B\rangle &= \frac{|+\rangle|-\rangle + |-\rangle|+\rangle}{\sqrt{2}} \\
|\mathbf{1}'\rangle &= \frac{|+\rangle|-\rangle - |-\rangle|+\rangle}{\sqrt{2}} \\
|\mathbf{2}_A, \pm\rangle &= \pm|0\rangle|\pm\rangle \\
|\mathbf{2}_B, \pm\rangle &= \pm|\pm\rangle|0\rangle \\
|\mathbf{2}_C, \pm\rangle &= |\mp\rangle|\mp\rangle
\end{aligned} \tag{C.19}$$

Using this, we have the 2-spin S_3 symmetric operator constrained by Schur's lemma

$$\hat{J} = J^{\mathbf{1}'}|\mathbf{1}'\rangle\langle\mathbf{1}'| + \sum_{\mu,\nu=A,B} J^{\mathbf{1}}_{\mu\nu}|\mathbf{1}_\mu\rangle\langle\mathbf{1}_\nu| + \sum_{\mu,\nu=A,B,C} J^{\mathbf{2}}_{\mu\nu}(|\mathbf{2}_\mu,+\rangle\langle\mathbf{2}_\nu,+| + |\mathbf{2}_\mu,-\rangle\langle\mathbf{2}_\nu,-|) \tag{C.20}$$

As in the case of 1-spin invariant operator, we can again read off the several independent symmetric 2-spin operators by simplifying Eq .C.20. However, since we need the operators to be Hermitian, we take Hermitian combinations of these operators. We finally list the non-trivial independent Hermitian

operators expressed in terms of spin-1 operators.

$$\begin{aligned}
\hat{J}_1 &= S^z \otimes S^z, \\
\hat{J}_2 &= (S^z)^2 \otimes (S^z)^2 \\
\hat{J}_3 &= (S^+)^2 \otimes (S^-)^2 + (S^-)^2 \otimes (S^+)^2 \\
\hat{J}_4 &= (S^+S^z) \otimes (S^-S^z) + (S^-S^z) \otimes (S^+S^z) + h.c \\
\hat{J}_5 &= (S^-S^z) \otimes (S^zS^+) + (S^+S^z) \otimes (S^zS^-) + h.c \\
\hat{J}_6 &= (S^+S^z) \otimes (S^+)^2 + (S^-S^z) \otimes (S^-)^2 + h.c \\
\hat{J}_7 &= (S^+)^2 \otimes (S^+S^z) + (S^-)^2 \otimes (S^-S^z) + h.c
\end{aligned}$$

To construct the Hamiltonian .5.5, we have used $(S^z)^2$ and $\hat{J}_1$ to build the disordered part H_d and $\hat{J}_3$, $\hat{J}_4$, $\hat{J}_7$ to build the thermal part of the Hamiltonian, H_t. Since $\hat{J}_5$ and $\hat{J}_6$ are mirrored versions of $\hat{J}_4$ and $\hat{J}_7$ respectively, we can keep our thermal term sufficiently generic even if leave them out. Note that while we have constructed a Hamiltonian for a 1D spin chain, the symmetric operators constructed using this formalism can be used to build Hamiltonians for any spatial dimensions.

C.2.2 General technique

We now give details of a general procedure that can be applied to obtain n-spin symmetric operators invariant under a representation of any on-site symmetry group. The schematic procedure is as follows

1. To construct symmetric n-spin operators, we first write down general operators that act on the Hilbert space of n spins.

2. We then demand the invariance of this operator under symmetry action.

3. Using Schur's lemma, we constrain the matrix elements of the n-spin operator and read off the independent operators.

4. If required, we finally take the hermitian combinations of the independent operators.

If G is the group we are considering, the most general local Hilbert space for the spin compatible with G-action can be an arbitrary number of copies of each irrep of G. Like mentioned in Sec C.1, we can choose the basis as $|\Gamma, m_\Gamma; d_\Gamma\rangle$ where the symbols have the same meaning as before. The matrix

representation of the group operators in this basis is block diagonal.

$$U(g) = \bigotimes_{i=1}^{L} V_i(g) \tag{C.21}$$

$$V_i(g) = \bigoplus_{\Gamma=1}^{N_R} \mathbb{1}_{D_\Gamma^i} \otimes \Gamma(g) \tag{C.22}$$

The "passive" group action on the basis is

$$g : |\Gamma, m_\Gamma; d_\Gamma\rangle \mapsto \sum_{n_\Gamma=1}^{|\Gamma|} \Gamma(g)_{n_\Gamma, m_\Gamma} |\Gamma, n_\Gamma; d_\Gamma\rangle \tag{C.23}$$

1-spin symmetric operator

Let us now start with symmetric 1-spin operators. The most general 1-spin operator we can write down is

$$\hat{\lambda} = \lambda^{\Gamma, m_\Gamma; d_\Gamma}_{\Gamma', m_{\Gamma'}; d_{\Gamma'}} |\Gamma, m_\Gamma; d_\Gamma\rangle\langle\Gamma', m_{\Gamma'}; d_{\Gamma'}| \tag{C.24}$$

Note that for notational convenience, here and henceforth, we assume summation over repeated indices. Demanding invariance under conjugation with $V(g)$, we have

$$\begin{aligned} V(g)\lambda V(g)^\dagger &= \lambda \\ \implies \Gamma(g)_{m_\Gamma, n_\Gamma} (\Gamma'(g)_{m_{\Gamma'}, n_{\Gamma'}})^* \lambda^{\Gamma, n_\Gamma; d_\Gamma}_{\Gamma', n_{\Gamma'}; d_{\Gamma'}} &= \lambda^{\Gamma, m_\Gamma; d_\Gamma}_{\Gamma', m_{\Gamma'}; d_{\Gamma'}}. \end{aligned} \tag{C.25}$$

In matrix form, the condition on λ becomes

$$[\Gamma(g)][\lambda^{\Gamma; d_\Gamma}_{\Gamma'; d_{\Gamma'}}] = [\lambda^{\Gamma; d_\Gamma}_{\Gamma'; d_{\Gamma'}}][\Gamma'(g)]. \tag{C.26}$$

This means that $[\lambda^{\Gamma; d_\Gamma}_{\Gamma'; d_{\Gamma'}}]$ is an intertwiner between the irreps Γ and Γ'. Such a matrix is constrained by Schur's lemma:

$$\begin{aligned} [\lambda^{\Gamma; d_\Gamma}_{\Gamma'; d_{\Gamma'}}] = 0 \quad &\text{if} \quad \Gamma \neq \Gamma' \\ \propto \mathbb{1}_\Gamma \quad &\text{if} \quad \Gamma = \Gamma' \\ \implies \lambda^{\Gamma, m_\Gamma; d_\Gamma}_{\Gamma', m'_{\Gamma'}; d'_{\Gamma'}} = 0 \quad &\text{if} \quad \Gamma \neq \Gamma' \\ \propto \delta_{m_\Gamma, m'_{\Gamma'}} \quad &\text{if} \quad \Gamma = \Gamma' \end{aligned} \tag{C.27}$$

Using this in Eq C.24, we get the form of a symmetric 1-spin operator,

$$\hat{\lambda} = \lambda^{\Gamma}_{d_\Gamma, d'_\Gamma} |\Gamma, m_\Gamma; d_\Gamma\rangle\langle\Gamma, m_\Gamma; d'_\Gamma|. \tag{C.28}$$

Here, the non-zero matrix elements $\lambda^{\Gamma}_{d_\Gamma, d'_\Gamma}$ are free parameters that act on the degenerate subspace associated with the outer multiplicity of each irrep.

2-spin symmetric operator

We now consider 2-spin symmetric operators. The most general operator that acts on the 2-spin Hilbert space is

$$\hat{J} = J^{(\Delta, m_\Delta; d_\Delta), (\Lambda, m_\Lambda; d_\Lambda)}_{(\Delta', m_{\Delta'}; d_{\Delta'}), (\Lambda', m_{\Lambda'}; d_{\Lambda'})} |\Delta, m_\Delta; d_\Delta\rangle\langle\Delta', m_{\Delta'}; d_{\Delta'}||\Lambda, m_\Lambda; d_\Lambda\rangle\langle\Lambda', m_{\Lambda'}; d_{\Lambda'}| \tag{C.29}$$

For this operator to be symmetric, it needs to be invariant under conjugation by $V_1(g) \otimes V_2(g)$,

$$[V_1(g) \otimes V_2(g)]\, J\, [V_1(g) \otimes V_2(g)]^\dagger = J. \tag{C.30}$$

To use the techniques like we did for the 1-spin operator in the previous subsection, we need to first block-diagonalize $V_1(g) \otimes V_2(g)$ using a suitable basis change and then use Schur's lemma. This redefinition of the basis states can be done using Clebsch-Gordan (CG) coefficients. Recall that the irrep content of a direct product of two irreps is schematically given by the CG series:

$$\Delta \otimes \Lambda = \bigoplus_\Gamma N^\Gamma_{\Delta\Lambda}\ \Gamma \tag{C.31}$$

$N^\Gamma_{\Delta\Lambda}$ denotes the number of copies of the Γ irrep that exists in the fusion outcome of $\Delta \otimes \Lambda$. At the level of representations, Eq .C.31 tells us that there exists a change of basis by a unitary matrix $C_{\Delta\Lambda}$ that fully reduces the direct product of the irreps $\Delta \otimes \Lambda$:

$$\Delta(g) \otimes \Lambda(g) \cong \bigoplus_\Gamma \mathbb{1}_{N^\Gamma_{\Delta\Lambda}} \otimes \Gamma(g), \tag{C.32}$$

$$C_{\Delta\Lambda}\, (\Delta(g) \otimes \Lambda(g))\, C^\dagger_{\Delta\Lambda} = \bigoplus_\Gamma \mathbb{1}_{N^\Gamma_{\Delta\Lambda}} \otimes \Gamma(g), \tag{C.33}$$

$$C^{\Gamma;\alpha_\Gamma}_{\Delta\Lambda}\, (\Delta(g) \otimes \Lambda(g))\, C^{\Gamma;\alpha_\Gamma\dagger}_{\Delta\Lambda} = \Gamma(g). \tag{C.34}$$

$C^{\Gamma;\alpha_\Gamma}_{\Delta\Lambda}$ are isometries whose matrix elements, $[C^{\Gamma;\alpha_\Gamma}_{\Delta\Lambda}]^{m_\Gamma}_{m_\Delta, m_\Lambda}$ are the CG coefficients that project $\Delta \times \Lambda$ onto the α^{th}_Γ copy of the irrep Γ, where, $\alpha_\Gamma = 1 \ldots N^\Gamma_{\Delta\Lambda}$. It is useful to look at the 'passive' action of the CG coefficients on

the basis kets to remind us of the actual "change-of-basis" action,

$$[C^{*\Gamma;\alpha_\Gamma}_{\Delta\Lambda}]^{m_\Gamma}_{m_\Delta,m_\Lambda}|\Delta,m_\Delta\rangle|\Lambda,m_\Lambda\rangle = |\Gamma,m_\Gamma,\alpha_\Gamma\rangle \tag{C.35}$$

Now, consider the following equivalences

$$\begin{aligned} V_1(g)\otimes V_2(g) &= \left[\bigoplus_\Delta \mathbb{1}_{D^1_\Delta}\otimes\Delta(g)\right]\otimes\left[\bigoplus_\Lambda \mathbb{1}_{D^2_\Lambda}\otimes\Lambda(g)\right] \\ &\cong \bigoplus_{(\Delta,\Lambda)}\left[\mathbb{1}_{D^1_\Delta\times D^2_\Lambda}\right]\otimes[\Delta(g)\otimes\Lambda(g)] \cong \bigoplus_{(\Delta,\Lambda)}\left[\mathbb{1}_{D^1_\Delta\times D^2_\Lambda}\right]\otimes\left[\bigoplus_\Gamma \mathbb{1}_{N^\Gamma_{\Delta\Lambda}}\otimes\Gamma(g)\right] \\ &\cong \bigoplus_\Gamma \mathbb{1}_{\mathcal{D}^{1,2}_\Gamma}\otimes\Gamma(g). \end{aligned} \tag{C.36}$$

Here,

$$\mathcal{D}^{1,2}_\Gamma = \sum_{(\Delta,\Lambda)|\Gamma\in\Delta\otimes\Lambda} D^1_\Delta\ D^2_\Lambda\ N^\Gamma_{\Delta\Lambda} \tag{C.37}$$

is the number of 'fusion channels' of the kind $\Delta\otimes\Lambda\to\Gamma$ available to produce the irrep Γ using the irreps in the 2-spin Hilbert space. In short, Eq [C.36] tells us that there exists some unitary matrix W which block diagonalizes $V_1(g)\otimes V_2(g)$

$$W\left[V_1(g)\otimes V_2(g)\right]W^\dagger = \tilde{V}(g) \tag{C.38}$$

$$\tilde{V}(g) = \bigoplus_{\Gamma\in\Delta\otimes\Lambda} \mathbb{1}_{\mathcal{D}^{1,2}_\Gamma}\otimes\Gamma(g). \tag{C.39}$$

When viewed as a matrix, W contains operations to both reorder indices appropriately as well as use the CG coefficients to reduce the direct product of irreps form V_1 and V_2 block-by-block. If we operate W on both sides of the Eq [C.30] and call $WJW^\dagger = K$, we get

$$\tilde{V}(g)K\tilde{V}(g)^\dagger = K \tag{C.40}$$

The matrix elements of K can be written in terms of those of J and CG coefficients.

$$K^{\Gamma,m_\Gamma;c_\Gamma}_{\Gamma',m_{\Gamma'};c_{\Gamma'}} = \left[C^{\Gamma;\alpha_\Gamma}_{\Delta\Lambda}\right]^{m_\Gamma}_{m_\Delta,m_\Lambda}\left[C^{*\Gamma';\alpha'_\Gamma}_{\Delta'\Lambda'}\right]^{m_{\Gamma'}}_{m_{\Delta'},m_{\Lambda'}} J^{(\Delta,m_\Delta;d_\Delta),(\Lambda,m_\Lambda;d_\Lambda)}_{(\Delta',m_{\Delta'};d_{\Delta'}),(\Lambda',m_{\Lambda'};d_{\Lambda'})} \tag{C.41}$$

Eq [C.40] is of the same form as Eq [C.25] and we can use Schur's lemma again to constrain the elements of K,

$$\begin{aligned} K^{\Gamma,m_\Gamma;c_\Gamma}_{\Gamma',m_{\Gamma'};c_{\Gamma'}} &= 0 \quad \text{if} \quad \Gamma \neq \Gamma' \\ &\propto \delta_{m_\Gamma,m_{\Gamma'}} \quad \text{if} \quad \Gamma = \Gamma'. \end{aligned} \tag{C.42}$$

Note that c_Γ is a collective index of compatible $(d_\Delta, d_\Lambda, \alpha_\Gamma)$ that runs over the $\mathcal{D}_\Gamma$ different fusion channels mentioned above. Also, note that we use the convention $\left[C^{\Gamma;\alpha_\Gamma}_{\Delta\Lambda}\right]^{m_\Gamma}_{m_\Delta,m_\Lambda} = 0$ if $\Gamma \notin \Delta \otimes \Lambda$. Finally, we can undo the transformation of W and get the elements of $\hat{J}$. Since it is important, we expand c_Γ:

$$J^{(\Delta,m_\Delta;d_\Delta),(\Lambda,m_\Lambda;d_\Lambda)}_{(\Delta',m_{\Delta'};d_{\Delta'}),(\Lambda',m_{\Lambda'};d_{\Lambda'})} = K^{\Gamma;(d_\Delta,d_\Lambda,\alpha_\Gamma)}_{(d_{\Delta'},d_{\Lambda'},\beta_\Gamma)} \left[C^{*\Gamma;\alpha_\Gamma}_{\Delta\Lambda}\right]^{m_\Gamma}_{m_\Delta,m_\Lambda} \left[C^{\Gamma;\beta_\Gamma}_{\Delta'\Lambda'}\right]^{m_\Gamma}_{m_{\Delta'},m_{\Lambda'}} \tag{C.43}$$

Plugging in Eq [C.43] into Eq [C.29], we get the general form of the symmetric 2-spin operator.

$$\begin{aligned} \hat{J} = K^{\Gamma;(d_\Delta,d_\Lambda,\alpha_\Gamma)}_{(d_{\Delta'},d_{\Lambda'},\beta_\Gamma)} &\left[C^{*\Gamma;\alpha_\Gamma}_{\Delta\Lambda}\right]^{m_\Gamma}_{m_\Delta,m_\Lambda} \left[C^{\Gamma;\beta_\Gamma}_{\Delta'\Lambda'}\right]^{m_\Gamma}_{m_{\Delta'},m_{\Lambda'}} \\ &|\Delta, m_\Delta; d_\Delta\rangle\langle\Delta', m_{\Delta'}; d_{\Delta'}||\Lambda, m_\Lambda; d_\Lambda\rangle\langle\Lambda', m_{\Lambda'}; d_{\Lambda'}|. \end{aligned} \tag{C.44}$$

This can be greatly simplified using Eq [C.35]

$$\hat{J} = K^{\Gamma;c_\Gamma}_{d_\Gamma} |\Gamma, m_\Gamma; c_\Gamma\rangle\langle\Gamma, m_\Gamma; c'_\Gamma|. \tag{C.45}$$

Where, we have once again reintroduced the short hand notation c_Γ to denote the fusion channels labeled by compatible $(d_\Delta, d_\Lambda, \alpha_\Gamma)$ to produce Γ. $K^{\Gamma;(d_\Delta,d_\Lambda,\alpha_\Gamma)}_{(d_{\Delta'},d_{\Lambda'},\beta_\Gamma)}$ are now the free parameters. In this form, we can clearly see the similarity with the symmetric 1-spin operator Eq [C.28]. This helps us see the general picture with arbitrary n-local operators. In a fully reduced basis of the n-spin Hilbert space, matrix elements of symmetric operators can only act on the outer multiplicity space of each irrep.

C.3 Detecting the irrep of the eigenstates

In this appendix, we give details of how we determine the irrep a given eigenstate transforms as. If $U(g) = \bigotimes_{i=1}^{L} V_i(g)$ is the many-body representation of the on-site symmetry, we want to find out the irrep Γ that an eigenstate

$|\epsilon\rangle$ or more generally, a set of degenerate eigenstates $\{|\epsilon\rangle_a\}$ transform as

$$U(g)|\epsilon\rangle_a = \sum_{b=1}^{|\Gamma|} \Gamma(g)_{ab}|\epsilon\rangle_b \tag{C.46}$$

This is an easy task for the symmetry group $SU(2)$, where, all we need to do is operate the eigenstates with the total angular momentum operator,

$$\boldsymbol{S}^2_{tot} = \sum_{a=x,y,z} \left(\sum_{i=1}^{L} S^a_i\right)\left(\sum_{i=1}^{L} S^a_i\right) \tag{C.47}$$

$$\boldsymbol{S}^2_{tot}|\epsilon\rangle = j(j+1)|\epsilon\rangle \tag{C.48}$$

This way, given an eigenstate that transforms as an irrep of $SU(2)$, we can extract the quantum number j which labels the irrep. For general finite groups, we are not aware of an equivalent technique. However, we now present a strategy that works well for the group S_3 in the form of the following theorem.

Theorem 3. *Given a normalized vector $|\epsilon\rangle$, $\langle\epsilon|\epsilon\rangle = 1$, that transforms as some irreducible representation of S_3, $\Gamma = \mathbf{1}, \mathbf{1}'$ or $\mathbf{2}$, we can determine Γ using the following two real numbers,*

$$\begin{aligned} \mathcal{X} &= \langle\epsilon|U(x)|\epsilon\rangle, \\ \mathcal{A} &= Real(\langle\epsilon|U(a)|\epsilon\rangle), \end{aligned}$$

where, a and x are the two generators of S_3 with presentation $\langle a, x|a^3 = x^2 = 1, xax = a^{-1}\rangle$. Specifically,

$$\begin{aligned} \mathcal{A} = -0.5 &\implies \Gamma = \mathbf{2} \\ (\mathcal{A}, \mathcal{X}) = (1,\ \ 1) &\implies \Gamma = \mathbf{1} \\ (\mathcal{A}, \mathcal{X}) = (1, -1) &\implies \Gamma = \mathbf{1}' \end{aligned}$$

Proof. Let us first consider the case when $|\epsilon\rangle$ is some vector in the 2D irrep $\mathbf{2}$. We can expand this vector in the orthonormal eigenbasis of the generator a of the $\mathbf{2}$ representation, $|\omega\rangle, |\omega^*\rangle$, with eigenvalues ω, ω^* respectively, where $\omega = e^{\frac{2\pi i}{3}}$ (see Appendix. C.2).

$$|\epsilon\rangle = \cos\theta|\omega\rangle + \sin\theta|\omega^*\rangle. \tag{C.49}$$

Acting on it by $U(a)$,

$$\begin{aligned} U(a)|\epsilon\rangle &= \omega\cos\theta|\omega\rangle + \omega^*\sin\theta|\omega^*\rangle \\ \langle\epsilon|U(a)|\epsilon\rangle &= \omega\cos^2\theta + \omega^*\sin^2\theta \\ Real(\langle\epsilon|U(a)|\epsilon\rangle) &= Real(\omega)(cos^2\theta + \sin^2\theta) \\ \implies \mathcal{A} &= Real(\omega) = -0.5 \end{aligned}$$

Let us now consider the case when $|\epsilon\rangle$ transforms as either of the 1D irreps. Since the representation of the generator a is simply 1 for both 1D irreps, we simply have

$$U(a)|\epsilon\rangle = |\epsilon\rangle \tag{C.50}$$

$$\implies \mathcal{A} = \langle\epsilon|U(a)|\epsilon\rangle = 1 \tag{C.51}$$

Thus, we can see that $\mathcal{A}$ can separate the 2D irrep **2** form the 1D irreps. Also, $\mathcal{A} = -0.5$ is necessary and sufficient for $|\epsilon\rangle$ to transform as **2**. Furthermore, if $\mathcal{A} = 1$, we can determine which 1D irrep $|\epsilon\rangle$ transforms as by considering the transformation under the generator x whose representation is ± 1 for Γ being **1** or **1′** respectively. Thus, if $\mathcal{A} = 1$,

$$\begin{aligned} U(x)|\epsilon\rangle &= \pm|\epsilon\rangle \\ \implies \mathcal{X} &= \langle\epsilon|U(x)|\epsilon\rangle = \pm 1 \end{aligned}$$

implies $|\epsilon\rangle$ transforms as **1** or **1′** respectively. This concludes the proof. □

In our numerics, we diagonalize our Hamiltonian in the 1D irrep sector by projecting it into the appropriate basis. As discussed above, this means that we need to restrict to the basis states that are left invariant under the action of $U(a) = \bigotimes_{i=1}^{L} V(a)_i$. To see how this is done, consider the action of operator $U(a)$ on a many-body basis state labeled by S^z eigenvalues on each spin

$$U(a)|m_1, m_2, \ldots, m_L\rangle = \omega^{m_1+m_2+\ldots+m_L}|m_1, m_2, \ldots, m_L\rangle \tag{C.52}$$

$$= \omega^{S^z_{tot}}|m_1, m_2, \ldots, m_L\rangle \tag{C.53}$$

We need $\omega^{S^z_{tot}} = 1$ which means

$$S^z_{tot} = \sum_{i=1}^{L} m_i = 0(mod\ 3). \tag{C.54}$$

Since 3^{L-1} of the 3^L basis states satisfy the condition of Eq .C.54, this helps us diagonalize an L site Hamiltonian for the price of $L-1$.

C.4 Spin glass diagnostics for S_3 subgroups

In this appendix, we give details of how the spin-glass (SG) order parameter used in Sec. 5.3.2 was constructed and also numerical evidence for the assertion that the high disorder region at $\kappa = 0$ does not in any form spontaneously break the S_3 symmetry.

First, let us list the elements of $S_3 = \{1, a, a^2, x, xa, xa^2\}$ and its five subgroups written in terms of the generators a, x defined in Sec. 5.2 and Appendix. C.2:

1. $\mathbb{Z}_3 = \{1, a, a^2\}$,
2. $\mathbb{Z}_{2A} = \{1, x\}$,
3. $\mathbb{Z}_{2B} = \{1, xa\}$,
4. $\mathbb{Z}_{2C} = \{1, xa^2\}$,
5. $\{1\}$.

For each subgroup $H \subset G$, we design a SG diagnostic that detects SSB of $G \to H$ and takes the form

$$\chi_H^{SG} = \frac{1}{L-1} \sum_{i \neq j=1}^{L} |\langle\epsilon|\mathcal{O}_{H;i}\mathcal{O}_{H;j}|\epsilon\rangle - \langle\epsilon|\mathcal{O}_{H;i}|\epsilon\rangle\langle\epsilon|\mathcal{O}_{H;j}|\epsilon\rangle|^2. \tag{C.55}$$

$\mathcal{O}_H$ are local Hermitian order parameters that are chosen to have the following properties under symmetry transformation by $U(g) = \bigotimes_{i=1}^{L} V(g)_i$

1. $\mathcal{O}_H$ transforms trivially under H: $U(g)\mathcal{O}_H U^\dagger(g) = \mathcal{O}_H$, $\forall g \in H$.
2. $\mathcal{O}_H$ transforms non-trivially under G/H: $U(g)\mathcal{O}_H U^\dagger(g) \neq \mathcal{O}_H$, $\forall g \notin H$.

Note that χ_H^{SG} is invariant under the redefinition $\mathcal{O}_H \to \mathcal{O}_H + \xi\mathbb{1}$. It can be checked that the following operators satisfy the above properties

- $\mathcal{O}_{\mathbb{Z}_3} = S^z$
- $\mathcal{O}_{\mathbb{Z}_{2A}} = S^z S^x + S^x S^z = \frac{1}{\sqrt{2}} \begin{pmatrix} 0 & 1 & 0 \\ 1 & 0 & -1 \\ 0 & -1 & 0 \end{pmatrix}$
- $\mathcal{O}_{\mathbb{Z}_{2B}} = V(a)\mathcal{O}_{\mathbb{Z}_{2A}} V^\dagger(a) = \frac{1}{\sqrt{2}} \begin{pmatrix} 0 & \omega & 0 \\ \omega^* & 0 & -\omega \\ 0 & -\omega^* & 0 \end{pmatrix}$

- $\mathcal{O}_{\mathbb{Z}_{2C}} = V^\dagger(a)\mathcal{O}_{\mathbb{Z}_{2A}}V(a) = \frac{1}{\sqrt{2}}\begin{pmatrix} 0 & \omega^* & 0 \\ \omega & 0 & -\omega^* \\ 0 & -\omega & 0 \end{pmatrix}$
- $\mathcal{O}_{\{1\}} = S^x$

Note that it is important to make sure that the disconnected part of the two point correlation function, $\langle\epsilon|\mathcal{O}_{H;i}|\epsilon\rangle\langle\epsilon|\mathcal{O}_{H;j}|\epsilon\rangle$ is subtracted when constructing χ_H^{SG}. In previous work like Ref [24], the local order parameter σ^z transformed as a non-trivial irrep of G/H ($\mathbb{Z}_2$ in their case). It is then automatically guaranteed that $\langle\epsilon|\sigma_i^z|\epsilon\rangle = 0$. Similarly, the local order parameter used in the main text to detect $S_3 \to \mathbb{Z}_3$ SSB, S_i^z transforms as a non-trivial irrep of $S_3/\mathbb{Z}_3 \cong \mathbb{Z}_2$ which also ensures $\langle\epsilon|S_i^z|\epsilon\rangle = 0$ and hence we leave out of the definition of $\chi_{\mathbb{Z}_3}^{SG}$. This would not be true if we used a different $\mathcal{O}_{\mathbb{Z}_3}$ like $S^z + \xi(S^z)^2$ or even $S^z + \xi\mathbb{1}$ both of which are equally good to detect $S_3 \to \mathbb{Z}_3$ SSB but would need subtraction of the disconnected part. Similarly, the other SG diagnostics we used namely $\mathcal{O}_{\mathbb{Z}_{2A/B/C}}$ and $\mathcal{O}_{\{1\}}$ also need subtraction.

Fig. C.1 shows the different SG diagnostics as a function of λ for $\kappa = 0, 1$ averaged over eigenstates across disorder realizations. It can be seen that only $\overline{\chi_{\mathbb{Z}_3}^{SG}}$, which detects SSB $S_3 \to \mathbb{Z}_3$ approaches a value that increases with system size in the region discussed in Sec. 5.3.2. The value of other SG diagnostics becomes increasingly smaller or approaches a constant value with system size for all λ and κ indicating that SSB to that residual subgroup has not taken place in the eigenstates.

One striking feature of Fig C.1 is that the plots for several order parameters, particularly for the different $\mathbb{Z}_2$ subgroups, look very similar. In fact, they are identical. This is because the above calculation using the three order parameters, $\mathcal{O}_{\mathbb{Z}_{2A}}, \mathcal{O}_{\mathbb{Z}_{2B}}, \mathcal{O}_{\mathbb{Z}_{2C}}$ is redundant. Spontaneous symmetry breaking of a group G does not occur down to a subgroup, H but rather the orbit of subgroups gHg^{-1} where $g \in G$. This is easy to see. Say there exists a ground state $|\psi\rangle$ that is invariant under a subgroup $H \subset G$. This means that

$$U(h)|\psi\rangle = |\psi\rangle \ \forall h \in H \tag{C.56}$$
$$U(g)|\psi\rangle = |\psi_g\rangle \neq |\psi\rangle \ \forall g \in G/H \tag{C.57}$$

Given a ground state $|\psi\rangle$, we can generate all the $|G/H|$ ground states by using the group operators corresponding to elements G/H. However, consider the ground state $|\psi_g\rangle$. This is invariant under the elements of $\{ghg^{-1}\}$.

$$U(ghg^{-1})|\psi_g\rangle = U(g)U(h)U^\dagger(g)U(g)|\psi\rangle = U(g)U(h)|\psi\rangle = U(g)|\psi\rangle = |\psi_g\rangle \tag{C.58}$$

It is easy to check that the elements $\{ghg^{-1}\} \cong gHg^{-1}$ form a group isomorphic to H. But this group need not be identical to H. In other words, the *isotropy subgroup* of G that leaves different ground states $|\psi_g\rangle$ invariant might be differnt but are isomorphic and belong to the orbit of subgroups gHg^{-1}. This is the case with the diffent $\mathbb{Z}_2$ subgroups in our model. It is easy to check that $\{\mathbb{Z}_{2A}, \mathbb{Z}_{2B}, \mathbb{Z}_{2C}\}$ form an orbit. Using any of the order parameters $\mathcal{O}_{\mathbb{Z}_{2A}}, \mathcal{O}_{\mathbb{Z}_{2B}}, \mathcal{O}_{\mathbb{Z}_{2C}}$ would have sufficed to detect SSB to this orbit which also explains the identical plot. A special case is when $H \triangleleft G$ is a normal subgroup like the case of $\mathbb{Z}_3 \triangleleft S_3$ when $gHg^{-1} = H \ \forall g \in G$ by definition in which case the orbit has just a single group, H.

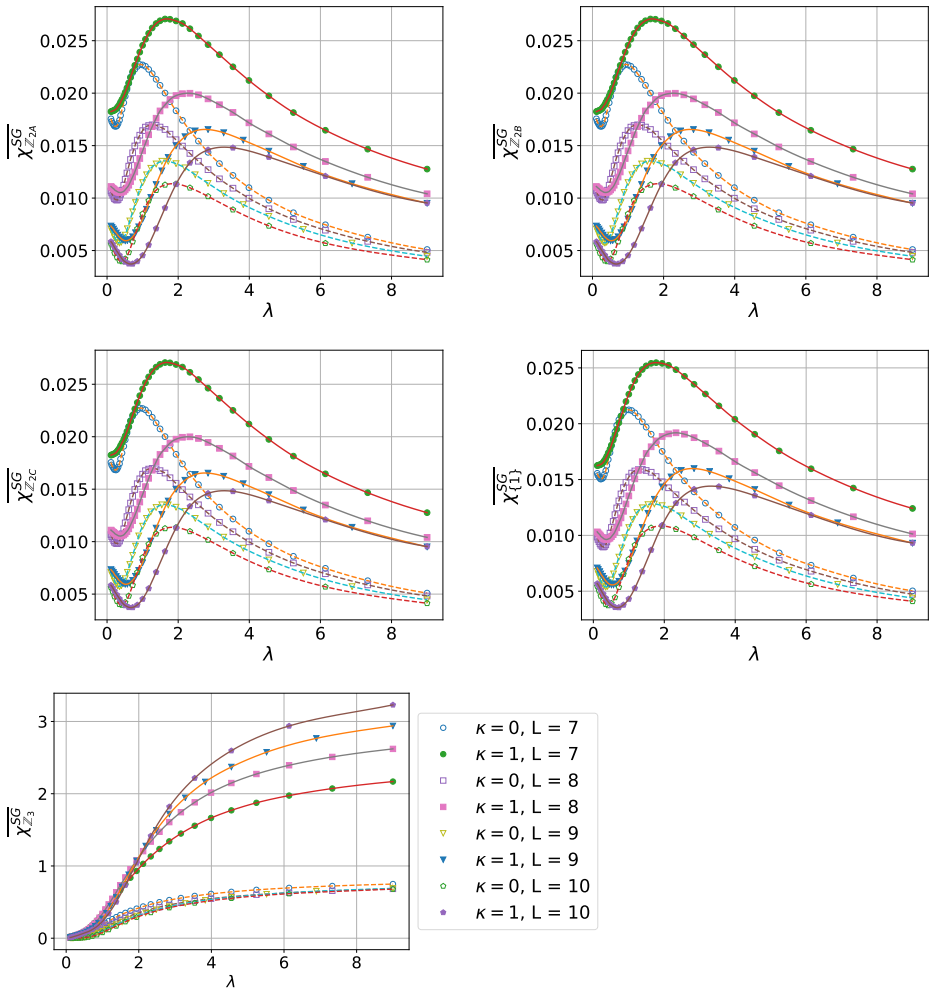

Figure C.1: SG diagnostics for different subgroups versus λ for $\kappa = 0$ and $\kappa = 1$ with spline fit (solid for $\kappa = 1$, dashed for $\kappa = 0$). 243 eigenstates per disorder realization that transform as 1D irreps sampled for 800 (7,8 sites), 879 (9 sites) and 715 (10 sites) disorder realizations respectively. The plot for $\overline{\chi^{SG}_{\mathbb{Z}_3}}$ is also shown in the main text.

Bibliography

[1] F. Westall and A. Brack, *The importance of water for life*, *Space Science Reviews* **214** (Feb, 2018) 50.

[2] D. G. Koch, W. Borucki, E. Dunham, J. Geary, R. Gilliland, J. Jenkins, D. Latham, E. Bachtell, D. Berry, W. Deininger, et al., *Overview and status of the kepler mission*, in *Optical, Infrared, and Millimeter Space Telescopes*, vol. 5487, pp. 1491–1501, International Society for Optics and Photonics, 2004.

[3] Wikipedia contributors, "Classical element — Wikipedia, the free encyclopedia." `https://en.wikipedia.org/w/index.php?title=Classical_element&oldid=843160922`, 2018. [Online; accessed 3-June-2018].

[4] Wikipedia contributors, "Scientific revolution — Wikipedia, the free encyclopedia." `https://en.wikipedia.org/w/index.php?title=Scientific_Revolution&oldid=844242240`, 2018. [Online; accessed 3-June-2018].

[5] Wikipedia contributors, "History of the periodic table — Wikipedia, the free encyclopedia." `https://en.wikipedia.org/w/index.php?title=History_of_the_periodic_table&oldid=843966012`, 2018. [Online; accessed 3-June-2018].

[6] Wikipedia contributors, "Humphry davy — Wikipedia, the free encyclopedia." `https://en.wikipedia.org/w/index.php?title=Humphry_Davy&oldid=841618764`, 2018. [Online; accessed 3-June-2018].

[7] Wikipedia contributors, "Phase transition — Wikipedia, the free encyclopedia." `https://en.wikipedia.org/w/index.php?title=Phase_transition&oldid=841551706`, 2018. [Online; accessed 3-June-2018].

[8] L. Landau and E. Lifshitz, *Statistical physics, part 1: Volume 5 (course of theoretical physics, volume 5)*, 1980.

[9] L. Michel, *Symmetry defects and broken symmetry. configurations hidden symmetry*, *Rev. Mod. Phys.* **52** (Jul, 1980) 617–651.

[10] K. v. Klitzing, G. Dorda, and M. Pepper, *New method for high-accuracy determination of the fine-structure constant based on quantized hall resistance*, *Phys. Rev. Lett.* **45** (Aug, 1980) 494–497.

[11] C. L. Kane and E. J. Mele, *Z_2 topological order and the quantum spin hall effect*, *Phys. Rev. Lett.* **95** (Sep, 2005) 146802.

[12] B. A. Bernevig, T. L. Hughes, and S.-C. Zhang, *Quantum spin hall effect and topological phase transition in hgte quantum wells*, *Science* **314** (2006), no. 5806 1757–1761, [http://science.sciencemag.org/content/314/5806/1757.full.pdf].

[13] M. König, S. Wiedmann, C. Brüne, A. Roth, H. Buhmann, L. W. Molenkamp, X.-L. Qi, and S.-C. Zhang, *Quantum spin hall insulator state in hgte quantum wells*, *Science* **318** (2007), no. 5851 766–770, [http://science.sciencemag.org/content/318/5851/766.full.pdf].

[14] P. W. Anderson, *Absence of diffusion in certain random lattices*, *Phys. Rev.* **109** (Mar, 1958) 1492–1505.

[15] D. Basko, I. Aleiner, and B. Altshuler, *Metal-insulator transition in a weakly interacting many-electron system with localized single-particle states*, *Annals of Physics* **321** (2006), no. 5 1126 – 1205.

[16] D. Huse and R. Nandkishore, *Many-body localization and thermalization in quantum statistical mechanics*, *Annual Review of Condensed Matter Physics* **6** (2015), no. 1.

[17] M. Srednicki, *Chaos and quantum thermalization*, *Phys. Rev. E* **50** (Aug, 1994) 888–901.

[18] D. S. Rokhsar and S. A. Kivelson, *Superconductivity and the quantum hard-core dimer gas*, *Phys. Rev. Lett.* **61** (Nov, 1988) 2376–2379.

[19] S. Sachdev, *Quantum phase transitions*. Cambridge university press, 2011.

[20] M. A. Levin and X.-G. Wen, *String-net condensation: A physical mechanism for topological phases*, *Phys. Rev. B* **71** (Jan, 2005) 045110.

[21] A. Kitaev, *Fault-tolerant quantum computation by anyons*, *Annals of Physics* **303** (2003), no. 1 2 – 30.

[22] A. C. Potter and A. Vishwanath, *Protection of topological order by symmetry and many-body localization*, *arXiv preprint arXiv:1506.00592* (2015).

[23] A. Chandran, V. Khemani, C. R. Laumann, and S. L. Sondhi, *Many-body localization and symmetry-protected topological order*, *Phys. Rev. B* **89** (Apr, 2014) 144201.

[24] J. A. Kjäll, J. H. Bardarson, and F. Pollmann, *Many-body localization in a disordered quantum ising chain*, *Physical review letters* **113** (2014), no. 10 107204.

[25] V. Khemani, A. Lazarides, R. Moessner, and S. L. Sondhi, *Phase structure of driven quantum systems*, *Phys. Rev. Lett.* **116** (Jun, 2016) 250401.

[26] L. Zhang, V. Khemani, and D. A. Huse, *A floquet model for the many-body localization transition*, *arXiv preprint arXiv:1609.00390* (2016).

[27] C. W. von Keyserlingk and S. L. Sondhi, *Phase structure of one-dimensional interacting floquet systems. ii. symmetry-broken phases*, *Phys. Rev. B* **93** (Jun, 2016) 245146.

[28] D. V. Else, B. Bauer, and C. Nayak, *Floquet time crystals*, *Phys. Rev. Lett.* **117** (Aug, 2016) 090402.

[29] A. C. Potter, T. Morimoto, and A. Vishwanath, *Classification of interacting topological floquet phases in one dimension*, *Phys. Rev. X* **6** (Oct, 2016) 041001.

[30] C. W. von Keyserlingk and S. L. Sondhi, *Phase structure of one-dimensional interacting floquet systems. i. abelian symmetry-protected topological phases*, *Phys. Rev. B* **93** (Jun, 2016) 245145.

[31] D. V. Else and C. Nayak, *Classification of topological phases in periodically driven interacting systems*, *Phys. Rev. B* **93** (May, 2016) 201103.

[32] D. V. Else, I. Schwarz, S. D. Bartlett, and A. C. Doherty, *Symmetry-protected phases for measurement-based quantum computation*, *Phys. Rev. Lett.* **108** (Jun, 2012) 240505.

[33] D. V. Else, S. D. Bartlett, and A. C. Doherty, *Symmetry protection of measurement-based quantum computation in ground states*, *New Journal of Physics* **14** (2012), no. 11 113016.

[34] R. Raussendorf, D.-S. Wang, A. Prakash, T.-C. Wei, and D. T. Stephen, *Symmetry-protected topological phases with uniform computational power in one dimension*, *Phys. Rev. A* **96** (Jul, 2017) 012302.

[35] D. T. Stephen, D.-S. Wang, A. Prakash, T.-C. Wei, and R. Raussendorf, *Computational power of symmetry-protected topological phases*, *Phys. Rev. Lett.* **119** (Jul, 2017) 010504.

[36] A. Prakash and T.-C. Wei, *Ground states of one-dimensional symmetry-protected topological phases and their utility as resource states for quantum computation*, *Phys. Rev. A* **92** (Aug, 2015) 022310.

[37] J. Miller and A. Miyake, *Resource quality of a symmetry-protected topologically ordered phase for quantum computation*, *Phys. Rev. Lett.* **114** (Mar, 2015) 120506.

[38] A. Prakash, C. G. West, and T.-C. Wei, *Detection of gapped phases of a one-dimensional spin chain with on-site and spatial symmetries*, *Phys. Rev. B* **94** (Jul, 2016) 045136.

[39] R. B. Laughlin, *Quantized hall conductivity in two dimensions*, *Phys. Rev. B* **23** (May, 1981) 5632–5633.

[40] R. B. Laughlin, *Anomalous quantum hall effect: An incompressible quantum fluid with fractionally charged excitations*, *Phys. Rev. Lett.* **50** (May, 1983) 1395–1398.

[41] W. X. Gang, *Quantum field theory of many-body systems: from the origin of sound to an origin of light and electrons*. Oxford University Press, Oxford, 2007.

[42] V. Kalmeyer and R. B. Laughlin, *Equivalence of the resonating-valence-bond and fractional quantum hall states*, *Phys. Rev. Lett.* **59** (Nov, 1987) 2095–2098.

[43] F. D. M. Haldane, *Nonlinear field theory of large-spin heisenberg antiferromagnets: Semiclassically quantized solitons of the one-dimensional easy-axis néel state*, *Phys. Rev. Lett.* **50** (Apr, 1983) 1153–1156.

[44] F. Haldane, *Continuum dynamics of the 1-d heisenberg antiferromagnet: Identification with the o(3) nonlinear sigma model*, *Physics Letters A* **93** (1983), no. 9 464 – 468.

[45] I. Affleck, T. Kennedy, E. H. Lieb, and H. Tasaki, *Rigorous results on valence-bond ground states in antiferromagnets*, *Phys. Rev. Lett.* **59** (Aug, 1987) 799–802.

[46] Z.-C. Gu and X.-G. Wen, *Tensor-entanglement-filtering renormalization approach and symmetry-protected topological order*, *Phys. Rev. B* **80** (Oct, 2009) 155131.

[47] F. Pollmann, E. Berg, A. M. Turner, and M. Oshikawa, *Symmetry protection of topological phases in one-dimensional quantum spin systems*, *Physical review b* **85** (2012), no. 7 075125.

[48] A. Mesaros and Y. Ran, *Classification of symmetry enriched topological phases with exactly solvable models*, *Phys. Rev. B* **87** (Apr, 2013) 155115.

[49] A. M. Essin and M. Hermele, *Classifying fractionalization: Symmetry classification of gapped $\mathbb{z}_2$ spin liquids in two dimensions*, *Phys. Rev. B* **87** (Mar, 2013) 104406.

[50] M. Hermele, *String flux mechanism for fractionalization in topologically ordered phases*, *Phys. Rev. B* **90** (Nov, 2014) 184418.

[51] X. Chen, Z.-C. Gu, and X.-G. Wen, *Classification of gapped symmetric phases in one-dimensional spin systems*, *Phys. Rev. B* **83** (Jan, 2011) 035107.

[52] X. Chen, Z.-C. Gu, and X.-G. Wen, *Complete classification of one-dimensional gapped quantum phases in interacting spin systems*, *Phys. Rev. B* **84** (Dec, 2011) 235128.

[53] L. Fidkowski and A. Kitaev, *Topological phases of fermions in one dimension*, *Phys. Rev. B* **83** (Feb, 2011) 075103.

[54] F. Pollmann and A. M. Turner, *Detection of symmetry-protected topological phases in one dimension*, *Phys. Rev. B* **86** (Sep, 2012) 125441.

[55] N. Schuch, D. Pérez-García, and I. Cirac, *Classifying quantum phases using matrix product states and projected entangled pair states*, *Phys. Rev. B* **84** (Oct, 2011) 165139.

[56] M. den Nijs and K. Rommelse, *Preroughening transitions in crystal surfaces and valence-bond phases in quantum spin chains*, *Phys. Rev. B* **40** (Sep, 1989) 4709–4734.

[57] T. Kennedy and H. Tasaki, *Hidden symmetry breaking and the haldane phase in $s = 1$ quantum spin chains*, *Comm. Math. Phys.* **147** (1992), no. 3 431–484.

[58] D. Pérez-García, M. M. Wolf, M. Sanz, F. Verstraete, and J. I. Cirac, *String order and symmetries in quantum spin lattices*, *Phys. Rev. Lett.* **100** (Apr, 2008) 167202.

[59] J. Haegeman, D. Pérez-García, I. Cirac, and N. Schuch, *Order parameter for symmetry-protected phases in one dimension*, *Phys. Rev. Lett.* **109** (Jul, 2012) 050402.

[60] G. Vidal, *Classical simulation of infinite-size quantum lattice systems in one spatial dimension*, *Phys. Rev. Lett.* **98** (Feb, 2007) 070201.

[61] J.-Y. Chen and Z.-X. Liu, *Symmetry protected topological phases in spin-1 ladders and their phase transitions*, *Annals of Physics* **362** (2015) 551–567.

[62] L. Tsui, H.-C. Jiang, Y.-M. Lu, and D.-H. Lee, *Quantum phase transitions between a class of symmetry protected topological states*, *Nuclear Physics B* **896** (2015) 330–359.

[63] L. Tsui, F. Wang, and D.-H. Lee, *Topological versus landau-like phase transitions*, *arXiv preprint arXiv:1511.07460* (2015).

[64] H. Ueda and S. Onoda, *Symmetry-protected topological phases and transition in a frustrated spin-1/2 xxz chain*, *arXiv preprint arXiv:1406.5382* (2014).

[65] P. Calabrese and J. Cardy, *Entanglement entropy and quantum field theory*, *Journal of Statistical Mechanics: Theory and Experiment* **2004** (2004), no. 06 P06002.

[66] F. Pollmann, S. Mukerjee, A. M. Turner, and J. E. Moore, *Theory of finite-entanglement scaling at one-dimensional quantum critical points*, *Phys. Rev. Lett.* **102** (Jun, 2009) 255701.

[67] D. Perez-Garcia, F. Verstraete, M. M. Wolf, and J. I. Cirac, *Matrix product state representations*, *Quantum Info. Comput.* **7** (July, 2007) 401–430.

[68] G. Vidal, *Efficient classical simulation of slightly entangled quantum computations*, *Phys. Rev. Lett.* **91** (Oct, 2003) 147902.

[69] M. B. Hastings, *An area law for one-dimensional quantum systems*, *Journal of Statistical Mechanics: Theory and Experiment* **2007** (2007), no. 08 P08024.

[70] I. Arad, Z. Landau, and U. Vazirani, *Improved one-dimensional area law for frustration-free systems*, *Phys. Rev. B* **85** (May, 2012) 195145.

[71] S. Singh, *Identifying quantum phases from the injectivity of symmetric matrix product states*, *Phys. Rev. B* **91** (Mar, 2015) 115145.

[72] G. Vidal, *Efficient simulation of one-dimensional quantum many-body systems*, *Phys. Rev. Lett.* **93** (Jul, 2004) 040502.

[73] R. Orús and G. Vidal, *Infinite time-evolving block decimation algorithm beyond unitary evolution*, *Phys. Rev. B* **78** (Oct, 2008) 155117.

[74] M. Suzuki, *General theory of higher-order decomposition of exponential operators and symplectic integrators*, *Physics Letters A* **165** (1992), no. 5 387–395.

[75] I. Omelyan, I. Mryglod, and R. Folk, *Optimized forest–ruth-and suzuki-like algorithms for integration of motion in many-body systems*, *Computer Physics Communications* **146** (2002), no. 2 188–202.

[76] J. Schachenmayer, *Dynamics and long-range interactions in 1d quantum systems*, Master's thesis, Technischen Universität, Muünchen, November, 2008.

[77] C. Lanczos, *An iteration method for the solution of the eigenvalue problem of linear differential and integral operators*. United States Governm. Press Office Los Angeles, CA, 1950.

[78] D. Calvetti, L. Reichel, and D. C. Sorensen, *An implicitly restarted lanczos method for large symmetric eigenvalue problems*, *Electronic Transactions on Numerical Analysis* **2** (1994), no. 1 21.

[79] D. C. Sorensen, *Implicitly restarted Arnoldi/Lanczos methods for large scale eigenvalue calculations*. Springer, 1997.

[80] X. Chen, Z.-X. Liu, and X.-G. Wen, *Two-dimensional symmetry-protected topological orders and their protected gapless edge excitations*, *Phys. Rev. B* **84** (Dec, 2011) 235141.

[81] D. E. Evans and R. Høegh-Krohn, *Spectral properties of positive maps on c*-algebras*, *Journal of the London Mathematical Society* **2** (1978), no. 2 345–355.

[82] H.-L. Wang, Y.-W. Dai, B.-Q. Hu, and H.-Q. Zhou, *Bifurcation in ground-state fidelity for a one-dimensional spin model with competing two-spin and three-spin interactions*, *Physics Letters A* **375** (2011), no. 45 4045–4048.

[83] A. Prakash, J. Wang, and T.-C. Wei, *Unwinding short-range entanglement*, *arXiv preprint arXiv:1804.11236* (2018).

[84] M. Z. Hasan and C. L. Kane, *Colloquium*, *Rev. Mod. Phys.* **82** (Nov, 2010) 3045–3067.

[85] X.-L. Qi and S.-C. Zhang, *Topological insulators and superconductors*, *Rev. Mod. Phys.* **83** (Oct, 2011) 1057–1110.

[86] C.-K. Chiu, J. C. Y. Teo, A. P. Schnyder, and S. Ryu, *Classification of topological quantum matter with symmetries*, *Rev. Mod. Phys.* **88** (Aug, 2016) 035005.

[87] A. W. W. Ludwig, *Topological phases: classification of topological insulators and superconductors of non-interacting fermions, and beyond*, *Physica Scripta* **2016** (2016), no. T168 014001.

[88] X.-G. Wen, *Colloquium: Zoo of quantum-topological phases of matter*, *Reviews of Modern Physics* **89** (Oct., 2017) 041004, [arXiv:1610.0391].

[89] I. Affleck, T. Kennedy, E. H. Lieb, and H. Tasaki, *Rigorous results on valence-bond ground states in antiferromagnets*, *Phys. Rev. Lett.* **59** (Aug, 1987) 799–802.

[90] F. Pollmann, A. M. Turner, E. Berg, and M. Oshikawa, *Entanglement spectrum of a topological phase in one dimension*, *Phys. Rev. B* **81** (Feb, 2010) 064439.

[91] F. Pollmann, E. Berg, A. M. Turner, and M. Oshikawa, *Symmetry protection of topological phases in one-dimensional quantum spin systems*, *Phys. Rev. B* **85** (Feb, 2012) 075125.

[92] J. Wang, X.-G. Wen, and E. Witten, *Symmetric Gapped Interfaces of SPT and SET States: Systematic Constructions*, *ArXiv e-prints* (May, 2017) [arXiv:1705.0672].

[93] A. Y. Kitaev, *Unpaired majorana fermions in quantum wires*, *Physics-Uspekhi* **44** (2001), no. 10S 131.

[94] F. Verstraete and J. I. Cirac, *Matrix product states represent ground states faithfully*, *Phys. Rev. B* **73** (Mar, 2006) 094423.

[95] N. Schuch, M. M. Wolf, F. Verstraete, and J. I. Cirac, *Entropy scaling and simulability by matrix product states*, *Phys. Rev. Lett.* **100** (Jan, 2008) 030504.

[96] X. Chen, Z.-C. Gu, Z.-X. Liu, and X.-G. Wen, *Symmetry protected topological orders and the group cohomology of their symmetry group*, *Phys. Rev. B* **87** (Apr, 2013) 155114.

[97] A. Vishwanath and T. Senthil, *Physics of three-dimensional bosonic topological insulators: Surface-deconfined criticality and quantized magnetoelectric effect*, *Phys. Rev. X* **3** (Feb, 2013) 011016.

[98] C. Wang and T. Senthil, *Boson topological insulators: A window into highly entangled quantum phases*, *Phys. Rev. B* **87** (Jun, 2013) 235122.

[99] F. J. Burnell, X. Chen, L. Fidkowski, and A. Vishwanath, *Exactly soluble model of a three-dimensional symmetry-protected topological phase of bosons with surface topological order*, *Phys. Rev. B* **90** (Dec, 2014) 245122.

[100] X.-G. Wen, *Classifying gauge anomalies through symmetry-protected trivial orders and classifying gravitational anomalies through topological orders*, *Phys. Rev. D* **88** (Aug, 2013) 045013.

[101] A. Kapustin and R. Thorngren, *Anomalous discrete symmetries in three dimensions and group cohomology*, *Phys. Rev. Lett.* **112** (Jun, 2014) 231602.

[102] D. V. Else and C. Nayak, *Classifying symmetry-protected topological phases through the anomalous action of the symmetry on the edge*, *Phys. Rev. B* **90** (Dec, 2014) 235137.

[103] E. Witten, *Fermion path integrals and topological phases*, *Rev. Mod. Phys.* **88** (Jul, 2016) 035001.

[104] L. Fidkowski, X. Chen, and A. Vishwanath, *Non-abelian topological order on the surface of a 3d topological superconductor from an exactly solved model*, *Phys. Rev. X* **3** (Nov, 2013) 041016.

[105] C. Wang, A. C. Potter, and T. Senthil, *Gapped symmetry preserving surface state for the electron topological insulator*, *Phys. Rev. B* **88** (Sep, 2013) 115137.

[106] P. Bonderson, C. Nayak, and X.-L. Qi, *A time-reversal invariant topological phase at the surface of a 3d topological insulator*, *Journal of Statistical Mechanics: Theory and Experiment* **2013** (2013), no. 09 P09016.

[107] X. Chen, F. J. Burnell, A. Vishwanath, and L. Fidkowski, *Anomalous symmetry fractionalization and surface topological order*, *Phys. Rev. X* **5** (Oct, 2015) 041013.

[108] M. A. Metlitski, C. L. Kane, and M. P. A. Fisher, *Symmetry-respecting topologically ordered surface phase of three-dimensional electron topological insulators*, *Phys. Rev. B* **92** (Sep, 2015) 125111.

[109] N. Seiberg and E. Witten, *Gapped boundary phases of topological insulators via weak coupling*, *Progress of Theoretical and Experimental Physics* **2016** (2016), no. 12.

[110] G. W. Moore, *Quantum symmetries and compatible hamiltonians*, *Notes available at http://www. physics. rutgers. edu/gmoore/QuantumSymmetryBook. pdf* (2014).

[111] H. J. Briegel and R. Raussendorf, *Persistent entanglement in arrays of interacting particles*, *Phys. Rev. Lett.* **86** (Jan, 2001) 910–913.

[112] R. Raussendorf and H. J. Briegel, *A one-way quantum computer*, *Phys. Rev. Lett.* **86** (May, 2001) 5188–5191.

[113] R. Raussendorf, D. E. Browne, and H. J. Briegel, *Measurement-based quantum computation on cluster states*, *Phys. Rev. A* **68** (Aug, 2003) 022312.

[114] W. Son, L. Amico, R. Fazio, A. Hamma, S. Pascazio, and V. Vedral, *Quantum phase transition between cluster and antiferromagnetic states*, *EPL (Europhysics Letters)* **95** (2011), no. 5 50001.

[115] W. Son, L. Amico, and V. Vedral, *Topological order in 1d cluster state protected by symmetry*, *Quantum Information Processing* **11** (Dec, 2012) 1961–1968.

[116] A. Miyake, *Quantum computation on the edge of a symmetry-protected topological order*, *Phys. Rev. Lett.* **105** (Jul, 2010) 040501.

[117] I. Schur, *Über die Darstellung der endlichen Gruppen durch gebrochene lineare Substitutionen.*, *J. Reine Angew. Math.* **127** (1904) 20–50.

[118] I. Schur, *Untersuchungen über die Darstellung der endlichen Gruppen durch gebrochene lineare Substitutionen.*, *J. Reine Angew. Math.* **132** (1907) 85–137.

[119] A. P. Schnyder, S. Ryu, A. Furusaki, and A. W. W. Ludwig, *Classification of topological insulators and superconductors*, *AIP Conference Proceedings* **1134** (2009), no. 1 10–21, [http://aip.scitation.org/doi/pdf/10.1063/1.3149481].

[120] A. Kitaev, *Periodic table for topological insulators and superconductors*, *AIP Conference Proceedings* **1134** (2009), no. 1 22–30, [http://aip.scitation.org/doi/pdf/10.1063/1.3149495].

[121] A. Kapustin, R. Thorngren, A. Turzillo, and Z. Wang, *Fermionic symmetry protected topological phases and cobordisms*, *Journal of High Energy Physics* **2015** (Dec, 2015) 1–21.

[122] D. S. Freed, *Short-range entanglement and invertible field theories*, *arXiv preprint arXiv:1406.7278* (2014).

[123] L. Fidkowski and A. Kitaev, *Effects of interactions on the topological classification of free fermion systems*, *Phys. Rev. B* **81** (Apr, 2010) 134509.

[124] R. Gade and F. Wegner, *The n = 0 replica limit of u(n) and u(n)so(n) models*, *Nuclear Physics B* **360** (1991), no. 2 213 – 218.

[125] R. Gade, *Anderson localization for sublattice models*, *Nuclear Physics B* **398** (1993), no. 3 499 – 515.

[126] R. Verresen, R. Moessner, and F. Pollmann, *One-dimensional symmetry protected topological phases and their transitions*, *Physical Review B* **96** (Oct, 2017).

[127] Y. Chen, A. Prakash, and T.-C. Wei, *Universal quantum computing using $(\mathbb{Z}_d)^3$ symmetry-protected topologically ordered states*, *Phys. Rev. A* **97** (Feb, 2018) 022305.

[128] M. Fannes, B. Nachtergaele, and R. F. Werner, *Finitely correlated states on quantum spin chains*, *Comm. Math. Phys.* **144** (1992), no. 3 443–490.

[129] H. Briegel, D. Browne, W. Dür, R. Raussendorf, and M. Van den Nest, *Measurement-based quantum computation*, *Nature Physics* **5** (2009), no. 1 19–26.

[130] M. Van den Nest, A. Miyake, W. Dür, and H. J. Briegel, *Universal resources for measurement-based quantum computation*, *Phys. Rev. Lett.* **97** (Oct, 2006) 150504.

[131] D. Gross and J. Eisert, *Novel schemes for measurement-based quantum computation*, *Phys. Rev. Lett.* **98** (May, 2007) 220503.

[132] D. Gross, J. Eisert, N. Schuch, and D. Perez-Garcia, *Measurement-based quantum computation beyond the one-way model*, *Phys. Rev. A* **76** (Nov, 2007) 052315.

[133] X. Chen, B. Zeng, Z.-C. Gu, B. Yoshida, and I. L. Chuang, *Gapped two-body hamiltonian whose unique ground state is universal for one-way quantum computation*, *Phys. Rev. Lett.* **102** (Jun, 2009) 220501.

[134] R. Raussendorf and T.-C. Wei, *Quantum computation by local measurement*, *Annual Review of Condensed Matter Physics* **3** (2012), no. 1 239–261, [http://dx.doi.org/10.1146/annurev-conmatphys-020911-125041].

[135] G. K. Brennen and A. Miyake, *Measurement-based quantum computer in the gapped ground state of a two-body hamiltonian*, *Phys. Rev. Lett.* **101** (Jul, 2008) 010502.

[136] T.-C. Wei, I. Affleck, and R. Raussendorf, *Affleck-kennedy-lieb-tasaki state on a honeycomb lattice is a universal quantum computational resource*, *Phys. Rev. Lett.* **106** (Feb, 2011) 070501.

[137] A. Miyake, *Quantum computational capability of a 2d valence bond solid phase*, *Annals of Physics* **326** (2011), no. 7 1656 – 1671.

[138] T.-C. Wei, I. Affleck, and R. Raussendorf, *Two-dimensional affleck-kennedy-lieb-tasaki state on the honeycomb lattice is a universal resource for quantum computation*, *Phys. Rev. A* **86** (Sep, 2012) 032328.

[139] T.-C. Wei, *Quantum computational universality of affleck-kennedy-lieb-tasaki states beyond the honeycomb lattice*, *Phys. Rev. A* **88** (Dec, 2013) 062307.

[140] J. Cai, A. Miyake, W. Dür, and H. J. Briegel, *Universal quantum computer from a quantum magnet*, *Phys. Rev. A* **82** (Nov, 2010) 052309.

[141] S. Singh, R. N. C. Pfeifer, and G. Vidal, *Tensor network decompositions in the presence of a global symmetry*, *Phys. Rev. A* **82** (Nov, 2010) 050301.

[142] S. Singh, R. N. C. Pfeifer, and G. Vidal, *Tensor network states and algorithms in the presence of a global u(1) symmetry*, *Phys. Rev. B* **83** (Mar, 2011) 115125.

[143] S. Singh and G. Vidal, *Tensor network states and algorithms in the presence of a global su(2) symmetry*, *Phys. Rev. B* **86** (Nov, 2012) 195114.

[144] S. Singh and G. Vidal, *Global symmetries in tensor network states: Symmetric tensors versus minimal bond dimension*, *Phys. Rev. B* **88** (Sep, 2013) 115147.

[145] J.-M. Cai, W. Dür, M. Van den Nest, A. Miyake, and H. J. Briegel, *Quantum computation in correlation space and extremal entanglement*, *Phys. Rev. Lett.* **103** (Jul, 2009) 050503.

[146] T. Morimae, *How to upload a physical quantum state into correlation space*, *Phys. Rev. A* **83** (Apr, 2011) 042337.

[147] S. D. Bartlett, G. K. Brennen, A. Miyake, and J. M. Renes, *Quantum computational renormalization in the haldane phase*, *Phys. Rev. Lett.* **105** (Sep, 2010) 110502.

[148] A. C. Doherty and S. D. Bartlett, *Identifying phases of quantum many-body systems that are universal for quantum computation*, *Phys. Rev. Lett.* **103** (Jul, 2009) 020506.

[149] G. Karpilovsky, *The schur multiplier*. Oxford University Press, Inc., 1987.

[150] I. Sakata, *A general method for obtaining clebsch-gordan coefficients of finite groups. i. its application to point and space groups*, *Journal of Mathematical Physics* **15** (1974), no. 10 1702–1709.

[151] W. Grimus and P. O. Ludl, *Finite flavour groups of fermions*, *Journal of Physics A: Mathematical and Theoretical* **45** (2012), no. 23 233001.

[152] P. Ramond, *Group theory: a physicist's survey*. Cambridge University Press, Cambridge, UK, 2010.

[153] J. Miller and A. Miyake, *Hierarchy of universal entanglement in 2d measurement-based quantum computation*, *npj Quantum Information* **2** (2016) 16036.

[154] J. Miller and A. Miyake, *Latent computational complexity of symmetry-protected topological order with fractional symmetry*, *Phys. Rev. Lett.* **120** (Apr, 2018) 170503.

[155] A. Prakash, S. Ganeshan, L. Fidkowski, and T.-C. Wei, *Eigenstate phases with finite on-site non-abelian symmetry*, *Phys. Rev. B* **96** (Oct, 2017) 165136.

[156] J. M. Deutsch, *Quantum statistical mechanics in a closed system*, *Phys. Rev. A* **43** (Feb, 1991) 2046–2049.

[157] V. Oganesyan and D. A. Huse, *Localization of interacting fermions at high temperature*, *Physical Review B* **75** (2007), no. 15 155111.

[158] A. Pal and D. A. Huse, *Many-body localization phase transition*, *Physical Review B* **82** (2010), no. 17 174411.

[159] B. Bauer and C. Nayak, *Area laws in a many-body localized state and its implications for topological order*, *Journal of Statistical Mechanics: Theory and Experiment* **2013** (2013), no. 09 P09005.

[160] S. Iyer, V. Oganesyan, G. Refael, and D. A. Huse, *Many-body localization in a quasiperiodic system*, *Phys. Rev. B* **87** (Apr, 2013) 134202.

[161] J. Z. Imbrie, *On many-body localization for quantum spin chains*, *Journal of Statistical Physics* **163** (2016), no. 5 998–1048.

[162] M. Serbyn, Z. Papić, and D. A. Abanin, *Local conservation laws and the structure of the many-body localized states*, *Phys. Rev. Lett.* **111** (Sep, 2013) 127201.

[163] A. Chandran, I. H. Kim, G. Vidal, and D. A. Abanin, *Constructing local integrals of motion in the many-body localized phase*, *Phys. Rev. B* **91** (Feb, 2015) 085425.

[164] D. A. Huse, R. Nandkishore, and V. Oganesyan, *Phenomenology of fully many-body-localized systems*, *Phys. Rev. B* **90** (Nov, 2014) 174202.

[165] V. Ros, M. Müller, and A. Scardicchio, *Integrals of motion in the many-body localized phase*, *Nuclear Physics B* **891** (2015) 420–465.

[166] S. Johri, R. Nandkishore, and R. Bhatt, *Many-body localization in imperfectly isolated quantum systems*, *Physical review letters* **114** (2015), no. 11 117401.

[167] K. Hyatt, J. R. Garrison, A. C. Potter, and B. Bauer, *Many-body localization in the presence of a small bath*, *Physical Review B* **95** (2017), no. 3 035132.

[168] A. Lazarides, A. Das, and R. Moessner, *Fate of many-body localization under periodic driving*, *Physical review letters* **115** (2015), no. 3 030402.

[169] W. De Roeck, F. Huveneers, M. Müller, and M. Schiulaz, *Absence of many-body mobility edges*, *Physical Review B* **93** (2016), no. 1 014203.

[170] W. De Roeck and J. Z. Imbrie, *Many-body localization: Stability and instability*, *arXiv preprint arXiv:1705.00756* (2017).

[171] R. Nandkishore and A. C. Potter, *Marginal anderson localization and many-body delocalization*, *Physical Review B* **90** (2014), no. 19 195115.

[172] X. Li, S. Ganeshan, J. Pixley, and S. D. Sarma, *Many-body localization and quantum nonergodicity in a model with a single-particle mobility edge*, *Physical review letters* **115** (2015), no. 18 186601.

[173] R. Modak and S. Mukerjee, *Many-body localization in the presence of a single-particle mobility edge*, *Physical review letters* **115** (2015), no. 23 230401.

[174] A. C. Potter and R. Vasseur, *Symmetry constraints on many-body localization*, *Phys. Rev. B* **94** (Dec, 2016) 224206.

[175] R. Vasseur, A. C. Potter, and S. A. Parameswaran, *Quantum criticality of hot random spin chains*, *Phys. Rev. Lett.* **114** (May, 2015) 217201.

[176] B. Kang, A. C. Potter, and R. Vasseur, *Universal crossover from ground state to excited-state quantum criticality*, *arXiv preprint arXiv:1607.03496* (2016).

[177] D. Pekker, G. Refael, E. Altman, E. Demler, and V. Oganesyan, *Hilbert-glass transition: New universality of temperature-tuned many-body dynamical quantum criticality*, *Phys. Rev. X* **4** (Mar, 2014) 011052.

[178] V. Khemani, S. Lim, D. Sheng, and D. A. Huse, *Critical properties of the many-body localization transition*, *arXiv preprint arXiv:1607.05756* (2016).

[179] X. Yu, D. J. Luitz, and B. K. Clark, *Bimodal entanglement entropy distribution in the many-body localization transition*, *Phys. Rev. B* **94** (Nov, 2016) 184202.

[180] S. F. Edwards and P. W. Anderson, *Theory of spin glasses*, *Journal of Physics F: Metal Physics* **5** (1975), no. 5 965.

[181] K. Binder and A. P. Young, *Spin glasses: Experimental facts, theoretical concepts, and open questions*, *Rev. Mod. Phys.* **58** (Oct, 1986) 801–976.

[182] H. Nishimori, *Statistical physics of spin glasses and information processing: an introduction*, vol. 111. Clarendon Press, 2001.

[183] A. B. Harris, *Upper bounds for the transition temperatures of generalized ising models*, *Journal of Physics C: Solid State Physics* **7** (1974), no. 17 3082.

[184] J. T. Chayes, L. Chayes, D. S. Fisher, and T. Spencer, *Correlation length bounds for disordered ising ferromagnets*, *Communications in Mathematical Physics* **120** (Sep, 1989) 501–523.

[185] J. T. Chayes, L. Chayes, D. S. Fisher, and T. Spencer, *Finite-size scaling and correlation lengths for disordered systems*, *Phys. Rev. Lett.* **57** (Dec, 1986) 2999–3002.

[186] A. Chandran, C. R. Laumann, and V. Oganesyan, *Finite size scaling bounds on many-body localized phase transitions*, *arXiv preprint arXiv:1509.04285* (2015).

[187] D. J. Luitz, N. Laflorencie, and F. Alet, *Many-body localization edge in the random-field heisenberg chain*, *Phys. Rev. B* **91** (Feb, 2015) 081103.

[188] V. Khemani, D. Sheng, and D. A. Huse, *Two universality classes for the many-body localization transition*, *arXiv preprint arXiv:1702.03932* (2017).

[189] D. Abanin, W. De Roeck, F. Huveneers, and W. W. Ho, *Asymptotic energy conservation in periodically driven many-body systems*, *arXiv preprint arXiv:1509.05386* (2015).

[190] D. V. Else, B. Bauer, and C. Nayak, *Pre-thermal time crystals and floquet topological phases without disorder*, *arXiv preprint arXiv:1607.05277* (2016).

[191] R. Vosk and E. Altman, *Many-body localization in one dimension as a dynamical renormalization group fixed point*, *Phys. Rev. Lett.* **110** (Feb, 2013) 067204.